



**UNIVERSITÀ DEGLI STUDI DI MILANO**

**Dottorato di Ricerca in Scienze Biochimiche  
XXX ciclo**

**Dipartimento di Biotecnologie Mediche  
e Medicina Traslazionale**

**GM1-mediated neurodifferentiation  
is promoted by  
OligoGM1-TrkA interaction**

**Margherita Maggioni**  
Matricola n. R10940

Docente guida:  
**Prof. Sandro Sonnino**

Tutor:  
**Dott.ssa Elena Chiricozzi**

Coordinatore del Dottorato:  
**Prof. Sandro Sonnino**

*Anno Accademico 2016/2017*

# ***Index***

|   |           |
|---|-----------|
| <b><i>Abstract</i></b>  | <b>1</b>  |
| <br>  |           |
| <b><i>Introduction</i></b>  | <b>4</b>  |
| Gangliosides  | 5         |
| <i>Chemical structure</i>   | 6         |
| <i>Cell topology and functions</i>                                      | 11        |
| GM1 ganglioside   | 19        |
| <i>Chemical properties and cell topology</i>                            | 21        |
| <i>GM1 neurofunctions</i>   | 26        |
| <br>  |           |
| <b><i>Aim</i></b>   | <b>33</b> |
| <br>  |           |
| <b><i>Materials &amp; Methods</i></b>                                   | <b>37</b> |
| Materials   | 38        |
| Methods   | 40        |
| Chemical synthesis and preparation of gangliosides and oligosaccharides | 40        |
| <i>Gangliosides</i>   | 40        |
| <i>Radiolabeled GM1</i>   | 40        |
| <i>Ganglioside Oligosaccharides</i>                                     | 42        |
| <i>Photoactivable Derivatives</i>                                       | 45        |
| <i>NMR, MS, HPTLC, and autoradiographic analyses</i>                    | 50        |
| Cell cultures   | 51        |
| Cell treatments   | 51        |

|   |           |
|---|-----------|
| <i>Ganglioside, Oligosaccharide and sugar treatments</i>        | 51        |
| <i>TrkA chemical inhibition</i>                                 | 52        |
| <i>siRNA mediated TrkA knockdown</i>                            | 52        |
| <i>Photolabeling experiments</i>                                | 53        |
| Assessment of cytotoxicity                                      | 54        |
| <i>Trypan blue assay</i>  | 54        |
| <i>MTT assays</i>   | 54        |
| Morphological analysis and neurite outgrowth evaluation         | 55        |
| Immunofluorescence analysis                                     | 56        |
| Study of interaction between OligoGM1 and N2a cells             | 57        |
| Protein analysis  | 58        |
| Molecular modeling  | 59        |
| <b><i>Results</i></b>   | <b>60</b> |
| GM1 and OligoGM1 effect on N2a cell viability and proliferation | 61        |
| Effect of GM1 derivatives on N2a cell morphology                | 63        |
| Neurite characterization  | 67        |
| <i>Physical characterization</i>                                | 67        |
| <i>Biochemical characterization</i>                             | 68        |
| OligoGM1 interaction with N2a cells                             | 70        |

|  |            |
|--|------------|
| OligoGM1 effect on TrkA receptor pathway                   | 72         |
| <i>TrkA receptor activation</i>                            | 72         |
| <i>Time course changing in TrkA-Erk signaling pathway</i>  | 75         |
| <i>TrkA receptor inhibition</i>                            | 78         |
| <i>TrkA receptor expression silencing</i>                  | 81         |
| Interaction between OligoGM1 and TrkA receptor             | 84         |
| <i>Covalent cross-linking interaction by photolabeling</i> | 84         |
| <i>Dynamic calculations for the TrkA-OligoGM1 complex</i>  | 88         |
| <br>   |            |
| <b><i>Discussion</i></b>                                   | <b>91</b>  |
| <br>   |            |
| <b><i>References</i></b>                                   | <b>100</b> |
| <br>   |            |
| <b><i>Appendix I</i></b>                                   | <b>113</b> |



# *Abstract*

The present study proposes a clarification on the molecular mechanism by which ganglioside GM1 promotes neurodifferentiation, demonstrating *in vitro* that neurotrophic functions are exerted by an interaction between the oligosaccharide portion (OligoGM1) and an extracellular domain of TrkA receptor.

Similarly to the entire molecule, the oligosaccharide portion of ganglioside GM1, rather than ceramide, is responsible for neurodifferentiation by augmenting neurite elongation and by increasing the expression of neurofilament proteins in mouse neuroblastoma cell line Neuro2a (N2a).

Conversely, the single components of OligoGM1 (asialo-OligoGM1, OligoGM2, OligoGM3, sialic acid or galactose) are not able to induce a neuro-like morphology. The neurodifferentiative effect is exerted instead by fucosyl-OligoGM1.

Contrarily to GM1, exogenous OligoGM1 never integrates in the plasma membrane composition and does not belong to the intracellular metabolism: the unique interaction with N2a is characterized by a weak non-covalent association to the plasma membrane that suggests the existence of an OligoGM1-stimulated target on the cell surface.

In fact, the neurotrophic properties of GM1 oligosaccharide are exerted by activating TrkA receptor and the following cascade leading to neurodifferentiation event.

The second part of this study elucidates the interaction between GM1 and TrkA, revealing a direct association of OligoGM1 to an extracellular domain of the receptor.

Photolabeling experiments, performed employing nitrogen azide radiolabeled GM1 derivatives, show a direct association of the oligosaccharide chain to TrkA.

Moreover, a bioinformatics study reveals that OligoGM1 fits perfectly in a pocket of the TrkA-NGF complex, stabilizing and favoring their intermolecular interactions as revealed by the increase in energy associated to the new complex TrkA-NGF-OligoGM1. A precise molecular recognition process between OligoGM1 and a specific extracellular domain of the TrkA receptor is

supposed. According to the weak association of OligoGM1 to the cell surface, no covalent bounds between OligoGM1 and TrkA-NGF complex were found.

For the first time the molecular mechanism by which GM1 exerts its neurodifferentiative potential was identified, finding out a direct interaction between the oligosaccharide portion and an extracellular domain of TrkA receptor responsible for enhancing the signal transduction related to the neurodifferentiation pathway.

# *Introduction*

## Gangliosides

Gangliosides are a large family of complex glycosphingolipids (GSLs) isolated for the first time from beef brain in 1942 by Klenk, who among the hydrolysis products identified their essential components: sphingosine, fatty acid, hexoses and sialic acid (Klenk, 1942; Svennerholm, 1964).

Ganglioside components are shown in figure I1 reporting chemical structure of the simplest ganglioside, GM3.

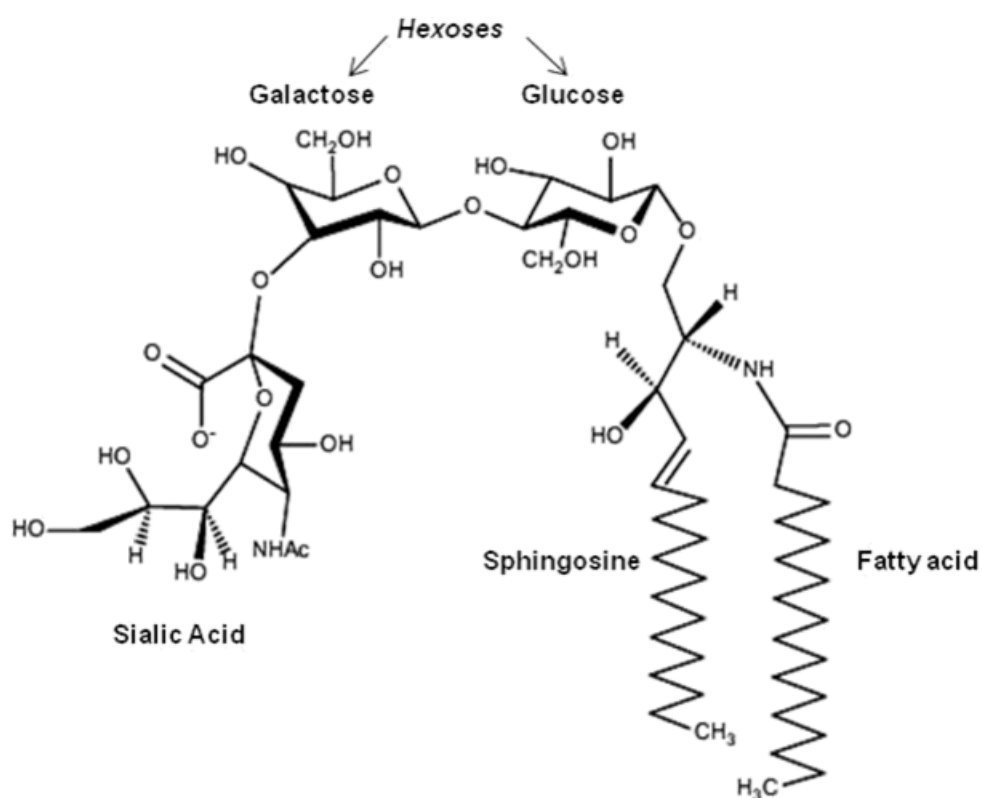


**Figure I1: Chemical structure of the simplest ganglioside GM3.** GM3 is reported to show typical components of gangliosides: sphingosine, fatty acid, sialic acid and hexoses. GM3 contains glucose and galactose.

### **Chemical structure**

Gangliosides are amphiphilic components typical of all deuterostomia cell plasma membranes that assume structural and functional outstanding roles internally to the lipid raft plasma membrane regions (Ghidoni *et al.* 1989; Senn *et al.* 1989; Valaperta *et al.* 2007; Merrill, 2011).

According to the general glycolipid features, gangliosides are inserted only in the outer leaflet of the plasma membrane integrating in the lipid core layer through a hydrophobic moiety and simultaneously protruding in the extracellular environment with a hydrophilic portion (Bertoli *et al.* 1981; Robert *et al.* 2011; Kolter, 2012; Shengrund, 2015).

Gangliosides are spread all over the tissues, but in mammals they are prevalent in plasma membranes of nervous cells, in particular in the gray matter, especially localized at the pre- and post-synaptic areas. Outside of the nervous system they are relevant in serum, vehiculated by lipoproteins, in spleen, and in erythrocytes (Svennerholm, 1964; Rösner *et al.* 1973; Hansson *et al.* 1977; Senn *et al.* 1989; Kolter, 2012).

As a matter of fact, the gangliosides are composed by ceramide, the hydrophobic core, resulting from a long chain fatty acid incorporation on the 2 position of a sphinganine basis promoted by the ceramide synthase acylation. Dihydroceramide can be finally desaturated introducing a double carbon bond between positions 4 and 5 of the acyl residue of sphingosine, derived generally by palmitate (Sribney, 1966; Merrill, 1991; Rother *et al.* 1992). The ceramide *de novo* synthesis, shown in figure I2, takes place in the endoplasmic reticulum (Miller Podrasa & Fishman, 1982; Schwarzmann & Sandhoff, 1990; Kolter, 2012).

According to the beginning discovery (Klenk, 1942), the hydrophilic head of gangliosides, the oligosaccharide chain, is always characterized by the presence of one or more residues of sialic acid (figure I3). The ceramide glycosylation arises from the progressive addition by specific glycosyltransferases of  $\beta$ -anomeric neutral monosaccharides from the nucleotide-activated forms, usually by UDP (Van Den Eijnden, 1973; Basu & Basu, 1982; Kolter, 2012). The transfer of sialic acid by a sialyltransferase stands out for the CMP-activated donor complex and for the formation of  $\alpha$ -glycosidic bond via

hydroxyl group at position 2 to a neutral monosaccharide unit or to another sialic acid residue (Schauer, 1982; Tettamanti & Riboni, 1993; Schnaar *et al.* 2014), as shown in figure 14.

These reactions occur in the luminal side of the Golgi apparatus explaining the topological asymmetric insertion of the gangliosides in the external layer of the plasma membrane (Ghidoni *et al.* 1989; Sandhoff & Kolter, 2003; Kolter *et al.* 2002).

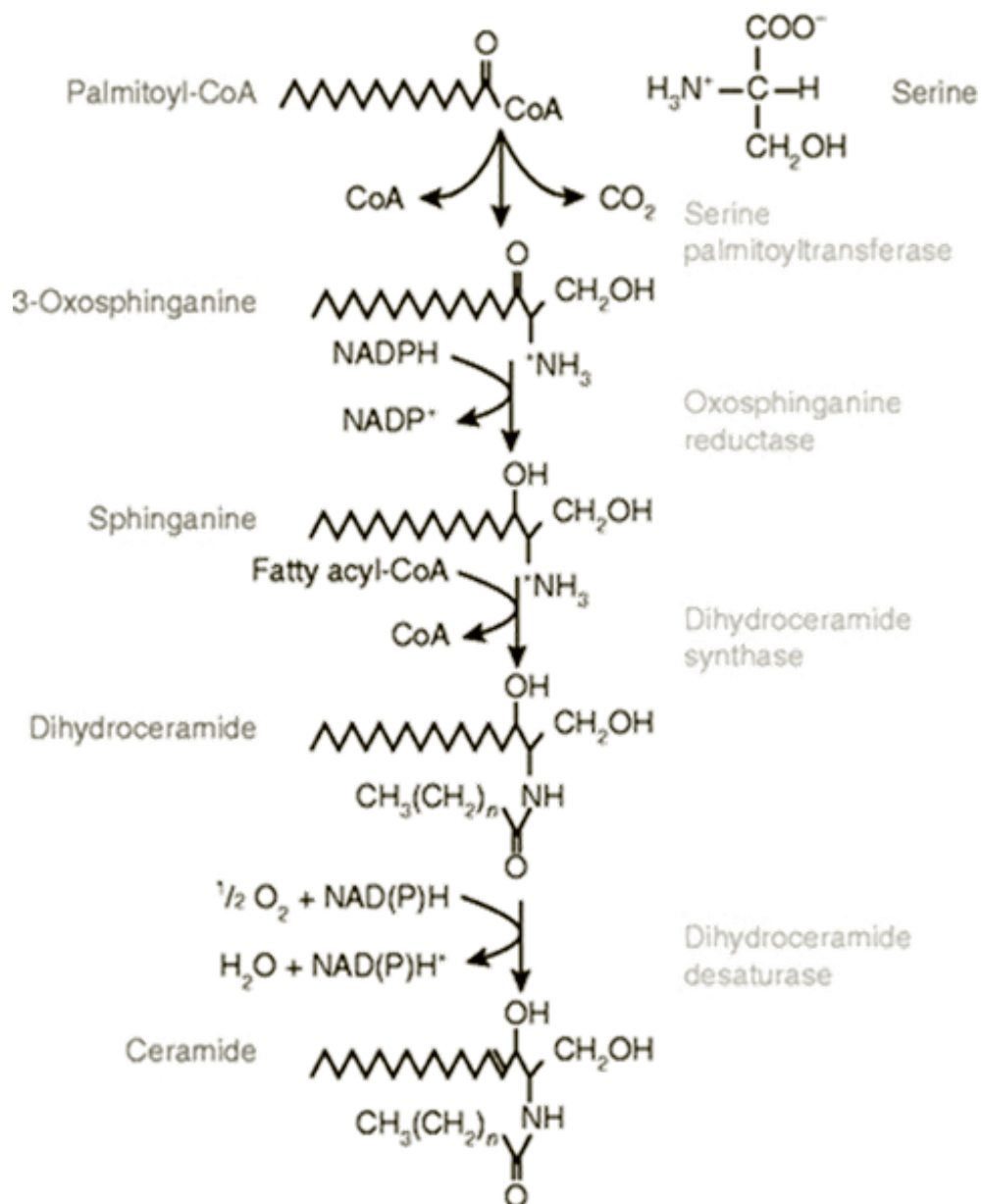


Figure 12: *De novo* ceramide biosynthesis.

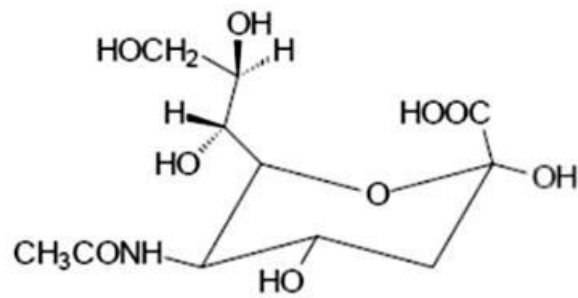
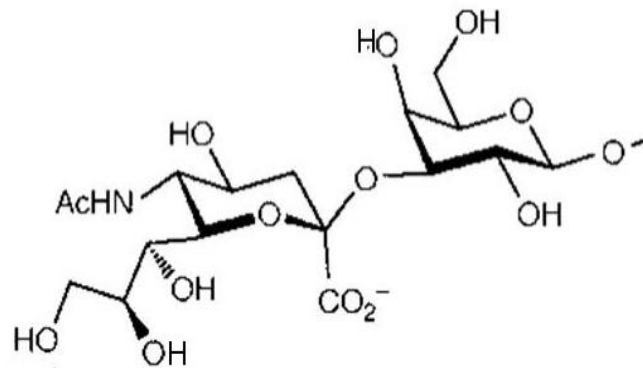


Figure I3: Structure of Sialic Acid.

a.



b.

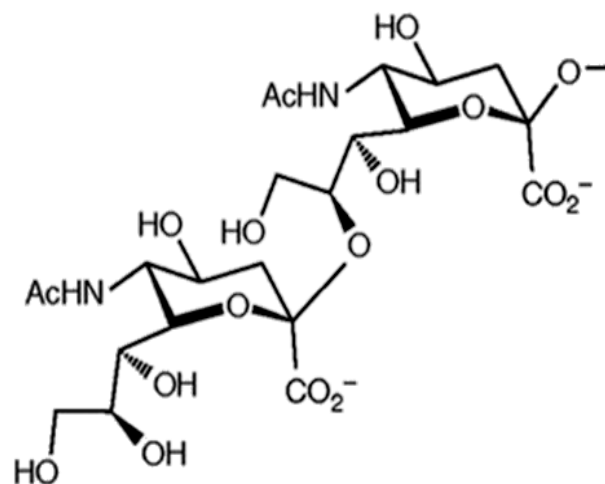


Figure I4: Sialic Acid linkages in gangliosides. Examples of an  $\alpha$ -(2-3) glycosidic linkage between sialic acid and a neutral monosaccharide typically represented by a galactose residue (a) and of an  $\alpha$ -(2-8) glycosidic linkage between sialic acid residues (b), characteristic of polysialylated brain gangliosides.



Beyond the conserved structure, gangliosides present an interesting heterogeneity given firstly by ceramide. It varies in relation to the sphingoid basis, a sphingosine or a sphinganine, presenting or omitting the desaturation respectively, and containing from 16 to 22 carbon atoms. Also the fatty acid differs among ceramide types commonly represented by the palmitic acid (16:0), stearic acid (18:0), oleic acid (18:1), and arachic acid (20:0) in the nervous system and by behenic acid (22:0), docosanoic acid (22:1), lignoceric acid (24:0) and nervonic acid (24:1) in extra nervous tissues (Schengrund & Garrigan, 1969; Karlsson 1970; Kolter, 2012).

Furthermore, the remarkable diversification in the oligosaccharide chains among the gangliosides have provided an instrument for their classification (Svennerholm & Fredman, 1980; Svennerholm, 1994) combined to the nomenclature formulation by IUPAC IUB Commission (IUPAC-IUBMB JCoBN, 1998).

According to the oligosaccharide core sequences, the gangliosides can be divided in six series: ganglio, gala, latte, neolatte, globo, isoglobo (Svennerholm, 1994; Kolter, 2012). The first letter is dependent on these categories: G stands for ganglio, that presents oligosaccharide  $\beta$ -D-Glucose- $\beta$ -D-Galactose-N-acetyl- $\beta$ -D-Galactosamine- $\beta$ -D-Galactose.

The ganglio sub classification (figure 15), based on the sialic acid residues number, is expressed by the second letters M, D, T, or Q, designing mono-, di-, tri- or tetra-sialyl groups respectively. The following number 1, 2 or 3 agrees with the order of migration of the ganglioside in thin layer chromatography (GM1 < GM2 < GM3), reflecting the presence of the entire oligosaccharide sequence, the lack of the external galactose or the disaccharide galactosyl-N-acetylgalactosamine respectively. The final letters evoke the role of the sialyltransferases in the ganglioside metabolism: letter "a" indicates the only presence of linkages between sialic acid and galactose, letters "b" and "c" the existence of linkages between two or three sialic acid residues respectively (Svennerholm, 1994; Kolter *et al.* 2002; Kolter, 2012).

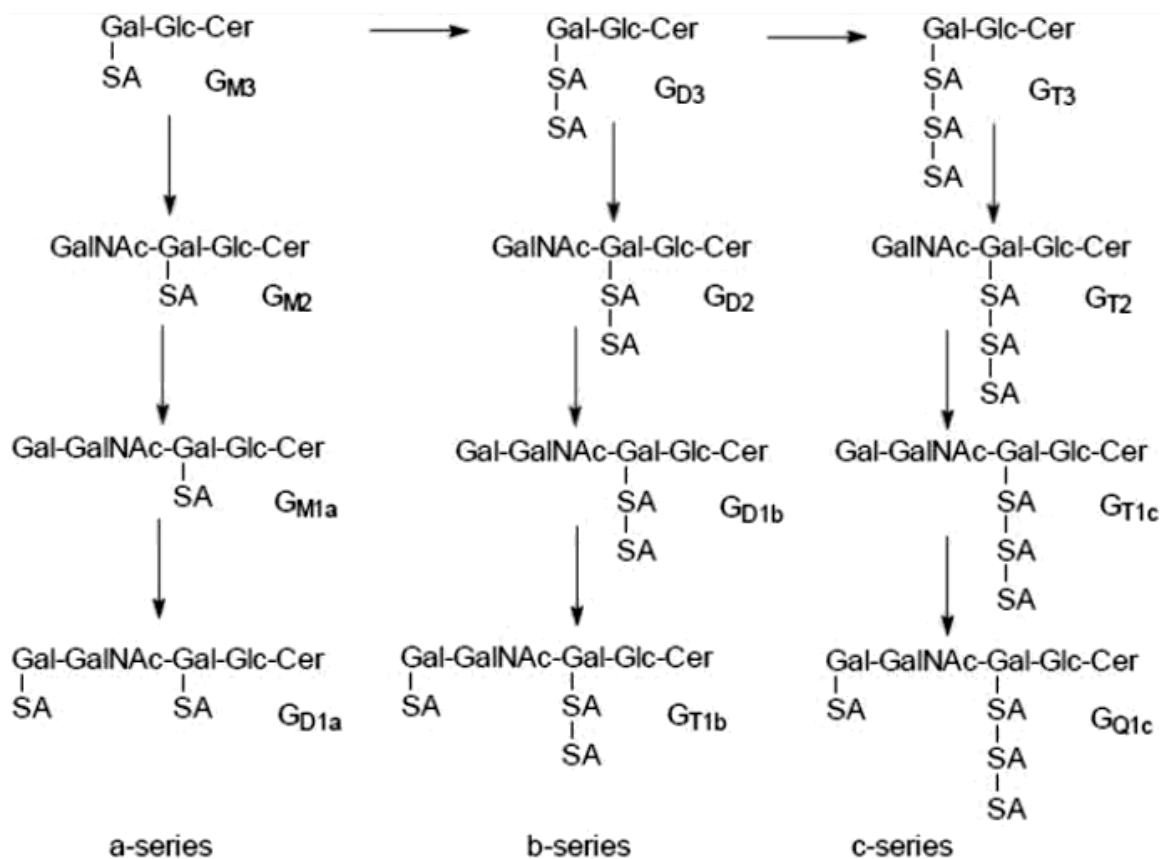


Figure 15: Classification of Ganglio series gangliosides (IUPAC-IUB JCoBN, 1998).

Currently, IUPAC-IUB commission on the biochemical nomenclature purposes a graphic symbology for glycans representation (IUPAC-IUBMB JCoBN, 1998). Monosaccharides typical of Ganglio series gangliosides are identified by symbols shown in figure 16.

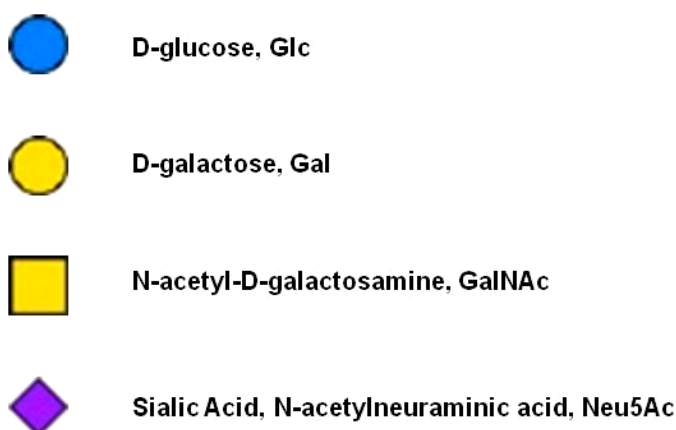


Figure 16: Symbols used for monosaccharides of Ganglio serie gangliosides (IUPAC-IUBMB JCoBN, 1998).

### **Cell topology and functions**

The substantial amphiphilic feature of gangliosides represents the basis beyond the structural ones, of their structural and physiological functions (Robert *et al.* 2011; Russo *et al.* 2016).

The ceramide portion, inserted in the plasma membrane outer layer, exerts an influence on the establishment of arrangement with other complex lipid and proteins, affecting the modulation of plasma membrane properties. On the other side, the carbohydrate moiety, projected in extracellular environment, offers many recognition and interaction sites for cell surrounding molecules playing a crucial role in the cell response to an external stimuli, in signal transduction and in mediation of cell activities (Bertoli *et al.* 1981; Hakomori, 1983; Arita *et al.* 1984; Merrill & Sandhoff, 2002; Kolter, 2004; Shengrund, 2015).

Starting from the ceramide contribute in ganglioside functions, a remarkable impact on plasma membrane organization is due to the presence of the *trans* double bond between sphingosine C4 and C5, combined with the presence of a saturated fatty acyl residue. These features allow the ganglioside hydrocarbon chains to pack in the plasma membrane lipid layer more tightly than other hydrophobic components, such as the phospholipids containing *cis* double bond related to unsaturated fatty acids, enhancing the association to cholesterol as well as to transmembrane protein domains (Shengrund & Garrigan, 1969; Tettamanti & Riboni, 1993; Shengrund, 2015). The following interactions originate the particularly enriched and specialized plasma membrane regions named lipid rafts (figure I7), that, according to their experimental isolation are defined as detergent-resistant assemblages (DRM) resulting as a low-density fractions from density-gradient ultracentrifugation (Simons & Ikonen, 1997; Simons & Sampaio, 2011; Ohmi *et al.* 2012; Kraft, 2013; Ledeen & Wu, 2015).

The Figure 17 purposes an overall representation of a plasma membrane lipid raft, presenting gangliosides among the characteristic elements (Malchiodi-Albedi *et al.* 2011).

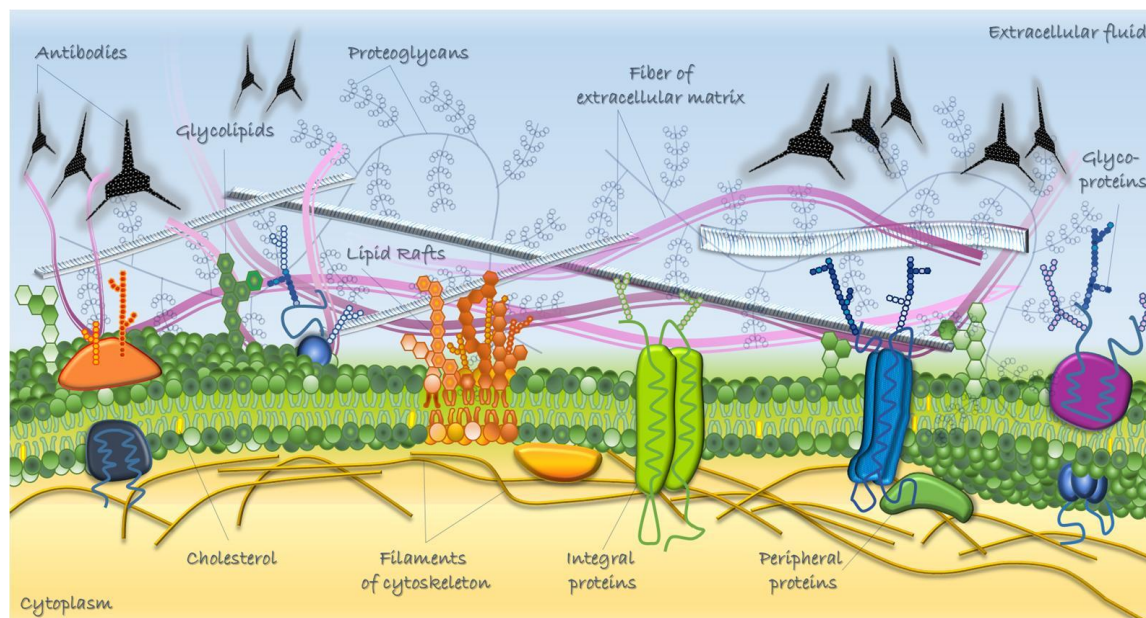


**Figure 17: Schematic representation of a LR in the cell membrane.** Enrichment in gangliosides, structurally and functionally correlated to cholesterol, proteoglycans, others glycolipids, transmembrane proteins (glycosylated and non-) and GPI-anchored proteins is shown.

The co-localization of gangliosides and cholesterol is important in maintaining the plasma membrane adequate structural equilibrium and physical characteristics such as the fluidity, the rigidity or the fusion temperature (Lingwood, 2000; Shengrund, 2015). Plasma membrane areas particularly enriched in gangliosides increase in rigidity (Bertoli *et al.* 1981).

Moreover, because the lipid tail region is critically smaller than polar moieties, in aqueous solution gangliosides, as well as for all the sphingolipids, aggregate in high molecular weight micelles, presenting a hydrophobic ceramide core and isolated from polar environment by the enclosing sugar chains as shown in figure 18 (Maggio *et al.* 1981; Sonnino *et al.* 1994; Sonnino & Prinetti, 2010).

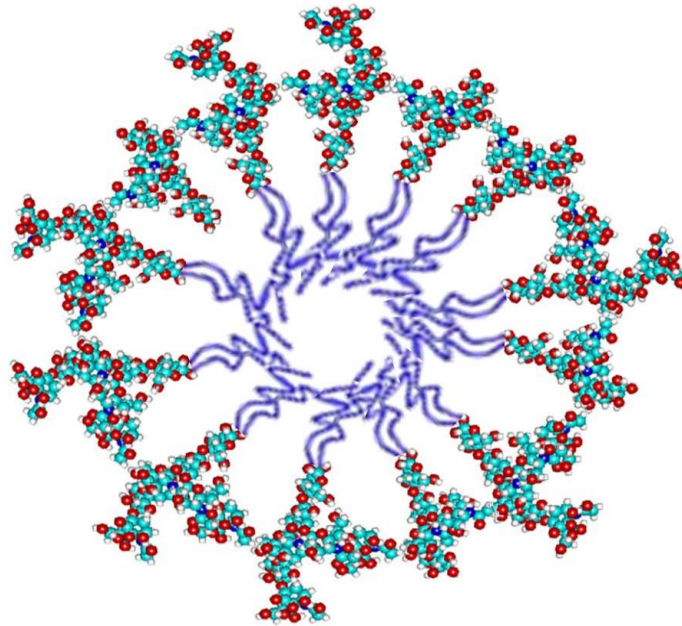


**Figure 18: Ganglioside micella.** The elevated volumetric ratio between hydrophilic head and hydrophobic tail of gangliosides originate high molecular weight micelles in aqueous solutions over a critical concentration.

In cell plasma membrane, the reported aggregative behavior produces physic modification of plasma membrane in particularly ganglioside-enriched clusters, introducing an increase in the layer curvature radius. In relation to the implication of gangliosides in plasma membrane invagination, an increase in endocytosis phenomena has been reported in correspondence to the leaf curvatures (Thompson & Tillack, 1985; Tettamenti *et al.* 1985; Fra *et al.* 1995; Ewers *et al.* 2010; Sonnino & Prinetti, 2010).

In addition to ceramide, the oligosaccharide portions confer to gangliosides as much structural properties finely correlated to biological functions. The monosaccharide units of a ganglioside establish cooperative contacts through hydrogen type binding that specifically offer an interactive potential to other molecules in extracellular environment (Sharom & Grant, 1978; Kiarash *et al.* 1994; Shengrund, 2015). Thanks to the oligosaccharide head, gangliosides can act as specific receptors for many molecular species such as viruses, bacteria, toxins (Yamakawa & Nagai, 1978; Borges *et al.* 2010; Ladisch & Liu, 2014), growth factors, peptides and hormones (Vengris *et al.* 1976; Shengrund, 2015; Russo *et al.* 2016).

Oligosaccharide chains of gangliosides, together with glycoproteins and proteoglycans, contribute to sialylated sugar-coat construction of glycan-rich glycocalyx associated to the plasma membrane (Schnaar *et al.* 2014; Linnartz-Gerlach *et al.* 2014; Shengrund, 2015; Ledeen & Wu, 2015). This structure supports different functions such as cell differentiation, cell to cell interactions and certainly signal transduction. In fact, the glycocalyx carbohydrate moiety, surrounding the outer leaflet of the plasma membrane surface is responsible for the recognition of other cells and for the attachment to extracellular components (Barrat *et al.* 1978; Kolter, 2012; Zeng & Tarbell, 2014; Shengrund, 2015). Furthermore, connecting directly or with mediator to internal elements (figure I9), the glycocalyx can initiate the communication and the realization of a specific response (Linnartz & Neumann, 2013; Shengrund, 2015).

The biochemical composition of glycocalyx sugar portion shows a strictly correlation to the functional meaning, presenting as a consequence, a considerably high level of specificity depending on cytological types, but also on the cycle phase or development stage of cells (Schnaar *et al.* 2014; Linnartz & Neumann, 2013). This evidences the fundamental role of oligosaccharide chains in determination of cell activities (Shengrund, 2015; Ledeen & Wu, 2015).

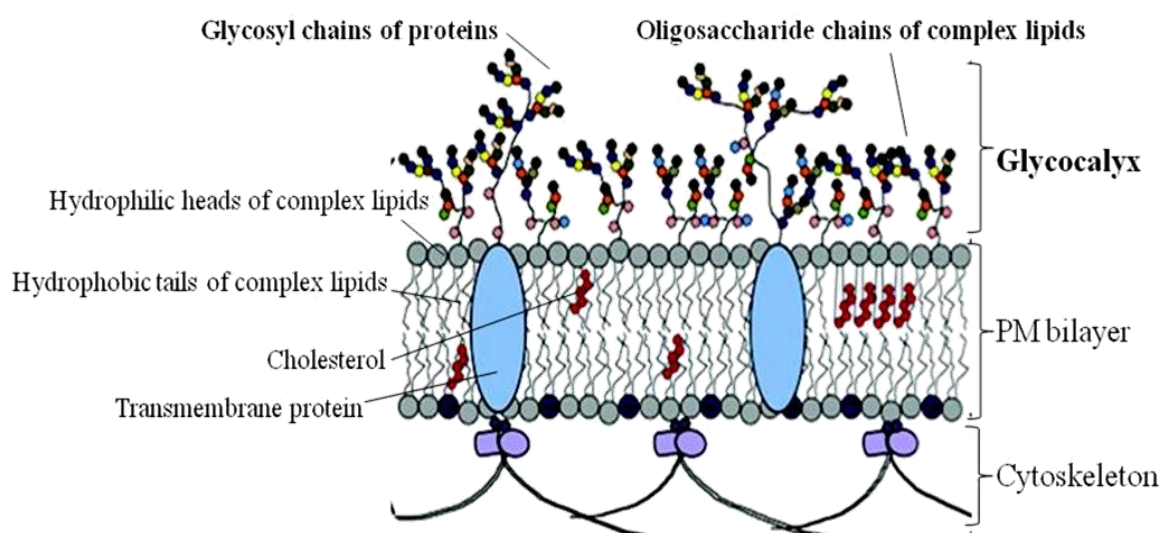


**Figure I9: Glycocalyx.** Oligosaccharide chains of gangliosides participate to the adequate composition of the cell glycocalyx that represents a crucial element for cell communication and response to external stimuli (Atukorale *et al.* 2015).



A well known phenomena that underscored the fundamental role of oligosaccharide chains in explicating cell ganglioside-dependent functions concerns their implication in cell differentiation and development (Schaal *et al.* 1985; Levine & Flynn, 1986; Yu *et al.* 1988; Shengrund, 1990; Kwak *et al.* 2006; Sonnino *et al.* 2010; Shengrund, 2015).

For what concerns the nervous system, where represent the main glycosphingolipids, the ganglioside content and pattern change during the neuron differentiation, aging and in neurodegenerative diseases. As shown in the figure I10, in undifferentiated neurons, GM3 and GD3 are the main gangliosides and they are characterized by a small hydrophilic head. Conversely, during the axons and synapses formation, GM3 and GD3 are displaced by the more complex gangliosides, such as GM1, GD1a, GT1b, and GQ1b (Shengrund, 1990; Shengrund, 2015). The modification of ganglioside composition reflects the differences in expression or in activities of specific glycosyltransferases (Yu *et al.* 1988; Shengrund, 1990; Sonnino *et al.* 2010; Aureli *et al.* 2011).

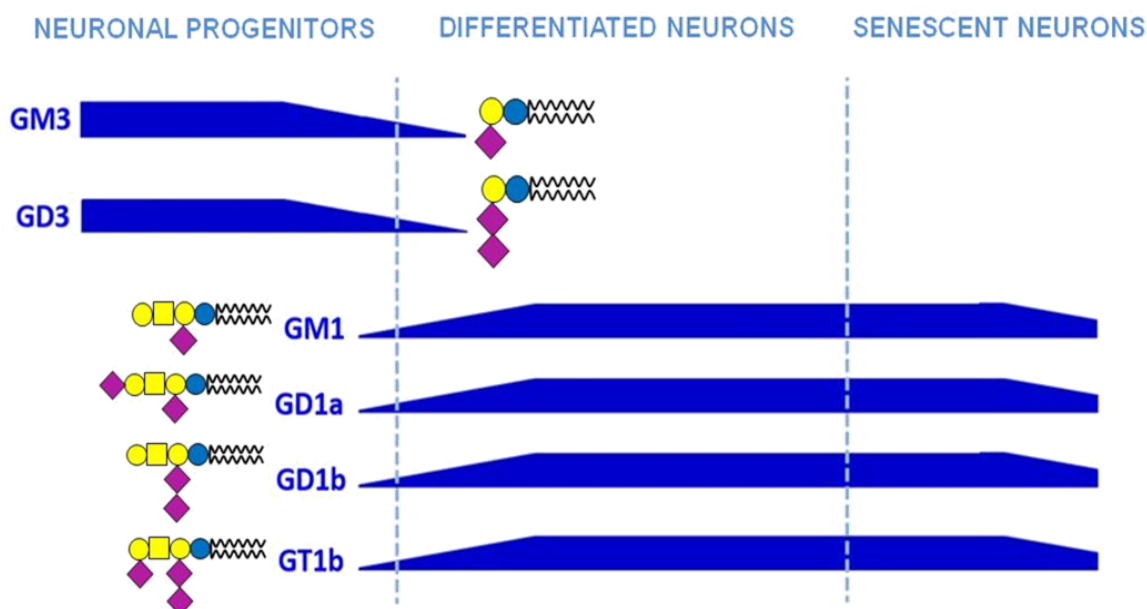


**Figure I10: Ganglioside changing in neurodifferentiation.** Modification in neuron ganglioside pattern during neurodifferentiation reflects the differences in glycosyltransferases and suggests an important role of oligosaccharide chains in the process.

The functional potential of oligosaccharide chains, peculiarly correlated to their specific composition, together with the described biophysical influence of the ceramide portion on plasma membrane regulation through the lateral partitioning, make the gangliosides exceptional players in recruiting membrane receptors and in promote initiation of signaling cascades (Tettamanti *et al.* 1985; Nagai, 1985; Ghidoni *et al.* 1989; Robert *et al.* 2011).

One of the results of the ceramide-enhanced ganglioside aggregation in plasma membrane specialized clusters is represented by the instauration of specific interaction between oligosaccharide chains and membrane receptors or glycoproteins, promoting the regulation of many pathways (Fueshko & Schengrund, 1992; Nagai, 1995; Aureli *et al.* 2011; Russo *et al.* 2016).

At this purpose, the changes in ganglioside oligosaccharide composition in specific sensing domains can act as an activator event of a co-localized tyrosine kinase receptor, as schematized in figure I11. One emblematic example concerns the activation of Epidermal Growth Factor (EGFR) receptor by modification of neighboring gangliosides (Russo *et al.* 2016).

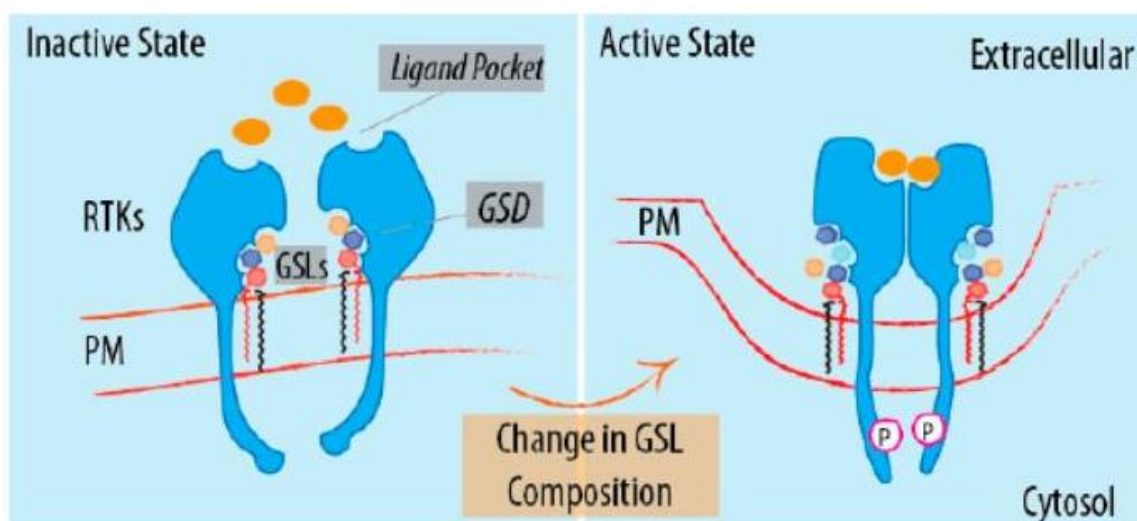


**Figure I11: Ganglioside changing in signaling regulation.** Modification in oligosaccharide chains of gangliosides, co-localized in sensing domains with tyrosine kinase receptors, can stimulates signaling activation promoting dimerization of receptor monomers and their autophosphorylation. PM, plasma membrane; GLSs, glycosphingolipids; GSD, glycosphingolipid sensing domain; RTKs, receptor tyrosine kinases (Russo *et al.* 2016).



This property can evolve also in regulation of membrane pores and channels, modulating molecule transit across the plasma membrane (Tettamanti *et al.* 1985; Ghidoni *et al.* 1989).

Moreover, another outcome imputable to the ganglioside specific features and organization, as well as for the others sphingolipids, is revealed by the sphingosine metabolites that can act themselves as a second messengers. In fact, an extracellular stimuli, such as the interleukin 1 or the interferon, receipted among a ganglioside clustering zone, can be translated in ceramide detachment, degradation or following modifications and metabolites can regulate intracellular enzymes (Svennerholm *et al.* 1994).

At this point, the requirement of ganglioside in signal transduction appears extremely important and actually implicated in cell functionality. As a consequence, pathologies and discordance from cell physiological state can arise from alteration in ganglioside metabolism. A concerning description is summarized and schematize in table I1 (Shengrund, 2015).

| GANGLIOSIDE or EFFECT of ENZYMATIC MODIFICATION | TARGET  | PATHWAY/ FUNCTION AFFECTED                               |
|---|---|--|
| GM3 synthase deficiency                         | Failure to synthesize GM3                                     | Severe CNS deficits in humans                            |
| GD3 and GM3                                     | Interact with gp120 on HIV-1                                  | Infection by HIV-1                                       |
| GD3 <sup>-/-</sup> + GM2/GD2 <sup>-/-</sup>     | Complement activation   | Inflammation /neural integrity                           |
| GM2 synthase deficiency                         | Failure to synthesize GM2                                     | Spastic paraplegia in humans                             |
| GM1   | ERK1/2 phosphorylation inhibited                              | Neuroprotective  |
|   | NE Na <sup>+</sup> /Ca <sup>2+</sup> exchanger                | Regulates Ca <sup>2+</sup> in nucleus                    |
|   | α5α1 Integrin initiating neurite outgrowth                    | Opens TRPC5 channels                                     |
|   | GDNF receptor complex   | Enhances Ret activity                                    |
|   | Lipid raft localization of caspr and glial neurofascin-155    | Maintenance of myelinated axons                          |
|   | Binding site for the prion protein                            | Prion protein-induced pathology                          |
| GM1 + laminin-1 → GM1 clusters                  | β-1 Integrin colocalizes to rafts containing Trk              | Activates Lyn, Akt, and MAPK enhancing neurite outgrowth |
| GD3   | Mitochondrial lipid rafts                                     | Release of apoptogenic factors                           |
|   | Paxillin tyr118 phosphorylation                               | Lyn is activated   |
|   | EGF receptor  | Maintains self-renewal ability of neural stem cells      |
| GT1b, GD1b                                      | Bradykinin B2 receptors                                       | Ca <sup>2+</sup> release from intracellular stores       |
| GD1a/GT1b-2b                                    | MAb Activates RhoA and ROCK                                   | Neurite growth arrest                                    |
| GT1α  | Functions in acetylcholine release                            | Learning and memory                                      |
| GT1b  | Akt dephosphorylation (inactivation)                          | Inhibits Akt, death of dopaminergic neurons              |
|   | Receptor for Clostridium tetani and botulinum toxins          | Tetanus and botulism                                     |
|   | Regulation of glutamate release                               | Neuronal glutamate signaling                             |
| GQ1b  | Regulates BDNF expression                                     | Neurotrophic factor-like actions                         |
| Polysialylated gangliosides                     | Plasma membrane Ca <sup>2+</sup> -ATPase                      | Enhances PMCA activity                                   |
| Plasma membrane associated Neu3                 | Catalyzes cleavage of sialic acid from gangliosides (not GM1) | Regulator of transmembrane signaling                     |
|   |   | Induces Akt phosphorylation                              |
|   |   | Needed for PNS axon regeneration                         |

**Table I1: Roles of gangliosides in signal transduction and cell functions** (modified form Shengrund, 2015).

## GM1 ganglioside

Ganglioside GM1 has continuously stirred up an exceptional outstanding attraction because its relevant implication and its key role in many signaling systems and cell regulatory pathways (Fang *et al.* 2000; Ledeen & Wu, 2015; Aureli *et al.* 2016). Abounding in the nervous system, GM1 appears involved in the essential mechanisms of neurodifferentiation and neurodevelopment on which its fame is continually depending such as the growing investigations about the dire pathological consequences of its alteration and lacking (Shengrund & Ringler, 1989; Shengrund & Mummert, 1998; Ledeen & Wu, 2015; Zhai *et al.* 2015).

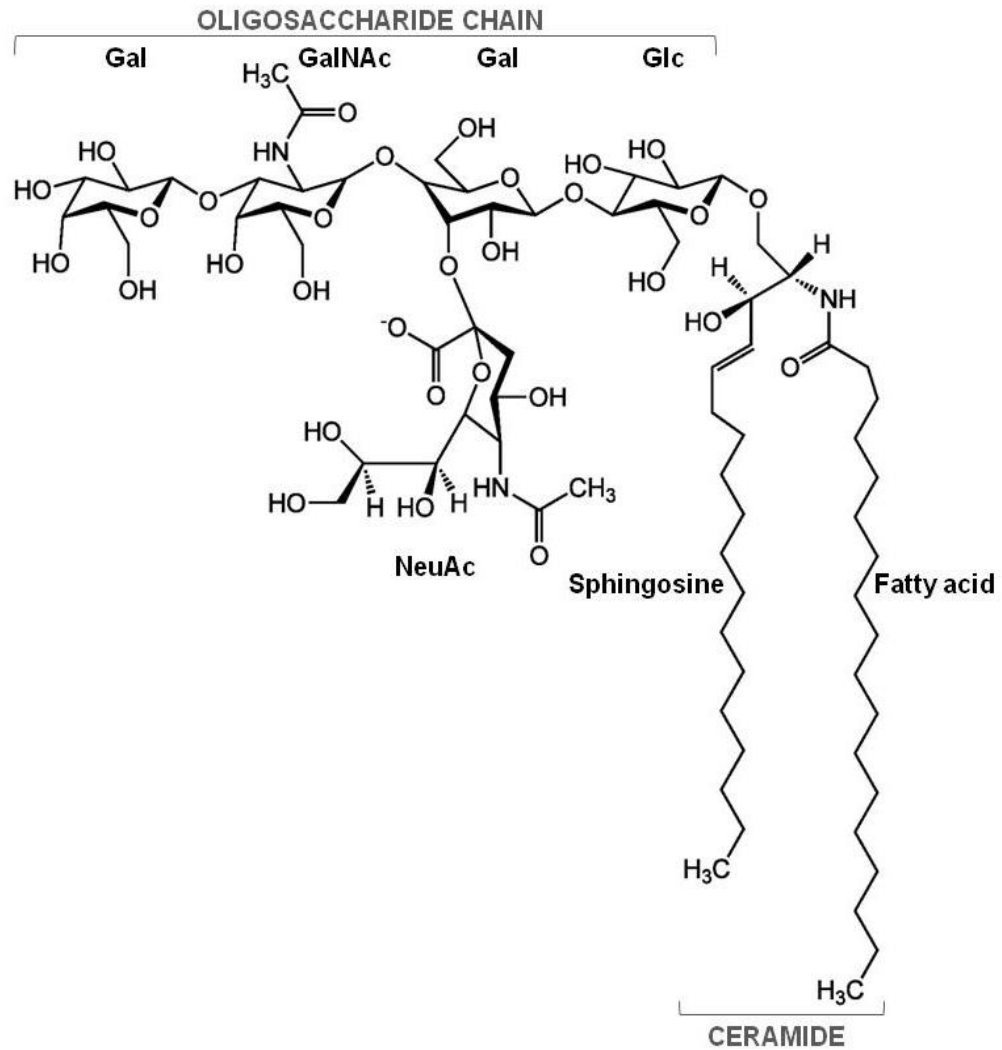
GM1 structure was depicted and elucidated for the first time by Kuhn and Wiegandt in 1963 in correspondence to its TLC separation (Kuhn & Wiegandt, 1963). According to classification and nomenclature (Svennerholm, 1980). GM1 is a monosialo- tetrahexoxylated glycosphingolipid and belongs to Ganglio series. Referring to IUPAC, GM1 formula is  $\beta$ -Gal-(1-3)- $\beta$ -GalNAc-(1-4)- $[\alpha$ -Neu5-(2-3)-] $\beta$ -Gal-(1-4)-Glc-(1-1)-Cer.

Conversely from the others major GM1-interacting gangliosides in the brain, GD1a, GD1b and GT1b, among which the typical sialic acid linkages are very susceptible to hydrolytic removal by endogenous sialidase, GM1 sialic acid is resistant to most forms of the mammalian enzyme (Sonnino *et al.* 2011, Mijagi & Yamaguchi, 2012).

GM1 derived from sequential addition of N-acetylgalactosamine and galactose units from UDP-activated forms to GM3 by specific glycosyltransferase (figure I5). The enzymatic complex for production of GM1 from GM3, occurring in the Golgi membranes, is called GM1 synthase (Robert *et al.* 2011; Kolter, 2012).

The GM1 chemical structure and the IUPAC symbolic representation are shown in figure I12.

a.



b.

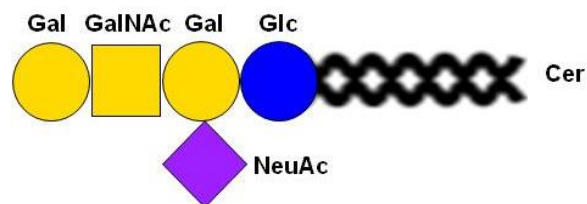


Figure I12: GM1.

a. Chemical structure of  $\beta$ -Gal-(1-3)- $\beta$ -GalNAc-(1-4)-[ $\alpha$ -Neu5-(2-3)]- $\beta$ -Gal-(1-4)-Glc-(1-1)-Cer.

b. IUPAC symbolic representation.

### **Chemical properties and cell topology**

GM1 shows a characteristic amphiphilic equilibrium, essential for the organization of membrane bilayer, given by the extended hydrophilic sugar domain combined with the hydrophobic moiety. The amphiphilic balance is easily perturbed by minimal modifications of ceramide or oligosaccharide chain (Sonnino *et al.* 2006; Sonnino *et al.* 2007; Aureli *et al.* 2016).

The presence of sialic acid confers to ganglioside GM1 a negative charge in biological environment, resulting however only the 16% of the expected value in aggregative status (Cantù *et al.* 1986). The particular aggregative behavior of GM1 is due once again both to the flexible and packable hydrophilic pentasaccharide chain, soluble in water and to the attached remarkably smaller hydrophobic ceramide moiety. In aqueous solutions these physicochemical properties determine the formation of micelles, according to the usual ganglioside penchant (Ulrich-Bott & Wiegandt, 1984; Cantù *et al.* 1986; Sonnino *et al.* 1994; Sonnino & Prinetti, 2010).

Among the GM1 micelles, the negative charge power of sialic acid residues is lowered by the polyelectrolyte effect and masked by the positive charges, explaining the cited phenomena (Sonnino *et al.* 1994; Aureli *et al.* 2016).

GM1 micelles present small ellipsoidal form caused by the original geometry of the monomer presenting a large hydrophilic head. For GM1, the critical micelles concentration (c.m.c.), determined by experimental approaches, ranging from  $10^{-8}$  to  $10^{-9}$  M and the free monomers never exceed the c.m.c. value, maintaining in equilibrium with aggregates at any GM1 concentration (Ulrich-Bott & Wiegandt, 1984; Cantù *et al.* 1986; Sonnino *et al.* 1994).

The aggregative properties of GM1 relevantly impact the interaction with cells and the modulation of cell membrane organization (Facci *et al.* 1984; Sonnino *et al.* 2006; Prinetti *et al.* 2007; Cantù *et al.* 2011; Khatun *et al.* 2014).

GM1 interaction with cell components and the effect on cell membranes has been studied *in vitro*, feeding cell cultures with the exogenous ganglioside.

Experimental evidences derived from GM1 administration to cultured neurons report that at the c.m.c. concentration, the GM1 monomers insert into the external layer of plasma membrane through lipid-lipid interactions, while the

micelles bind to the cell surface proteins and can be endocytosed reaching then lysosomes (Saqr *et al.* 1993). A prolonged treatment was proved to advance the insertion of GM1 monomers into the plasma membrane. On the other hand, the gradually augmenting in GM1 concentration, over the c.m.c. increase the aggregative process (Tomasi *et al.* 1980; Venerando *et al.* 1982; Facci *et al.* 1984).

A study performed on fibroblasts agrees with time and concentration dependence of exogenous GM1 behavior, underlining its modality of association to cells. In fact, increasing the GM1 concentration over the c.m.c. up to  $10^{-4}$  M, the weakly association of GM1 to plasma membrane, typical of the micelle forms, appears progressively more favorable. Alternatively, at the c.m.c. the monomeric GM1, stably associated to cells and introduced in the cell metabolism, prevails after 120 minutes treatment (Chigorno *et al.* 1985). These outcomes are reported and detailed in figure I13.

Moreover, if c.m.c. value is increased, meaning that an unusual higher GM1 molarities are required to initiate aggregation process, the half-life of micelles is reduced and the process is perturbed by the facilitated release of monomers (Cantù *et al.* 1991).

GM1 monomers are stabilized into the outer layer of plasma membrane establishing hydrogen bonds with surrounding glycerophospholipids and can interact with proteins and membrane receptors. According to the typical ganglioside properties, GM1 monomers integrated into plasma membrane tends to segregate in specialized domains characterized by peculiar interaction with others components and between themselves, that physically reflects its amphiphilic balance (Prioni *et al.* 2004; Sonnino *et al.* 2006; Sonnino *et al.* 2007; Aureli *et al.* 2016). In particular, at the aqueous/lipid interface the dynamic is reduced by a network of hydrogen bonds created by the amide group of the ceramide that acts both as a donor and as an acceptor of protons (Brocca *et al.* 1993). The oligosaccharide heads interact reciprocally by hydrogen bonds too, allowed by water molecules insinuated as linking bridges between two chains (Acquotti *et al.* 1990; Brocca *et al.* 1998; Brocca *et al.* 2000).

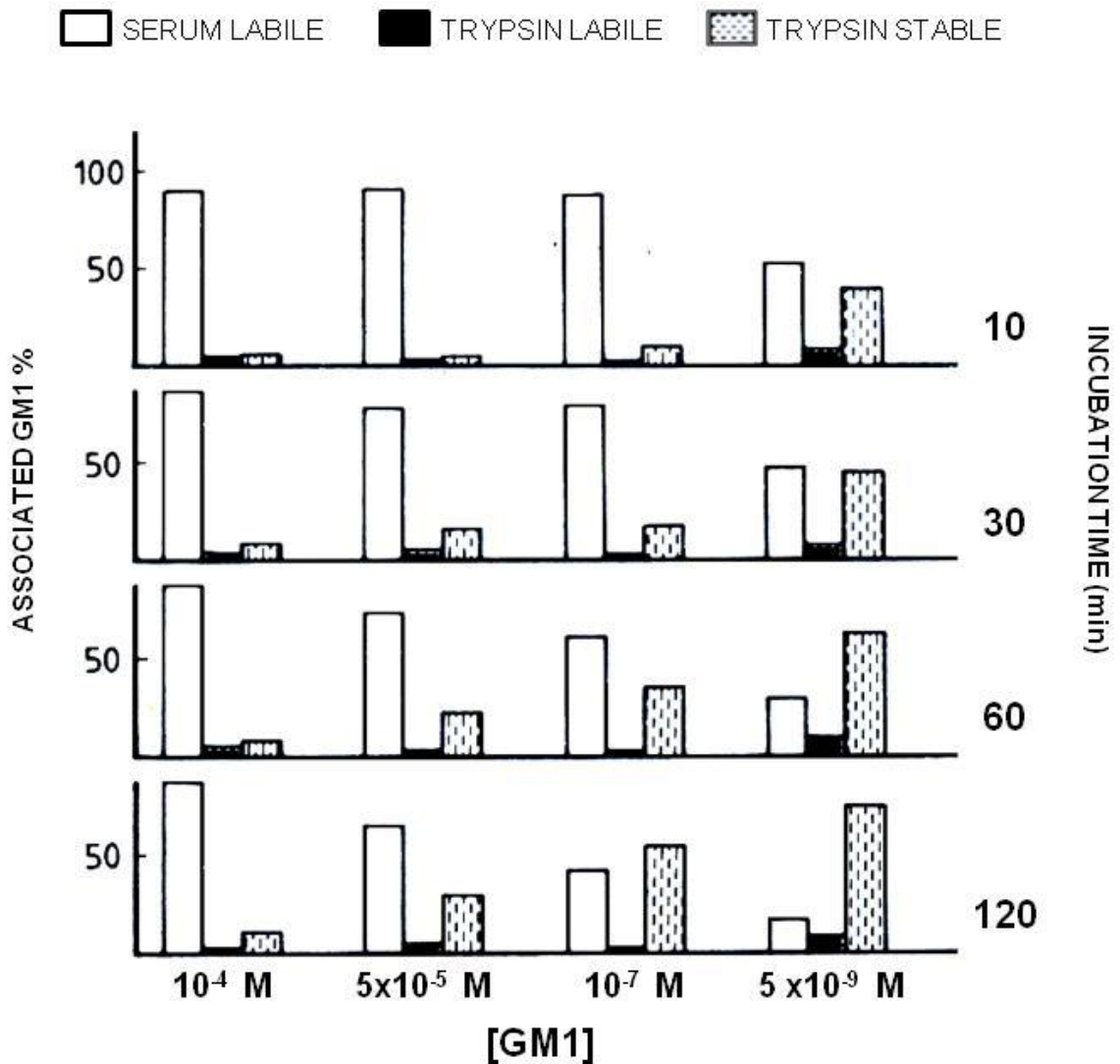


**Figure I13: Exogenous Ganglioside GM1 association to cultured fibroblasts.** GM1 interaction with cells is based on its aggregative properties depending on time and concentration. Over the c.m.c. ( $10^{-9}$  M), the promoted state is progressively represented by the micelles that weakly bind the external cell surface and are easily removed by exchange with serum component (SERUM LABILE). This tendency however decrease in time and at fixed c.m.c. after 120 minutes, most GM1 administrated stays in monomer forms. Monomeric GM1, integrated into the plasma membrane, participating to the cell metabolism, can be isolated after cell treatment with trypsin (TRYPSIN STABLE). A third dynamic, intermediate and vulnerable state corresponds to simple monomers or micelles of GM1 interacting with some proteins protruding from the external layer of the cell membrane (TRYPSIN LABILE).

As previously mentioned in relation to overall ganglioside properties, also GM1 chemical features, effectively decisive for its structural relations and arrangement, play a determinant role in peculiar tendency to the lateral segregation in the plasma membrane lipid rafts (Simons & Sampaio, 2011; Aureli *et al.* 2016).

Firstly, the above mentioned coexistence of opposite forces in the hydrogen bonds proton exchanging and in the ceramide influence on the hydrophobic packing, drive the physical phase separation of ganglioside from the fluidity of the glycerophospholipid bilayer (Sonnino & Prinetti, 2010; Sonnino & Prinetti, 2013).

Moreover, an extremely important factor to determine the GM1 segregation is represented by the bulkiness of the large surface area occupied by its oligosaccharide chain. This characteristic has an impact not only on the packing of the ganglioside, considering the volume ratio to the ceramide moiety (Acquotti *et al.* 1990; Sonnino & Prinetti, 2010), but also on the acquisition of a spontaneous positive curvature of the plasma membrane that affects the local lateral organization favoring the phase separation of GM1 enriched microdomains (Sonnino *et al.* 1994; Fra *et al.* 1995; Ewers *et al.* 2010; Patel *et al.* 2016).

GM1 in lipid rafts have been detected and localized thanks to its capacity to bind subunit B of cholera toxin (Holmgren *et al.* 1973). The receptor activity was proved to be imputable to GM1 oligosaccharide chain: the B pentameric subunit binds to the five monomers independently from both the A subunit and the ceramide with a low binding constant ranging from  $10^{-9}$  to  $10^{-12}$  M (Masserini *et al.* 1992; Kuziemko *et al.* 1996).

Alternatively, GM1 can be recognized also by using antibodies for which employing techniques and the improvement in their specificity have been implementing for many years (Wu & Ledeen, 1991; Watarai *et al.* 1994; Taylor *et al.* 1996; Kaji & Kimura, 1999; Iglesias-Bartolomé *et al.* 2009; Ledeen & Wu, 2015).

GM1 is one of the physiologically essential ganglioside in neuronal plasma membrane lipid rafts, concentrating at the presynaptic and postsynaptic membranes of nerve endings and segregating especially with sphingomyelin, phosphatidylinositols, glycosylphosphatidylinositols, cholesterol and others gangliosides (Simons & Sampaio, 2011; Sonnino *et al.* 2007).



From the analysis of lipid rafts in cerebellar granule cells, gangliosides have been found to represent only the 6-7% of the total lipid content, constituted over 50% by glycerophospholipids (Sonnino *et al.* 2007). The most representative gangliosides in these differentiated neurons are GD1a and GT1b and, regardless of the minor quantity, their co-localization with GM1 justifies from a functional point of view their physiological essentiality (Sonnino *et al.* 2011; Shengrund, 2015).

In fact, mice genetically deficient in gangliosides show a distortion in lipid microdomains, indicating their necessity in formation, stabilization and dynamicity of lipid rafts. The overexpression of gangliosides is correlated to an abnormal functioning of the process too (Sonnino *et al.* 2007; Pavlov *et al.* 2009; Furukawa *et al.* 2011; Ohmi *et al.* 2012).

Neurological disorders that further accompany this situation are explained by the alteration in physiological GM1 concomitance with proteins among the lipid rafts (Fang *et al.* 2000; Sonnino *et al.* 2007; Ledeen & Wu, 2015; Russo *et al.* 2016). As a matter of fact, different proteins crucial for neural functions have been identified to present glycolipid-binding domains, being interacting partners of GM1, or to belong to a related pathway. Just to make some examples:  $\beta$ -amyloid peptide (Fantini *et al.* 2013),  $\alpha$ -synuclein (Fantini *et al.* 2011),  $\text{Na}^+/\text{Ca}^{2+}$  exchanger, integrins (Ledeen & Wu, 2015; Xie *et al.* 2002), transient receptor potential channel 5 (Wu *et al.* 2007), opioid receptors (Shen & Crain, 1990; Wu *et al.* 1997) and Trk receptor (Mutoh *et al.* 2002; Nishio *et al.* 2004).

Moreover, an association of GM1 and GD1a to the plasma-membrane-bound sialidase has been reported too, suggesting a reserve-role of GD1a for GM1 and as a consequence, the existence of a tightly regulated cell content and requirement of GM1, supporting its functional relevance (Sonnino *et al.* 2010; Sonnino *et al.* 2011; Miyagi & Yamaguchi, 2012; Ledeen & Wu, 2015).

### **GM1 neurofunctions**

Thence, the impact of GM1 on plasma membrane microdomain assessment and specialization, leading to its involvement in the regulation of the cell signal transduction and in the modulation of several pathways, appears unavoidable element to consider and to clearly realize the GM1 biological potential (Fueshko & Shengrund, 1992; Nagai, 1995; Pavlov *et al.* 2009; Aureli *et al.* 2016; Ledeen & Wu, 2015).

Because of the GM1 relevant presence in the nervous system, most of the GM1 biological properties have been studied in neuronal models, following biological or pharmacological approaches by manipulating the endogenous GM1 or by treating cell cultures and animals with the exogenous one respectively (Ledeen & Wu, 2015). Nevertheless, because of the evaluation of the GM1 potential in extra nervous areas such as immune system, liver, kidney or lungs (Ozkök *et al.* 1999; Saito & Sugiyama, 2000; Ledeen & Wu, 2015), it has been recently defined a "factotum of nature" (Ledeen & Wu, 2015).

A lot of studies have been performed *in vitro* in order to identify GM1 targets in initiation of neurodifferentiation and neurotrophic effects. Even if the most experiences were conducted following a pharmacological approach, by administering exogenous GM1 to cells in culture or to animal models, some results offer a physiological meaningful (Ledeen & Wu, 2015). It happened because they appeared reproducible also manipulating endogenous GM1 enhancing sialidase (Wu *et al.* 1998; Monti *et al.* 2000) or GM1 synthase activities (Mutoh *et al.* 2002; Dong *et al.* 2002), ascertaining the insertion of GM1 into specialized domains of the cell membrane (Ledeen & Wu, 2015) or proving the natural increase in the GM1 content occurring during spontaneous neurodeveloping processes (Fang *et al.* 2000; Hasegawa *et al.* 2000).

According to above described physicochemical parameters and characteristics, the effects exerted by GM1 occurs when its content increases in plasma membrane lipid rafts (Hakomori *et al.* 1998; Dietrich *et al.* 2001; Mitsuda *et al.* 2002; Mutoh *et al.* 2002; Dong *et al.* 2002; Pavlov *et al.* 2009; Sonnino *et al.* 2010; Coskun & Simons 2011; Sonnino *et al.* 2011; Ledeen & Wu, 2015), as represented in figure I14.

Effectively, the membrane local GM1 enrichment can support biological functions in two main ways:

- i.* indirectly, by the GM1 content-dependent membrane reorganization, followed by membrane properties modifications that ensure physical parameters required for protein activities;
- ii.* by the GM1-proteins direct interactions allowing the modification in the protein conformation and the signal onset.

The simultaneously occurrence of both phenomena is also contemplated (Coskun & Simons 2011).

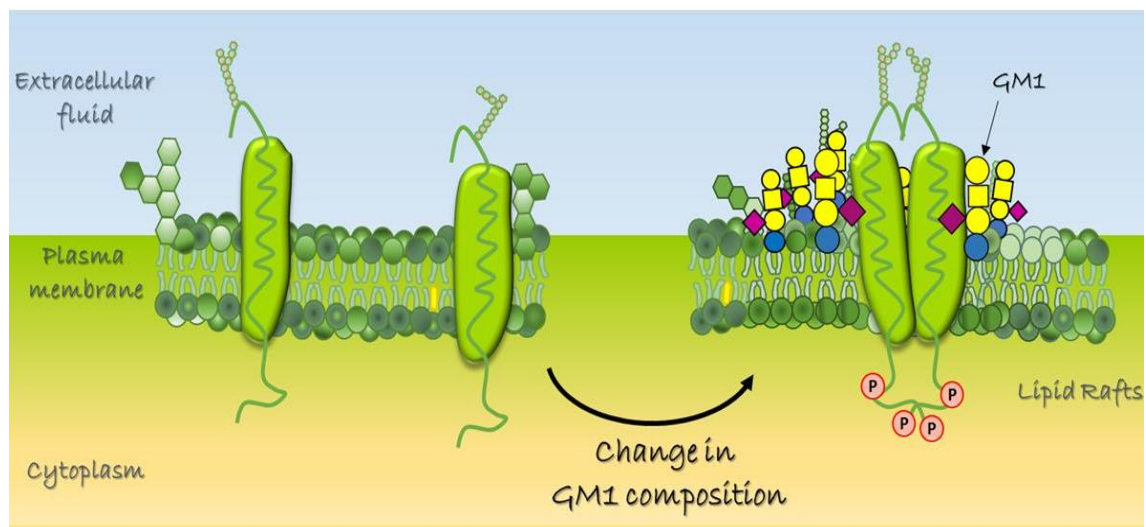


**Figure I14: GM1 content augmenting in lipid rafts is the basis for its functions.** GM1 concentration in lipid rafts causes modifications in protein activity *i.* indirectly, through a rearrangement of membrane parameters; *ii.* directly by interactions between GM1 and proteins.

Different authors describe the involvement of GM1 in the neuronal development and in the maturation of mammalian brain (Ledeen *et al.* 1998; Ledeen & Wu, 2009; Schnaar *et al.* 2014; Aureli *et al.* 2016; Schengrund, 2015). As mentioned above, GM1 appears with other complex gangliosides during neuronal differentiation- and specialization-correlated processes, reflecting its participation in neurite sprouting, elongation and in synaptogenesis (Arita *et al.* 1984; Facci *et al.* 1984; Ledeen, 1984; Ledeen & Wu, 2015).

Among the biological roles of GM1, its contribution to the regulation of the intracellular neuronal calcium homeostasis has emerged from many studies. GM1 has been proved to induced  $\text{Ca}^{2+}$  influx in different neuroblastoma cell lines (Wu & Ledeen, 1991; Wu *et al.* 1998; Fang *et al.* 2000; Hasegawa *et al.* 2000; Monti *et al.*

2000) and in primary cultures of hippocampal neurons (Abad-Rodriguez *et al.* 2001), interacting directly with T type channels (Wu & Ledeen, 1991; Fang *et al.* 2000). The effect is evidenced both by enhancing of sialidase activity (Wu & Ledeen, 1991) and by administering the exogenous ganglioside (Wu *et al.* 1998).

Alternatively, Ca<sup>2+</sup> influx has been recorded as a consequence of GM1 crosslinking with B subunit of cholera toxin that allows the co-crosslinking of GM1-associated proteins such as the integrins (Fang *et al.* 2000; Milani *et al.* 1992). The following autophosphorylation of associated kinases induce the signaling that trigger the activation of TRPC5 channels (Montell, 2004; Wu *et al.* 2007).

In both reported examples, the downstream result of the GM1-promoted Ca<sup>2+</sup> influx is represented by the genesis and the outgrowth of neurite processes (Wu & Ledeen, 1991; Fang *et al.* 2000; Hasegawa *et al.* 2000; Abad-Rodriguez *et al.* 2001; Wu *et al.* 2007).

Another related effect concerns the regeneration of damaged peripheral nerve appearing concomitant to the Ca<sup>2+</sup> influx and to the enhancement in sialidase activity (Kappagantula *et al.* 2014).

GM1 has been further proved to modulate the Ca<sup>2+</sup> efflux by Na<sup>+</sup>/Ca<sup>2+</sup> exchanger interaction, also in nucleus membrane (Xie *et al.* 2002), and by Ca<sup>2+</sup>-ATPase association in sarco/endoplasmic reticulum (Leon *et al.* 1981; Nowycky *et al.* 2014).

An overall scheme of GM1 contribution in Ca<sup>2+</sup> cell flux regulation is reported in figure I15 (Ledeen & Wu, 2015).

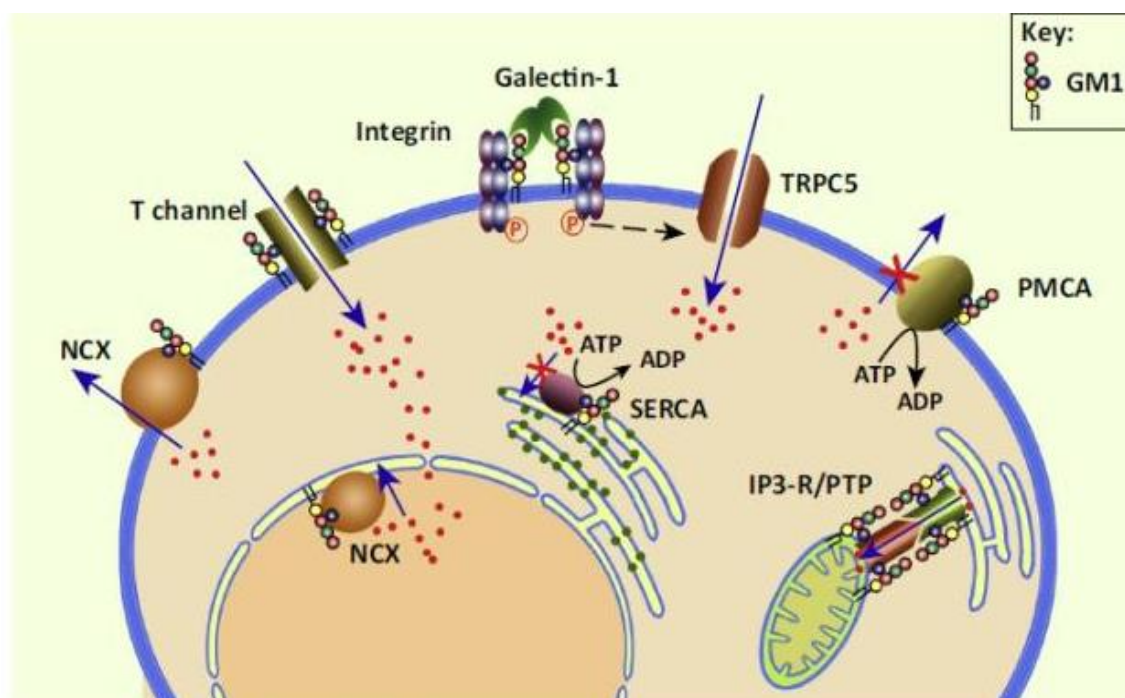


**Figure I15: Influence of GM1 on the regulation of calcium flux.** GM1 can interact directly or indirectly with different proteins responsible to mediate influx or efflux of Ca<sup>2+</sup> across cell membranes. NCX, Na<sup>+</sup>/Ca<sup>2+</sup> exchanger; TRPC5, transient receptor potential channel 5; PMCA, plasma membrane Ca<sup>2+</sup>-ATPase pump; SERCA, sarco/endoplasmic Ca<sup>2+</sup>-ATPase pump; PTP, IP3-R, inositol-3-phosphate receptor; PTP, permeability transition pore (Ledeen & Wu, 2015).

In addition to the regulation of calcium flux, to explain GM1-promoted neuritogenic effects (Abad-Rodriguez *et al.* 2001; Wu *et al.* 2007), another elucidated pathway claimed for its involvement in GM1-mediated neurodifferentiation is the TrkA receptor/MAP Kinases one (Ferrari *et al.* 1995; Mutoh *et al.* 1995; Farooqui *et al.* 1997; Bachis *et al.* 2002; Duchemin *et al.* 2002; Rabin *et al.* 2002).

GM1 has been reported to promote neurite outgrowth in rat pheochromocytoma PC12 cells and in dorsal root ganglion binding directly laminin-1 and promoting the constitution of a focal microdomain in the membrane. In this way, laminin-1 induces large clustering of GM1 in lipid rafts that causes translocation and enrichment in  $\beta$ 1 integrin. This aggregation allows the co-localization and autophosphorylation of TrkA enhancing signal transduction by activation of Lyn, Akt and MAPK promoting neurite outgrowth (Ichikawa *et al.* 2009).

An overall representation of TrkA-mediated pathways and of the downstream signaling are represented in figure I16. GM1 is supposed to colocalized with TrkA receptor and to influence its activation (Ferrari *et al.* 1995; Mutoh *et al.* 1995; Farooqui *et al.* 1997; Bachis *et al.* 2002; Duchemin *et al.* 2002; Rabin *et al.* 2002).

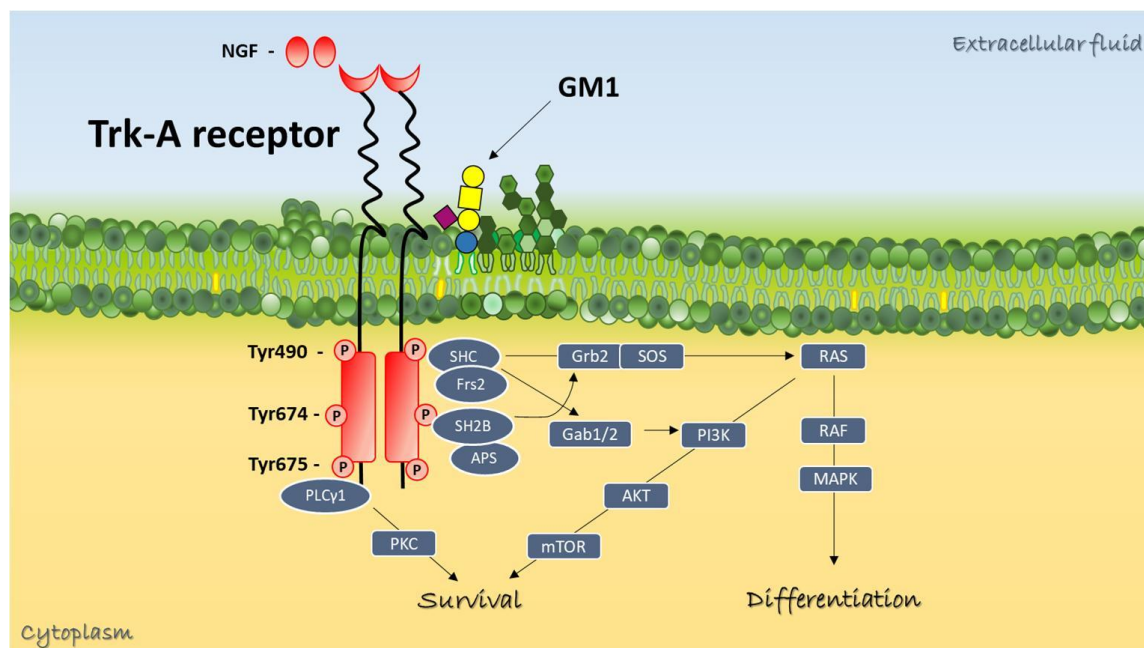


**Figure I16: Overview of TrkA-mediated pathways promoted by interaction with GM1.** NGF, Nerve Growth Factor; PLC $\gamma$ 1, Phospholipase C gamma 1; PKC, Phosphokinase C; SHC, Src homology 2 domain Containing protein; Grb2, Growth factor Receptor Binding protein 2; SOS, Son of Sevenless; RAS, RAF, Reticular Ascendant System proteins; MAPK, Mitogen Activated Protein Kinase; Frs2, Fibroblast Growth Factor Receptor Substrate 2; SH2B, Signal Transduction Adapter protein 2b; Gab1/2, GRB associated binding proteins; PI3K, Phospho-inositide 3 Kinase, AKT, alpha serine/threonine-protein Kinase; mTOR, mammalian Target of Rapamycin.

Another study reveals a direct and tight association of GM1 with TrkA, that strongly enhances the neurite outgrowth and the neurofilament expression in rat PC12 cells. Elicitation of cells by a low dose of NGF alone was insufficient to induce neuronal differentiation. The potentiating of NGF activity has been observed in the presence of GM1 in the culture medium increasing autophosphorylation of TrkA as compared with NGF alone. A GM1 direct enhancement of NGF-activated autophosphorylation of *in vitro* immunoprecipitated TrkA was also found. Monosialoganglioside GM1, but not polysialogangliosides, was tightly associated with immunoprecipitated TrkA. Furthermore, a tight association of GM1 and TrkA was not observed with other growth factor receptors, such as low-affinity NGF receptor, p75<sup>NGR</sup> and epidermal growth factor receptor, EGFR, (Mutoh *et al.* 1995). A similar study agrees with this evidence, reporting an increase in the TrkA mediated neuritogenesis and NGF-stimulated apoptosis prevention in GM1-treated PC12 cells in a dose and time dependent manner (Farooqui *et al.* 1997).

Another example is reported to prove GM1 induction of Trk and Erk phosphorylation in brain slice of striatum, hippocampus and frontal cortex, underlining a higher level of specificity for TrkA with respect to TrkB and C and an elicited activation of Erk2 superior than of Erk1. The time and dose dependency was set also in this study (Duchemin *et al.* 2002).

A study revealed that GM1 deficient NG108 cells don't locate TrkA receptor in plasma membrane and doesn't show any autophosphorylation. The stable transfection of GM1 synthase into these cells restores the expression of TrkA in plasma membrane and its activation, suggesting that GM1 is required for normal maintaining and functionality of TrkA (Mutoh *et al.* 2002).

Focusing on neurotrophic and neuroprotective properties of GM1, Trk pathway seems to be once again implicated.

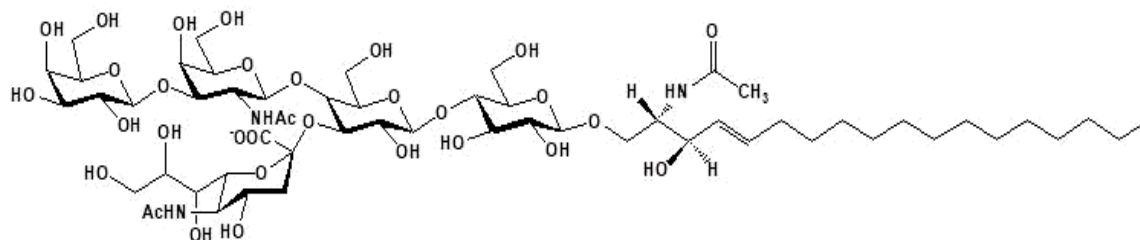
GM1 was found to rescue cells from apoptotic death using serum-deprived cultures of wild type and TrkA overexpressing PC12 cells. GM1-promoted survival was demonstrated to be mediated by both TrkA and TrkB, and potentially by tyrosine kinase receptors for additional neurotrophic growth factors. To support these findings, K-252a, an inhibitor of Trk kinases, was employed in PC12 cells overexpressing a dominant inhibitory form of Trk, revealing that a portion of the survival-promoting activity of GM1 is due to receptor dimerization and autophosphorylation (Ferrari *et al.* 1995).

Moreover, GM1 was proved to increase the survival of PC12 cells to hydrogen peroxide and others reactive oxygen species. The TrkA receptor implication and the downstream activation of Erk and Akt were considered target of GM1 because the ganglioside-promoted cell viability was abolished by TrkA inhibitor (Zakharova *et al.* 2014).

Concerning the neurotrophic role shown by GM1 after exogenous administration, the gathered pharmacological potential has open a window onto development of semisynthetic derivatives of GM1, the LIGA series (Kharlamov *et al.* 1993). Their remarkable difference from the parent compound reside in the incremented membrane permeability and, therefore, enhanced capability to penetrate the blood-brain barrier (BBB) and neuronal plasma membrane. These property is imputable to the replacement the long-chain fatty acid of

ceramide by shorter groups, such as acetyl (LIGA4) or dichloroacetyl (LIGA20), as shown in figure I17.

a.



b.

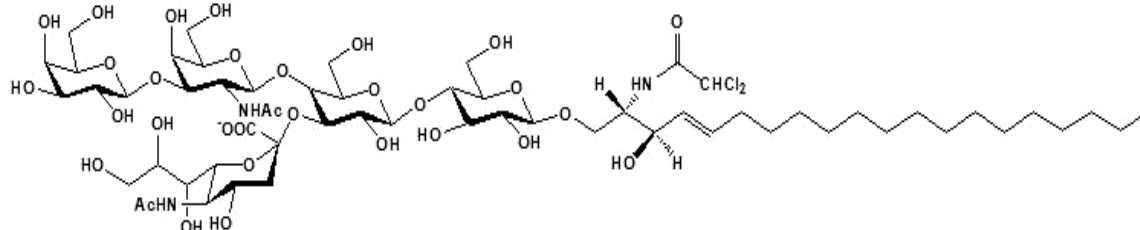


**Figure I17: Semisynthetic GM1 derivatives chemical structures.**

**a. LIGA 4**

**b. LIGA 20**

LIGA20 provided examples of others neuroprotection activities, including attenuation of ethanol-induced apoptosis in rat cerebellar granule neurons (Saito *et al.* 1999). LIGA20 exhibit *in vivo* a protective behavior against enhanced kainate-induced seizures (Wu *et al.* 2005). It also succeeded in ameliorating Parkinsonian symptoms in a rodent model of Parkinson disease (Schneider & Di Stefano, 1995)

LIGA20, as well as GM1 ganglioside, demonstrates different effects on neurotrophic processes, even though the only structural modification realized on fatty acid and the sphingosine moieties while the oligosaccharide chain stayed unchanged.



*Aim*

Among all features of GM1 biological potential, neurodifferentiation, neuroprotection and neurodevelopment are certainly the impacted processes predominantly studied and debated.

Many cell pathways have been considered and investigated in order to accurately clarify and completely dissect the biological role of endogenous GM1 in the nervous system.

Even if different GM1 targets have been successfully identified by several studies, the precise dynamic interaction between GM1 and candidate proteins such as the related molecular mechanisms at the bases of the observed effects still remain elusive.

Moreover, the findings obtained following the pharmacological approaches don't explain utterly the physiological reasoning, opening and implementing however the GM1 therapeutic employment as alternative research field.

The involvement of GM1 in neuronal differentiation has been demonstrated using different experimental approaches *in vitro*:

*i.* in murine neuroblastoma cell line, N2a, a micromolar GM1 administration have proved its capability to influence neurodifferentiation process by inducing neuritogenesis (Facci *et al.* 1984)

*ii.* in hippocampal neurons, the overexpression of sialidase Neu3 allowed the formation of GM1-enriched platforms inducing membrane structure modifications. The resulting membrane configuration induces the Trk dimerization and activation. This turn on a specific signaling cascade resulting in the actin depolymerization generating axon protrusion and elongation (Abad-Rodriguez *et al.* 2001; Da Silva *et al.* 2005).

*iii.* in murine neuroblastoma cell line, N2a, Neu3 silencing and the following decrease in enzymatic activity has been demonstrated to induce neurite sprouting too (Valaperta *et al.* 2007).

The evidence of the neurodifferentiation promotion obtained manipulating the endogenous GM1 by two opposed mechanisms, augmenting or silencing the plasma membrane-associated sialidase Neu3, suggests an important influence

of the oligosaccharide chain in the fine-tuning of the processes beginning at the level of plasma membranes, figure A1.

The value of glyco-mediated signaling has been further strongly described for gangliosides.

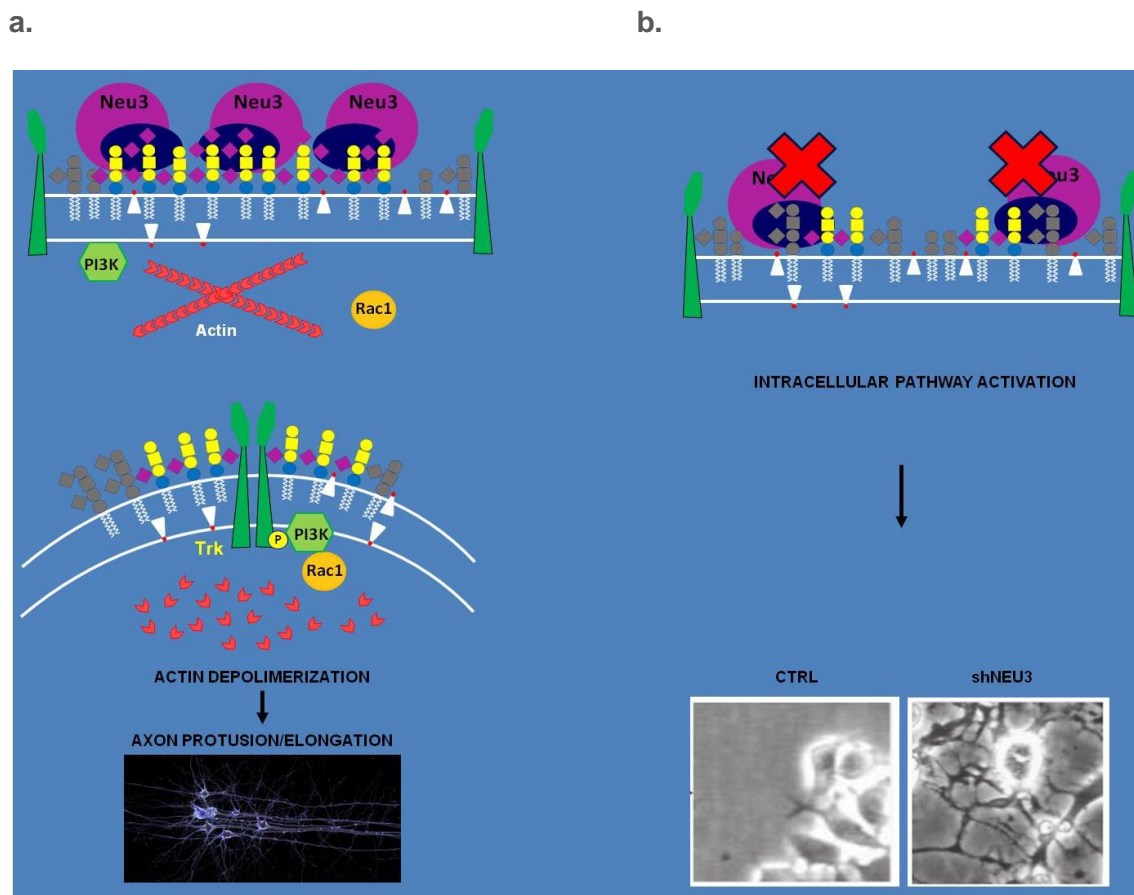


**Figure A1: Neurodifferentiative effect promoted by the modification of the Neu3 sialidase activity.**

**a. Increasing Neu3 activity.** In hippocampal neurons GM1 augmenting, due to the Neu3 activity enhancement, leads to the plasma membrane reorganization in GM1-enriched lipid rafts where dimerization and autophosphorylation of Trk receptor can occur. Trk pathway activation provokes the downstream actin depolymerization promoting axon protrusion.

**b. Silencing Neu3.** In mouse neuroblastoma cells, silencing Neu3 activity, resulting in about 50% GM1 reduction, causes neurite sprouting and elongation.

In addition, the studies carried on using LIGA 20 GM1 derivative revealed a responses both in differentiative and therapeutic employments. The only structural difference concerns the fatty acid portion, unchanging the oligosaccharide chain constitution and their feasible association with glycol-sensitive protein domains but affecting only the GM1 availability to biological membrane systems.

The conditions and premises above mentioned encourage to suppose that the crucial point for GM1 to exert its tasks depend on the “quality” of the oligosaccharide chain into the lipid rafts, which promotes selective interaction with plasma membrane specific proteins.

The aim of the proposed research is the clarification of the molecular mechanism and the recognizing of the protein targets by which GM1 accompany and enhance neurodifferentiation process in cells, hypothesizing the implication of its oligosaccharide chain.

On the bases of previous studies the attention is focused on TrkA signaling, employing the murine neuroblastoma cell line, Neuro2a (N2a) as an *in vitro* model. N2a have been in fact demonstrate to differentiate in neurons-like phenotype under treatment with GM1 and by increasing its endogenous content (Facci *et al.* 1984).

In the present study, the exogenous administration of OligoGM1 is really employed with the purpose to demonstrate the essential implication of the hydrophilic head in the natural GM1-promoted neuritogenesis, aspiring to confer to achieving results a physiological significance.

*Materials*  
&  
*Methods*

## Materials

The murine neuroblastoma cell line, Neuro2a (N2a, RRID: CVCL\_0470), Phosphate-buffered saline (PBS), Trizma Base (Tris), Ethylenediaminetetraacetic acid (EDTA), Sodium orthovanadate (Na<sub>3</sub>VO<sub>4</sub>), Bovine Serum Albumin (BSA), 1,4-Dithiothreitol (DTT), 3-(4,5,-dimethylthiazole-2yl)-2,5-diphenyltetrazolium bromide (MTT), Triethylamine (TEA), Sodium dodecil sulfate (SDS), Tween, Glycerol, Paraformaldehyde, Triton X-100, Methanol, 2-propanol, Formic acid, Blue bromophenol, Trypan blue, Donkey serum, powder milk, anti-rabbit FITC conjugate, and mouse  $\alpha$ -tubulin antibodies galactose, sialic acid were purchased from Sigma-Aldrich (St. Louis, MO, USA).

Corning<sup>®</sup> cell culture flasks, dishes, and Corning<sup>®</sup> Costar<sup>®</sup> cell culture plates, and Corning<sup>®</sup> Transfectagro<sup>™</sup> reduced serum medium were purchased from Corning (Corning, NY, USA).

Dulbecco's modified Eagle's high glucose medium (DMEM HG), fetal bovine serum (FBS), L-glutamine (L-Glut), Penicillin (10000 U/mL), Streptomycin (10 mg/mL), and acrylamide, were purchased from EuroClone (Paignton, UK).

Gibco<sup>™</sup> Opti-MEM<sup>™</sup> I reduced serum medium, Lipofectamine<sup>®</sup> 2000 reagent, ammonium persulfate (APS), goat anti-mouse IgG (H+L) antibody (RRID: AB\_228307) were from Thermo Fischer Scientific (Waltham, MA, USA).

TrkA inhibitor (CAS 388626-12-8) and high performance thin-layer chromatography (HPTLC) were from Merk Millipore Merk Millipore (Billerica, MA, USA).

The short interfering RNAs (siRNAs) were from Quiagen (Velno, Netherlands).

Rabbit anti-TrkA (RRID: AB\_10695253), rabbit antiphospho-TrkA (tyrosine 490, Tyr490) (RRID: AB\_10235585), rabbit anti-p44/42 MAPK (Erk1/2) (RRID: AB\_390779), rabbit antiphospho-p44/42 MAPK (pErk1/2) (Thr202/Tyr204) (RRID:AB\_2315112) and anti-rabbit IgG (RRID: AB\_2099233) antibodies were from Cell Signaling Technology (Danvers, MA, USA). Rabbit anti-pan Neurofilament (NF) antibody (RRID: AB\_10539699) was from Biomol International (Plymouth Meeting, PA, USA).

Protein assay kit and TEMED were from BioRad (Hercules, CA, USA).

Chemiluminescent kit for western blot was purchased from Cyanagen (Bologna, Italy). Ultima gold was purchased from Perkin Elmer (Waltham, MA, USA). Dako Fluorescent mounting medium was purchased from Agilent (Santa Clara, CA, USA). Polyvinylidene difluoride (PVDF) membrane was from GE Healthcare Life Sciences (Chigago, IL, USA).

Commercial chemicals were of the highest purity available, common solvents were distilled before use and water was doubly distilled in a glass apparatus.

## Methods

### Chemical synthesis and preparation of gangliosides and oligosaccharides

#### ***Gangliosides***

Fucosyl-GM1, GM1, GM2, and GM3 gangliosides were obtained from total ganglioside mixture extracted from pig brains (Tettamanti *et al.* 1973), by sialidase hydrolysis and chromatographic purification (Acquotti *et al.* 1994). To obtain desialylated GM1 (asialoGM1), GM1 underwent acid hydrolysis and chromatographic purification (Ghidoni *et al.* 1976).

Gangliosides were solved in methanol and stored at -20 °C.

#### ***Radiolabeled GM1***

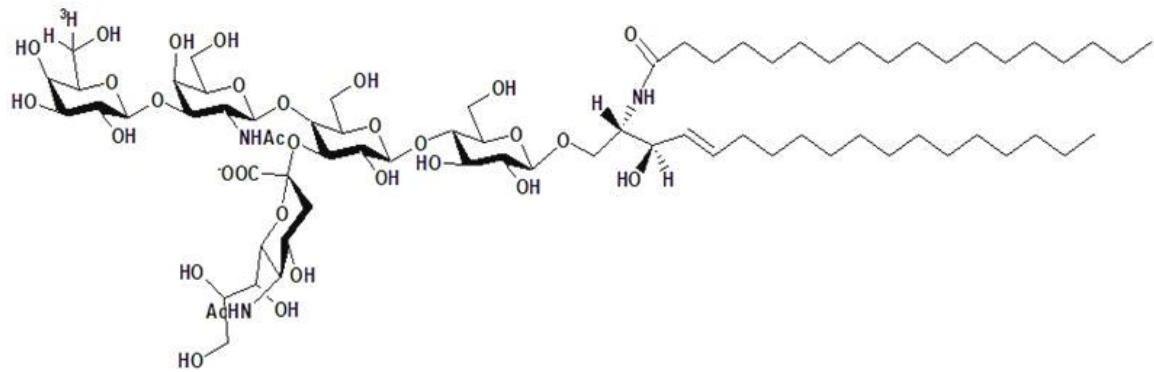
GM1 containing tritium at position 6 of external galactose ([Gal-6-<sup>3</sup>H]GM1, figure M1a) was obtained by an enzymatic oxidation reaction using galactose oxidase followed by reduction with sodium boro[<sup>3</sup>H]hydride (Sonnino *et al.* 1992).

On the other hand, GM1 containing tritium at 3-position of sphingosine ([Sph-3-<sup>3</sup>H]GM1, figure M1b) resulted from a chemical approach by oxidation of ganglioside at the 3-position sphingosine with 2,3-dichloro-5,6-dicyanobenzoquinone (DDQ), a reagent that is specific for allylic hydroxyl groups. Once again, the oxidation was followed by reduction with boro[<sup>3</sup>H]hydride (Ghidoni *et al.* 1981).

Radiolabeled GM1 were solved in methanol and stored at 4 °C.



a.



b.

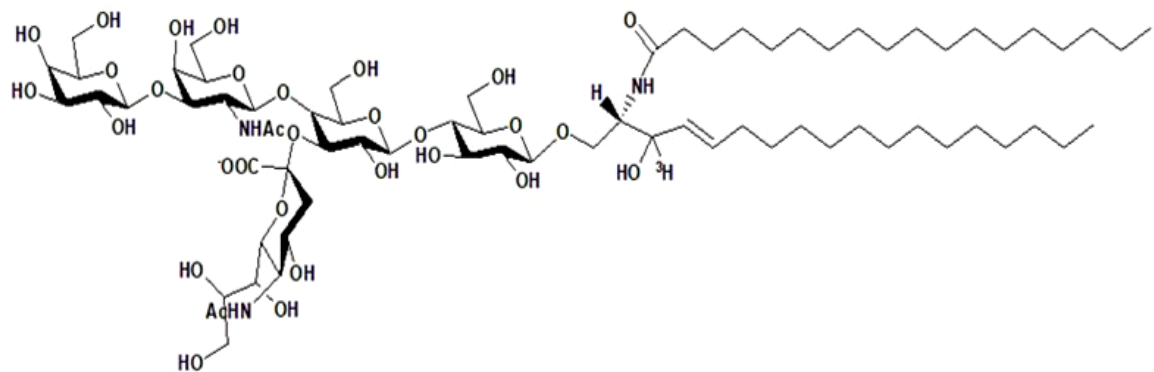


**Figure M1: Radiolabeled GM1 derivative structures:**

**a. [Gal-6- $^3\text{H}$ ]GM1.** An enzymatic oxidation was employed to obtain tritium labeling at the 6-position of the external galactose.

**b. [Sph-3- $^3\text{H}$ ]GM1.** tritium labeling at position 3 of the sphingosine is obtained by a chemical oxidation with DDQ.

***Ganglioside oligosaccharides***

The oligosaccharides Fuc-OligoGM1, OligoGM1, [Gal-6-<sup>3</sup>H]OligoGM1, asialoOligoGM1, OligoGM2, and OligoGM3 were prepared by ozonolysis followed by alkaline degradation with triethylamine (Wiegandt & Bucking, 1970) of Fuc-GM1, GM1, (<sup>3</sup>H)GM1, asialoGM1, GM2, and GM3 respectively.

Oligosaccharides were solved in methanol and stored at -20 °C. Radiolabeled derivatives are stored at 4 °C.

OligoGM1 chemical synthesis and MS analysis are shown in figure M2 and M3.

.

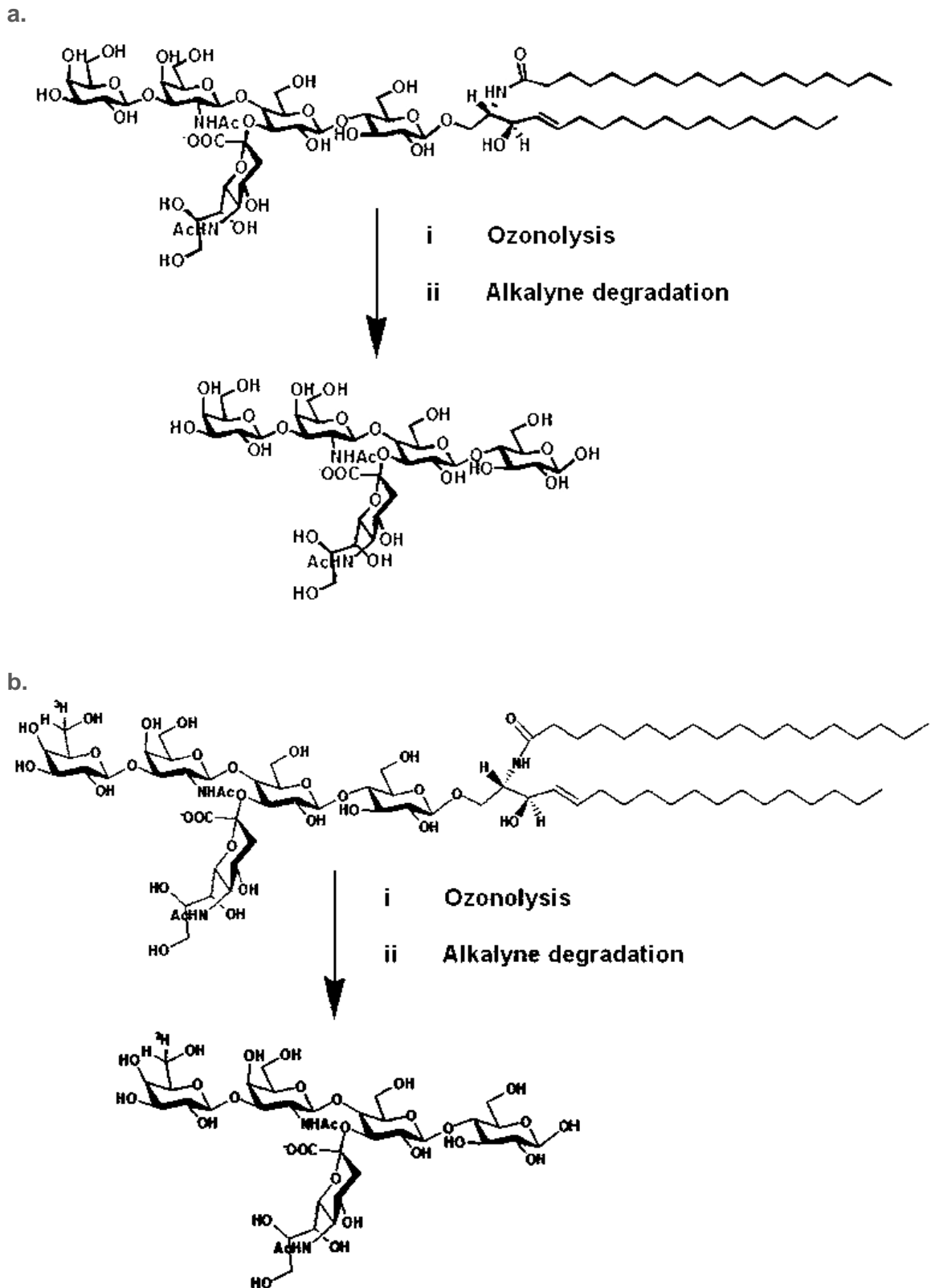


**Figure M2: Chemical synthesis of OligoGM1 (a) and [Gal-6-<sup>3</sup>H]OligoGM1 (b).** Ozone-alkali fragmentation procedure was used to obtain desphingosino-gangliosides. Ozonolysis organic reaction cleaved unsaturated bond between sphingosine 4 and 5 carbons. Subsequently, the alkaline degradation with triethylamine released the oligosaccharide chain from the residue.

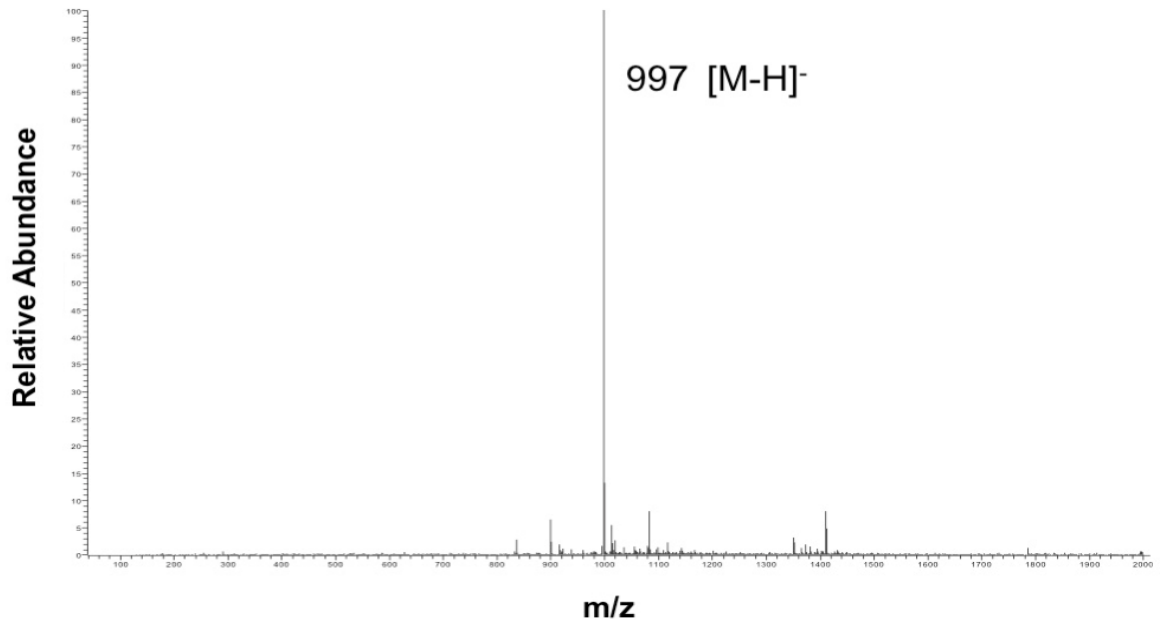


Figure M3: OligoGM1 MS analysis.

### **Photoactivable derivatives**

Photoactivable OligoGM1, [Gal-6-<sup>3</sup>H]OligoGM1(Glc-N<sub>3</sub>), bearing the photosensitive group on the glucose, as well as GM1 photoactivable on the fatty acid moiety, [Gal-6-<sup>3</sup>H]GM1(Cer-N<sub>3</sub>) were prepared from galactose-tritiated GM1, shown in figure M1a.

On the other side, GM1 tritiated on sphingosine (figure M1b), was the precursor for the GM1 with the photoactivable group on the last galactose residue, [Sph-3-<sup>3</sup>H]GM1(Gal-N<sub>3</sub>).

To prepare photoactivable OligoGM1 on glucose (figure M5), an amount of 52 μmol of radiolabeled OligoGM1 (obtained by ozonolysis and alkaline degradation of tritiated GM1) were dissolved in 33% ammonia and treated with 1 mg of ammonium hydrogen carbonate. The reaction was maintained under stirring for 48 hours at 40 °C. The solution was then immediately freeze-dried (Lubineau *et al.* 1995). The same approach was followed for the preparation of photosensitive GM1 on the external galactose (figure M4). In this case, however, tritiated GM1 was firstly submitted to enzymatic oxidation at position 6 of the last galactose by galactose oxidation.

To insert the photoactivable group on fatty acid residue, galactose-tritiated GM1 was submitted to alkaline hydrolysis to remove the stearic acid residue, followed by acid coupling with 12-aminododecanoic acid (figure M6). The reaction occurred adding 350 μmol of 12-aminododecanoic acid, dissolved in 2.5 mL of dry tetrahydrofuran to 1.5 mL of dimethylformamide containing 80 μmol of deAcyl-GM1, Triton X-100 (1 mL), and dry triethylamine (15 mL) under continuous magnetic stirring for 24 hours at 23 °C. The mixture was evaporated under vacuum to 1 mL, and 25 mL of ethyl acetate was added (Sonnino *et al.* 1989).

Finally, all amino-derivatives were properly treated to insert the chosen photoactivable group. In particular, the azide labeling procedure (figure M4-6) started with the dissolution of the crude amino-derivatives obtained by previous reactions in 0.5 mL of dry dimethylformamide. Subsequently, 1 mg of 2-nitro-4-fluorophenylazide and 1 μL of tributylamine were added under dark conditions

in 25  $\mu$ L of dry DMSO. Maintaining dark conditions for all the process, the reaction mixture was stirred over night at 80°C. After solvent evaporation, desired compounds were purified by flash chromatography using chloroform/methanol/2-propanol/water 60:35:5:5 v/v/v/v as eluent for OligoGM1 (Mauri *et al.* 2003) and chloroform/methanol/water 60:35:8 v/v/v for GM1 series (Sonnino *et al.* 1989).

All derivatives were dissolved in methanol and stored at 4 °C.

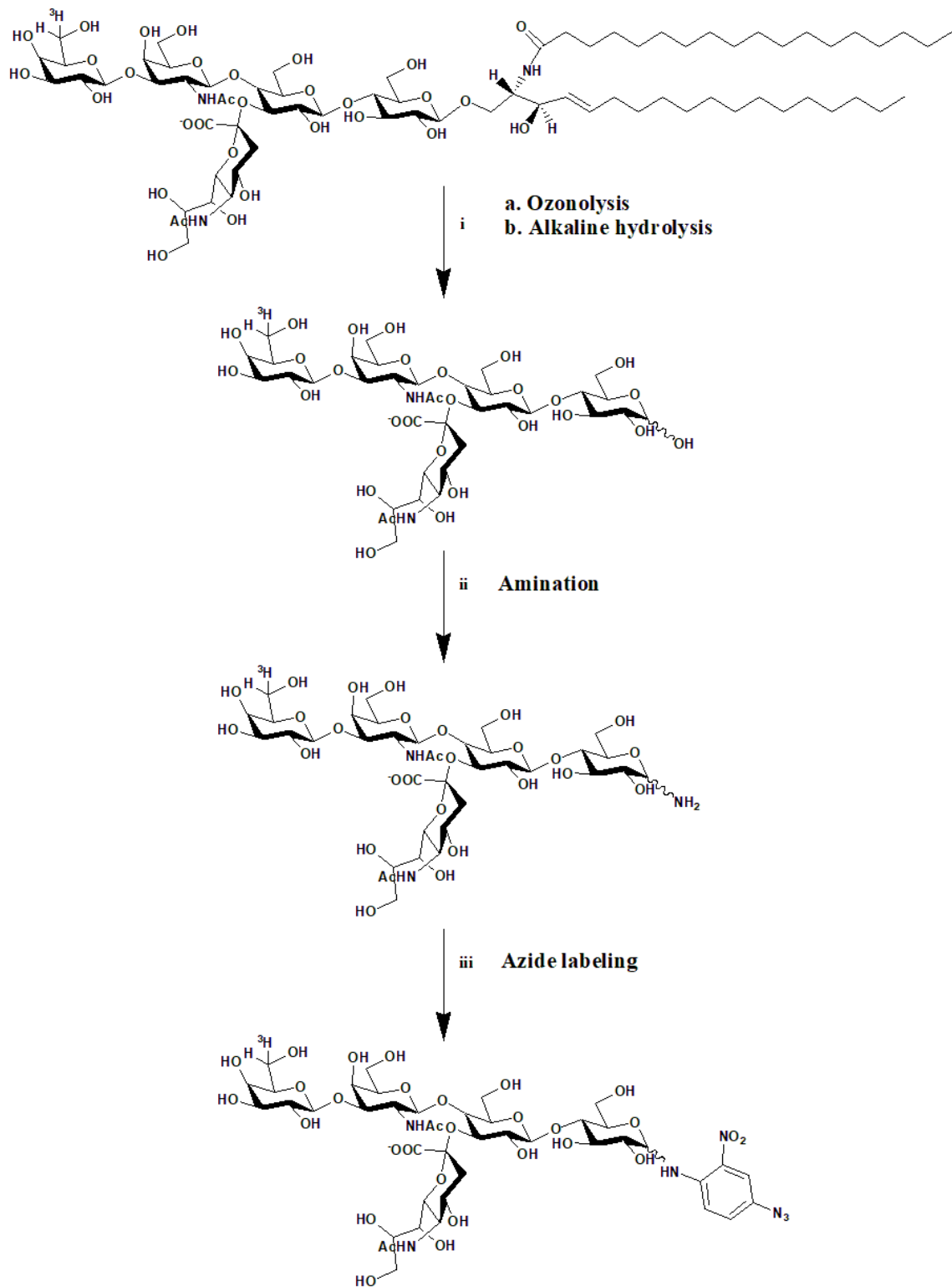


Figure M4: Synthesis of [Gal-6-<sup>3</sup>H]OligoGM1(Glc-N<sub>3</sub>).

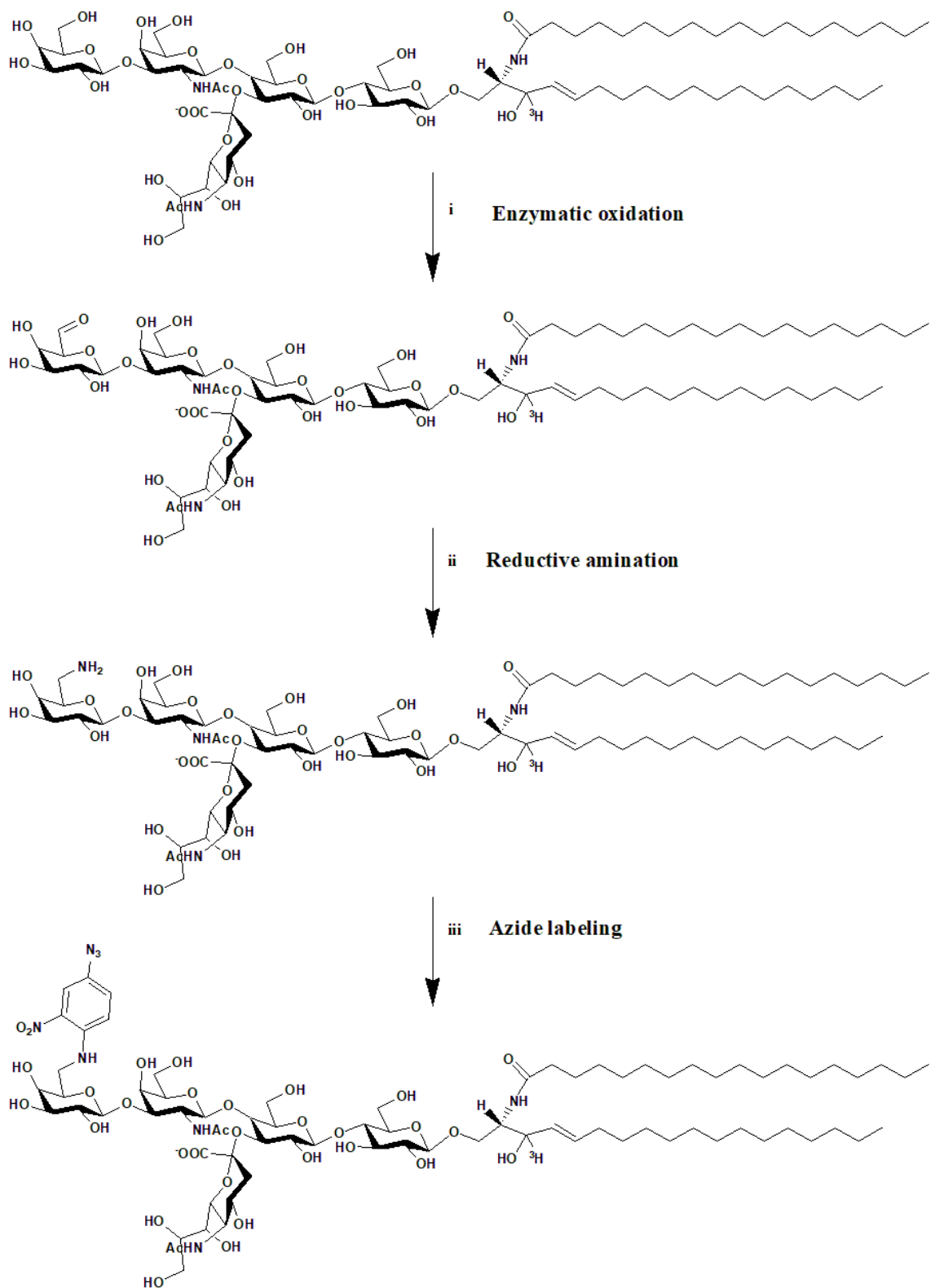
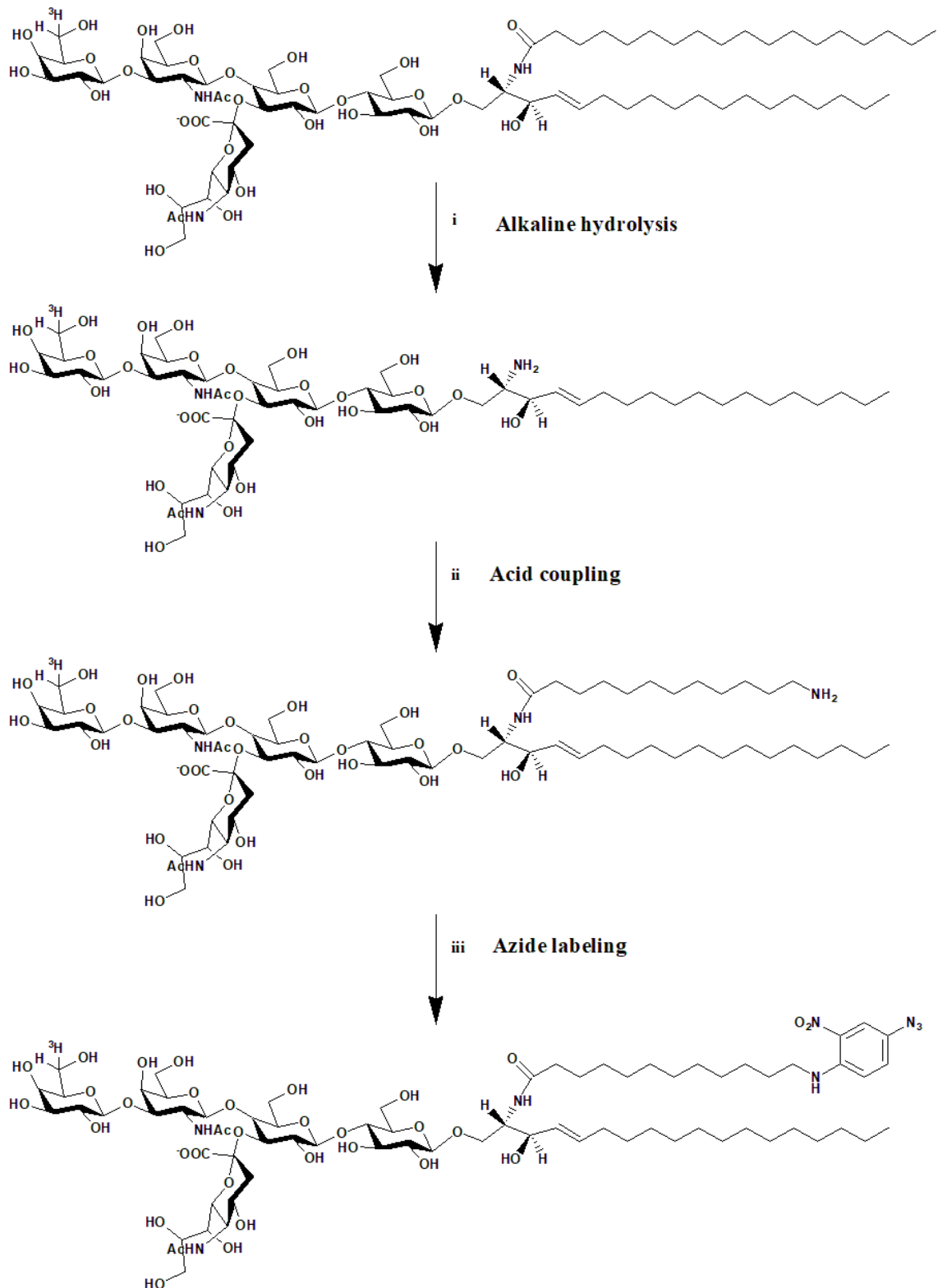


Figure M5: Synthesis of [Sph-3-<sup>3</sup>H]GM1(Gal-N<sub>3</sub>).



Figure M6: Synthesis of [Gal-6-<sup>3</sup>H]GM1(Cer-N<sub>3</sub>).

***NMR, MS, HPTLC, and autoradiographic analyses***

Altogether, NMR, MS, HPTLC, and autoradiographic analyses showed a homogeneity over 99% for all the prepared gangliosides and oligosaccharides.

NMR spectra were recorded with a Bruker AVANCE-500 spectrometer at a sample temperature of 298 K. NMR spectra were recorded in CDCl<sub>3</sub> or CD<sub>3</sub>OD and calibrate using the TMS signals internal reference.

Mass spectrometric analysis were performed in positive or negative ESI-MS. MS spectra were recorded on a Thermo Quest Finningan LCQTM DECA ion trap mass spectrometer, equipped with a Finnigan ESI interface.

All reactions were monitored by HPTLC on silica gel 60 plates.

## Cell cultures

Neuro2a (N2a) cells were cultured and propagated on 75 cm<sup>2</sup> flasks in high glucose Dulbecco's modified Eagle's medium (DMEM HG) supplemented with 10% fetal bovine serum (FBS), 1% L-glutamine and 1% penicillin/streptomycin (P/S, v/v), at 37 °C in a humidify atmosphere of 95% air / 5% CO<sub>2</sub>. Cells were sub-cultured to a fresh culture twice a week at reaching of 90% confluence (i.e. every 3-4 days). In sub-cultures passages cells were washed twice with PBS and detached by 0.02% EDTA - 0.6% glucose in PBS (w/v).

N2a cells were employed in experiments between the 5<sup>th</sup> and the 30<sup>th</sup> passages.

For all cell culture procedures sterilized condition were maintained by using sterile solutions and by working under the laminar flow cabinet.

## Cell treatments

For all experiments N2a cells were plated at  $5 \times 10^3$  / cm<sup>2</sup>, on 6-well plates if not specified, and incubated for 24 hours in complete DMEM HG medium to allow cells attachment. Cells were counted by Bürker chamber system (Denham *et al.* 1971).

Control cells were always plated and incubated under identical conditions but omitting any addition.

### ***Ganglioside, Oligosaccharide and sugar treatments.***

Growth medium was removed and cells were conditioned for at least 30 minutes at 37 °C in a humidify atmosphere of 95% air / 5% CO<sub>2</sub> in pre-warmed Transfectagro medium supplemented with 2% FBS, 1% L-glutamine, 1% P/S (v/v). Cell treatments were performed in 2% FBS medium to minimize interactions between serum and added components (Facci *et al.* 1984). Subsequently, cells were incubated at 37 °C up to 48 hours in the presence of 50 µM gangliosides, oligosaccharides, galactose, or sialic acid.

Gangliosides, oligosaccharides and sugars were solved in methanol. To perform cell treatment, they were dried by nitrogen gas, and dissolved in

Transfectagro complete medium by vortex agitation and by sonication in water bath 3 times each for 30 seconds.

### ***TrkA chemical inhibition***

In order to block TrkA activity in N2a cells, 120 nM TrkA inhibitor (Wood *et al.* 2004) was added to the conditioning Transfectagro medium 1 hours before the addition of GM1 or OligoGM1.

### ***siRNA mediated TrkA knockdown***

TrkA expression silencing was achieved by RNA interference experiments applying siRNA.

Three different siRNAs were employed to silence TrkA:

- i.* Mm\_Ntrk1\_1 (sense 50-CCAUCAUAAUAGCAAUUUAUTT-30, antisense 50-AUAAUUGCUAUUAUGGAT-30);
- ii.* Mm\_Ntrk1\_5 (sense 50-GGUGGCUGCUGGUAUGGUATT-30, antisense 50-UACCAUACCAGCAGCCACCTG-30 );
- iii.* Mm\_Ntrk1\_6 (sense 50-CCUUCUUGUGCUCAACAAATT-30, antisense 50-UUUGUUGAGCACAAGAAGGAG-30 ).

Non-silencing siRNA with no homology to any known mammalian gene was used (sense 50-UUCUUCGAACGUGUCACGUdTdT-30, antisense 50-ACGUGACACGUUCGGAGAAdTdT-30) and the cells transfected by scramble were considered the control condition for the experiment.

Transfection was performed 24 hours after cell plating in antibiotic and serum free OptiMEM culture media containing 0.25% Lipofectamine 2000 (v/v) and 50 nM siRNA, previously solved in sterilized, deionized and nuclease free water (16.7 nM of each siRNA). After 6 hours, the transfection medium was changed to complete DMEM HG culture medium. The day after the silencing, cells were treated with 50  $\mu$ M GM1 or OligoGM1 as described above.

### **Photolabeling experiments**

Cells were incubated with 50  $\mu$ M [Sph-3- $^3$ H]GM1(Gal-N<sub>3</sub>) (figure M4), [Gal-6- $^3$ H]OligoGM1(Glc-N<sub>3</sub>) (figure M5), and [Gal-6- $^3$ H]GM1(Cer-N<sub>3</sub>) (figure M6), for 3 hours at 37 °C in a humidify atmosphere of 95% air / 5% CO<sub>2</sub> in obscure room. After incubation, medium was removed and cells were illuminated for 40 minutes under UV light ( $\lambda$ = 360 nm) maintaining the plates on ice to induce photo-activation.

All the procedures before exposure to UV light were performed in dark room, under red safelight.

The cells were lysed by sample buffer containing 0.15 M DTT, 94 mM Tris-HCl, 15% glycerol (v/v), 3% SDS (w/v), 0.015% blue bromophenol (v/v), sonicated by probe (50 W, 30 kHz) and boiled for 5 minutes at 99 °C. Denatured proteins underwent to 4–20% SDS-polyacrylamide gel electrophoresis (SDS–PAGE) and blotted on PVDF membrane by trans-blot turbo system. Digital autoradiography of the PVDF membrane was performed with Beta-Imager 2000. PVDF membranes were then blocked, incubated with anti-TrkA antibody and processed as follow described in the paragraph “Protein analysis” (Sonnino *et al.* 1989; Sonnino *et al.* 1992; Chigorno *et al.* 1990; Loberto *et al.* 2003; Chiricozzi *et al.* 2015).

## **Assessment of cytotoxicity**

### ***Trypan blue assay***

Cell viability was determined by Trypan blue exclusion assay after 24 and 48 hour treatments with 50  $\mu$ M GM1 or OligoGM1. Cells were detached by 25 cm<sup>2</sup> flasks. The numbers of living and death cells were discriminated according to Trypan blue staining that selectively distinguished necrosis and apoptotic cells from living ones (Mehlen *et al.* 1988; Aureli *et al.* 2011).

### ***MTT assays***

Cell proliferation was monitored after 12, 24 and 48 hour treatment with 50  $\mu$ M GM1 or OligoGM1 according to MTT method firstly described by Mosmann in 1983.

Briefly, cells were seeded on 24-well plates for MTT test.

At the end of incubation period, treatment medium was replaced with 2.4 mM MTT (dissolved 4 mg/mL in PBS) diluted in Transfectagro complete medium. Plates were re-incubated for 4 hours at 37 °C. Subsequently, MTT containing medium was carefully removed and the cells were lysed with 2-propanol : formic acid, 95 : 5 (v/v) in order to solve resulting formazan crystals. Plates were gently agitated for 5 minutes to homogenate cell purple solution prior to read the absorbance at 570 nm with microplate spectrophotometer.

### **Morphological analysis and neurite outgrowth evaluation**

Cultured cells, treated with 50  $\mu$ M GM1, oligosaccharides or sugars up to 48 hours, were observed by phase contrast microscopy.

The neurite-like processes length was measured after treatment with GM1 or OligoGM1 on bidimensional images and expressed as the ratio between neurite length and cell body diameter (Schengrund & Prouty, 1988; Sato *et al.* 2002).

Five random fields were examined from each well, giving a total cell count of at least 200 cells per well.

### **Immunofluorescence analysis**

After 24 hour treatment with 50  $\mu$ M GM1 or OligoGM1, cells, attached to the glass inserts, were washed with cold PBS and fixed in 4% paraformaldehyde for 20 minutes at 23 °C. Cells were washed, got permeable by 0.1% Triton X-100 for 30 minutes and then treated for 1 hour at 23 °C with the blocking solution (5% donkey serum and 0.2% Triton X-100 in PBS, v/v). Cells were incubated with rabbit polyclonal antibody anti-Neurofilament (NF) for 2 hours at 23 °C. After three washing with PBS, cells were incubated 1 hour with secondary anti-rabbit antibody FITC-conjugated.

Fluorescence signal was detected by fluorescence microscope and the images were processed by ImageJ software.



### Study of interaction between OligoGM1 and N2a cells

The fate of OligoGM1 administered to cells was determined using tritium-labeled derivative shown in figure M2b.

After the cell loading with [Gal-6-<sup>3</sup>H]OligoGM1 for 0.5, 1, 6, and 24 hours the medium was removed and the following treatments were performed sequentially:

*i.* cells were washed 5 times/10 minutes each with 10% FBS-DMEM HG medium to remove the amount of [Gal-6-<sup>3</sup>H]OligoGM1 weakly associated to the cell was collected removable from the cell plasma membrane by the affinity to the serum components. The resulting solution was called "serum labile fraction (SL)";

*ii.* cells were treated with 0.1% trypsin-EDTA solution in PBS (v/v) for 1 minute to obtain the [Gal-6-<sup>3</sup>H]OligoGM1 covalently linked to extracellular domain of plasma membrane proteins. Trypsin removable-derived solution fraction was called "trypsin labile fraction" (TL);

*iii.* cells were lysed by trypsin-EDTA solution (0.05%-0.02%, w/v in PBS) in order to evaluate the quantity of [Gal-6-<sup>3</sup>H]OligoGM1 internalized by the cells. This fraction underwent to probe sonication (50 W, 30 kHz) and the relative homogenate is called "trypsin labile fraction" (TS).

Radioactivity associated with collected solutions was determined by liquid scintillation counting.

The procedure was previously established to determine at the cell culture level the fate of exogenously administered gangliosides (Chigorno *et al.* 1985).

## **Protein analysis**

At the end of treatments, cells were washed with cold PBS containing 0.5% of 2 mM Na<sub>3</sub>VO<sub>4</sub> (v/v), lysed by hot lysis Buffer (0.15 M DTT, 94 mM Tris-HCl, 15% glycerol, v/v, 3% SDS w/v, 0.015% blue bromophenol, v/v) and detached using scrapers. DC protein assay was performed in order to quantify sample proteins. After the probe sonication (50 W, 30 kHz) and the boiling of the lysed samples for 5 minutes at 99 °C, equal amounts of denatured proteins derived from treated and untreated cells were separated on 7.5% polyacrylamide gels, and transferred to PVDF membranes.

Electrophoresis was performed at 23 °C, applying 100 V constant voltage in the stacking gel, augmenting at 170 V in the running. Blot transferring was performed at 4 °C, maintaining for 3 hours constant current at 200 mA. PVDF membranes were blocked with 5% milk (w/v) in TBS-0.1% tween (v/v) at 23 °C for 2 hours under gently shaking.

The presence of Neurofilament (NF), TrkA, p-TrkA, extracellular signal-regulated protein kinases 1 and 2 (ERK1/2) and p-ERK1/2 was determined by specific rabbit primary antibodies, diluted 1:1000 in 5% BSA (w/v) in TBS-0.1% tween.  $\alpha$ -tubulin, used as loading, was detected by the specific mouse primary antibody diluted 1:40000 in 5% milk (w/v) in TBS-0.1% tween (v/v). The incubation was performed over night at 4 °C under gently shaking.

PVDF membrane were washed three times with TBS-0.1% tween. The reaction with secondary horseradish peroxidase (HPR)-conjugated antibodies was following performed at 23 °C in agitation, after 1:2000 dilution of anti-rabbit antibody in 5% BSA (w/v) in TBS-0.1% tween and 1:30000 dilution of anti-mouse antibody in 5% milk (w/v) in 0.1% TBS-tween.

After three washes with TBS-0.1% tween, PVDF signal, originated from luminol chemiluminescence reaction, was acquired and analyzed by Uvitec. Quantitative estimation were performed using ImageJ software.

## Molecular modeling

Crystallographic structure of the extracellular segment of human TrkA in complex with nerve growth factor (NGF) (RCSB PDB ID: 2IFG) was used for molecular docking calculations. Protein complex was submitted to the Molecular Operating Environment 2016.0802 (MOE) Structure Preparation application, in order to fix all issues and to prepare structures for subsequent computational analyses.

The OligoGM1 structure was built with the MOE Carbohydrate Builder and a geometry optimization was carried out with MOPAC7 and the PM6 basis set.

Molecular docking was carried out through the MOE Dock program, setting as receptor the complex between TrkA and NGF, as ligand the optimized OligoGM1 structure. The binding site was identified at the interface between the two proteins. Before placement procedure, 20 000 rotamers of the ligand was generated, exploring all the molecule rotatable bonds. Alpha PMI placement algorithm, specifically developed for tight binding pocket, was selected. The London dG empirical scoring function was used for sorting the poses. The 30 top-scoring poses was refined through molecular mechanics, considering the receptor as a rigid body, and the refined complexes were scored through the GBVI/WSA dG empirical scoring function, keeping the five top-scoring poses.

The top-scoring pose from the docking procedure was refined by using the MOE QuickPrep procedure aimed at relaxing and refining the complex before calculating the approx. binding free energy via the GBVI/WSA dG empirical scoring function (Naim *et al.* 2007).

# *Results*

### GM1 and OligoGM1 effect on N2a cell viability and proliferation

GM1 and OligoGM1 concentration for cell treatments was fixed at 50  $\mu$ M (Rabin *et al.* 2002; Chiricozzi *et al.* 2017).

Trypan blue assay was preliminary performed after 24 and 48 hour treatment in order to evaluate a possible toxic effect of 50  $\mu$ M GM1 or OligoGM1 on N2a cells (Mehlen *et al.* 1988; Strober, 2001; Aureli *et al.* 2011).

As shown in figure R1a, no significant difference in cell viability was observed with respect to untreated cells (Chiricozzi *et al.* 2017).

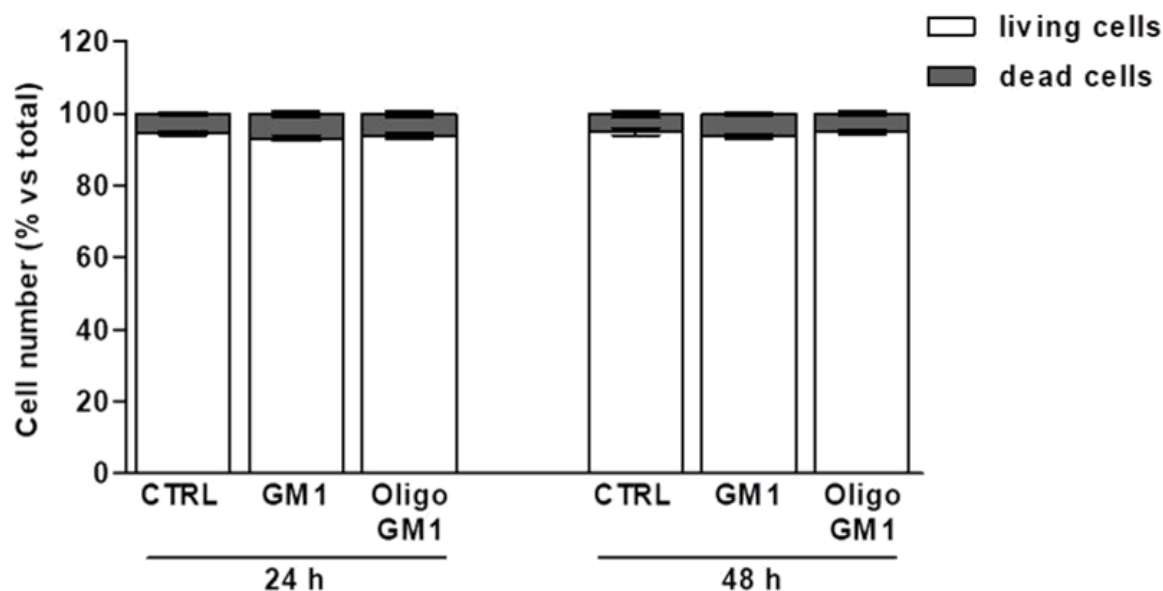


**Figure R1a: Effect of GM1 and OligoGM1 on cell viability.** N2a cells were treated for 24 and 48 hours with 50  $\mu$ M GM1 or OligoGM1. The numbers of living and dead cells were determined according to the Trypan blue exclusion assay and expressed in percentage of the total cell number. Bars show the mean values  $\pm$  SEM of 5 different cell culture preparations ( $n = 5$ ).

MTT reduction assay was additionally done after 12, 24 and 48 hours from administration of 50  $\mu$ M GM1 or OligoGM1 to check on cell proliferation (Mosmann, 1983; Berridge *et al.* 1996).

The assay revealed a remarkable slowdown of cell proliferation for both GM1 and OligoGM1 treatments (Chiricozzi *et al.* 2017), suggesting a possible differentiative effect of oligosaccharide portion of GM1 on N2a cells (figure R1b).

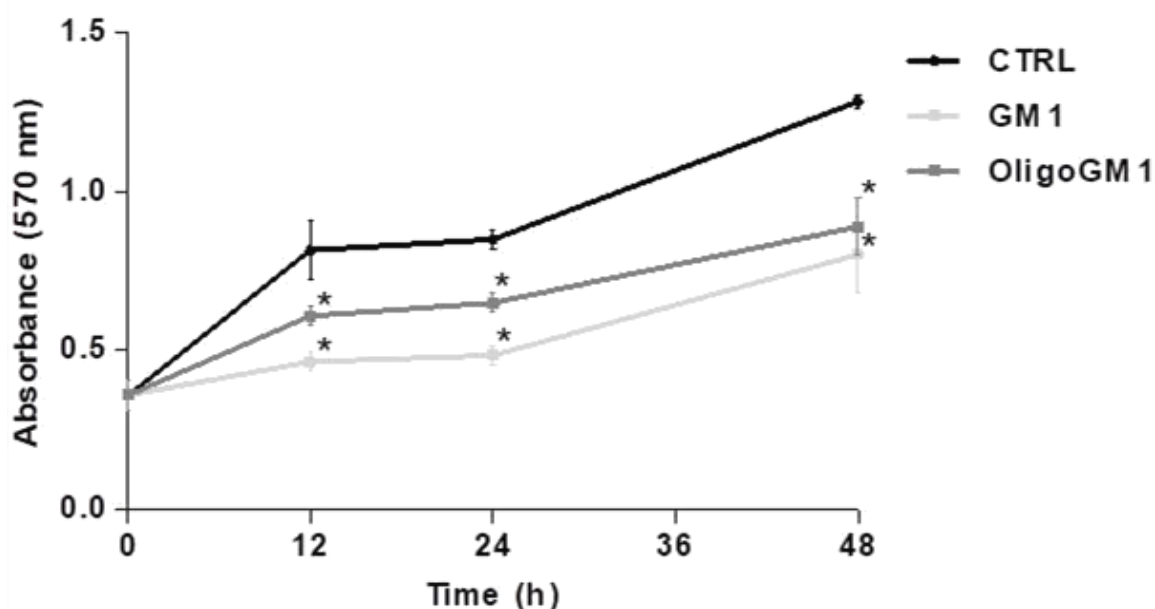


**Figure R1b: Effect of GM1 and OligoGM1 on cell proliferation.** N2a cell proliferation rate was monitored performing MTT reduction assay at different time point during 48 hour treatment with 50  $\mu$ M GM1 or OligoGM1. Formazan absorbance values at  $\lambda=570$  nm are directly proportional to the number of proliferative cells. The points represent the mean  $\pm$  SEM of background-reduced absorbance values of 5 different culture preparations ( $n = 5$ , \* = statistical significant difference,  $p < 0.05$ , TWO-WAY ANOVA vs CTRL).

## Effect of GM1 derivatives on N2a cell morphology

In order to investigate a possible differentiative role of GM1 derivatives, treated N2a cells were subjected to morphological analysis by phase contrast microscopy 24 and 48 hours after treatments.

GM1 was employed as a positive control for the proved capacity to induce neurite formation in N2a cells (Roisen *et al.* 1981; Leon *et al.* 1982; Facci *et al.* 1984; Rabin *et al.* 2002).

OligoGM1 administration to N2a cells induced a neuron-like morphology in 24 hours, accentuated after 48 hours (figure R2). The effect was evidenced by the enhanced sprouting and progressive elongation of cell extension, conversely inappreciable in round-shaped control cells (Chiricozzi *et al.* 2017).

In order to clearly rationalize on the minimal GM1 oligosaccharide-included portion essentially required to initiate neurodifferentiation process, N2a cells were treated with 50  $\mu$ M galactose, sialic acid, OligoGM3, OligoGM2 or asialo-OligoGM1. OligoGM1 components were not able to induce any relevant morphological changes in N2a cells after 48 hour incubation (figure R3). The morphological effect was only obtained by using the entire OligoGM1 molecule suggesting that all included sugars are necessary to limit cell proliferation and to induce neurite sprouting (Chiricozzi *et al.* 2017).

In addition, N2a cells were treated also with the fucosylated OligoGM1, since Fuc-GM1 was able to induce neurodifferentiation (Masserini *et al.* 1992). As shown in figure R4, Fuc-OligoGM1 was still able to induce neurite sprouting and reduction in cell proliferation, similarly to OligoGM1 (Chiricozzi *et al.* 2017).

The obtained results suggest that the GM1 enhanced neurite sprouting in N2a cells requires specifically  $\beta$ -Gal-(1-3)- $\beta$ -GalNAc-(1-4)-[ $\alpha$ -Neu5Ac-(2-3)]- $\beta$ -Gal-(1-4)- $\beta$ -Glc structure and that the  $\alpha$ -fucose addition at the 2 position of the external galactose is irrelevant for impacting differentiative process.

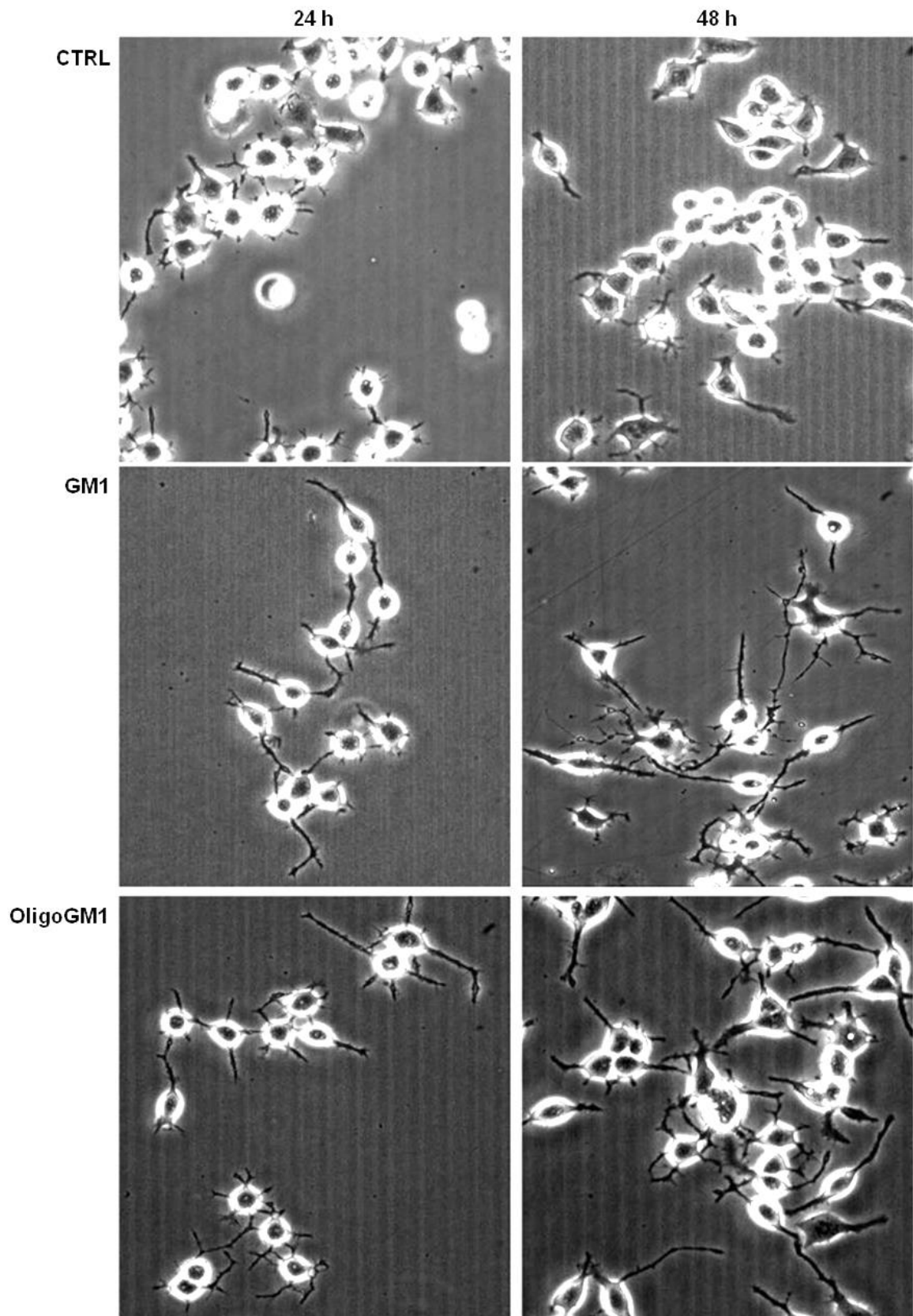


Figure R2: Morphological outcomes of N2a cells following 24 and 48 hours incubation with 50  $\mu$ M GM1 or OligoGM1. Cells were examined with phase contrast microscopy with 200X magnification. Images are representative of 10 independent experiments ( $n = 10$ ).



48 h

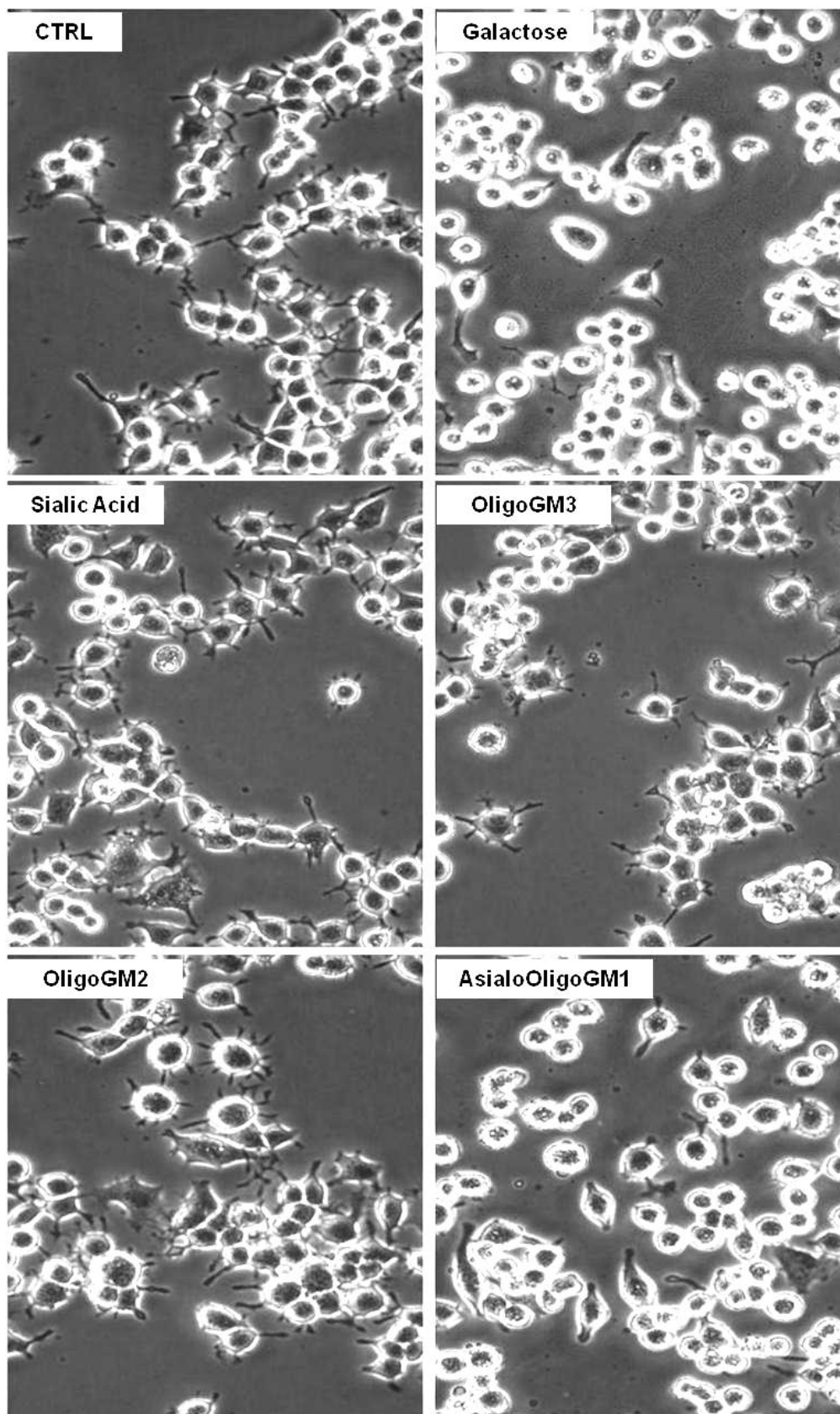


Figure R3: Morphological outcomes of N2a cells grown with 50  $\mu$ M galactose, sialic acid, OligoGM3, OligoGM2 and asialo-OligoGM1 for 48 hours. Cells were observed by phase contrast microscopy with 200X magnification. Images are representative of 3 independent experiments ( $n = 3$ ).

48 h

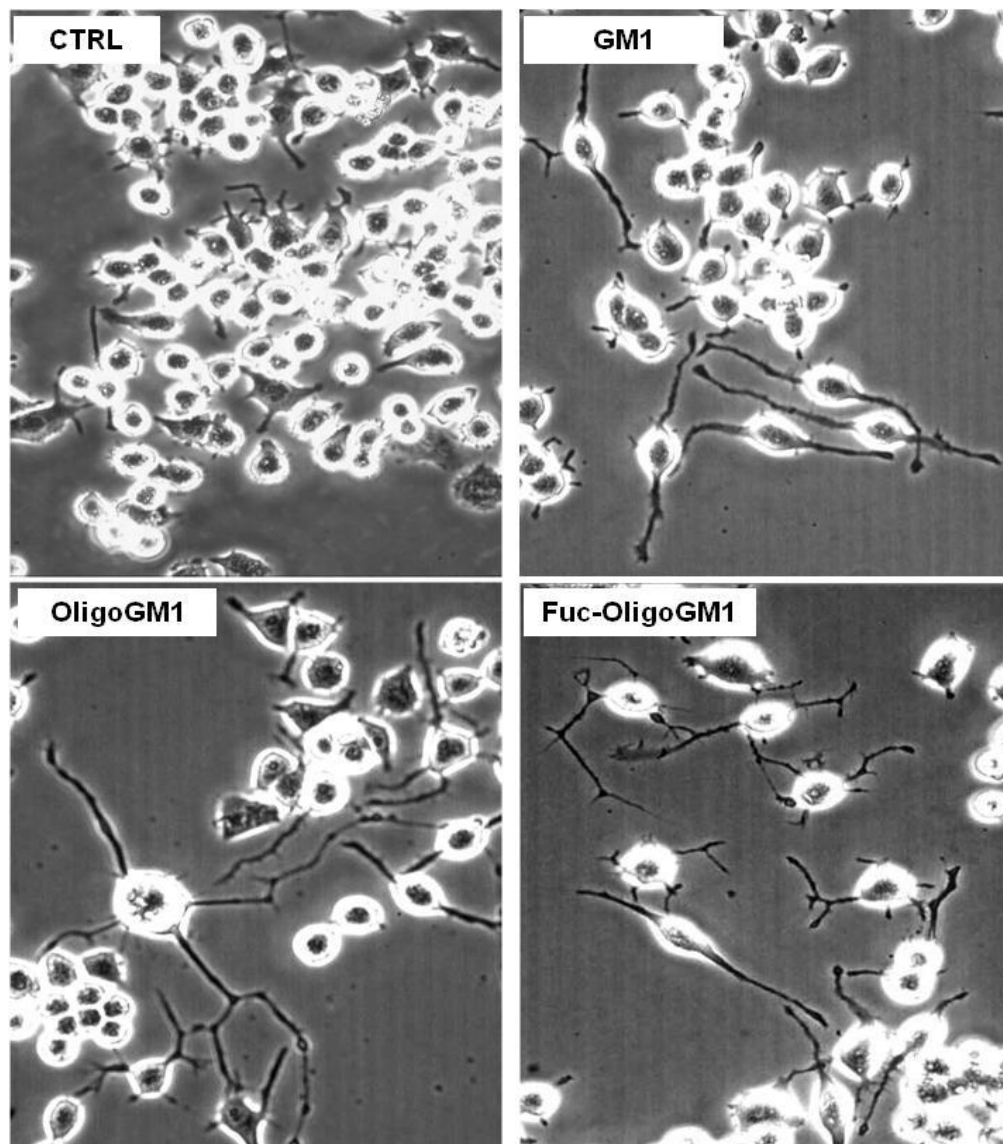


Figure R4: Morphological outcomes of N2a cells grown with 50  $\mu$ M GM1, OligoGM1 and fuco-OligoGM1 for 48 hours. Cells were observed by phase contrast microscopy with 200X magnification. Images are representative of 3 independent experiments ( $n = 3$ ).

## Neurite characterization

Neurite outgrowth was analyzed to characterize from a physical and biochemical points of view the morphological evidence of neuron-like cell differentiation induced by OligoGM1.

### **Physical characterization**

Neurite extensions were measured and expressed by the ratio between the length of processes and the diameter of cell body (Schengrund & Prouty 1988; Sato *et al.* 2002).

The values related to treated cells resulted significantly higher than control cells after 24 hours, increasing two fold more up to 48 hours (Chiricozzi *et al.* 2017). Values obtained with OligoGM1 were comparable to GM1 (figure R5).

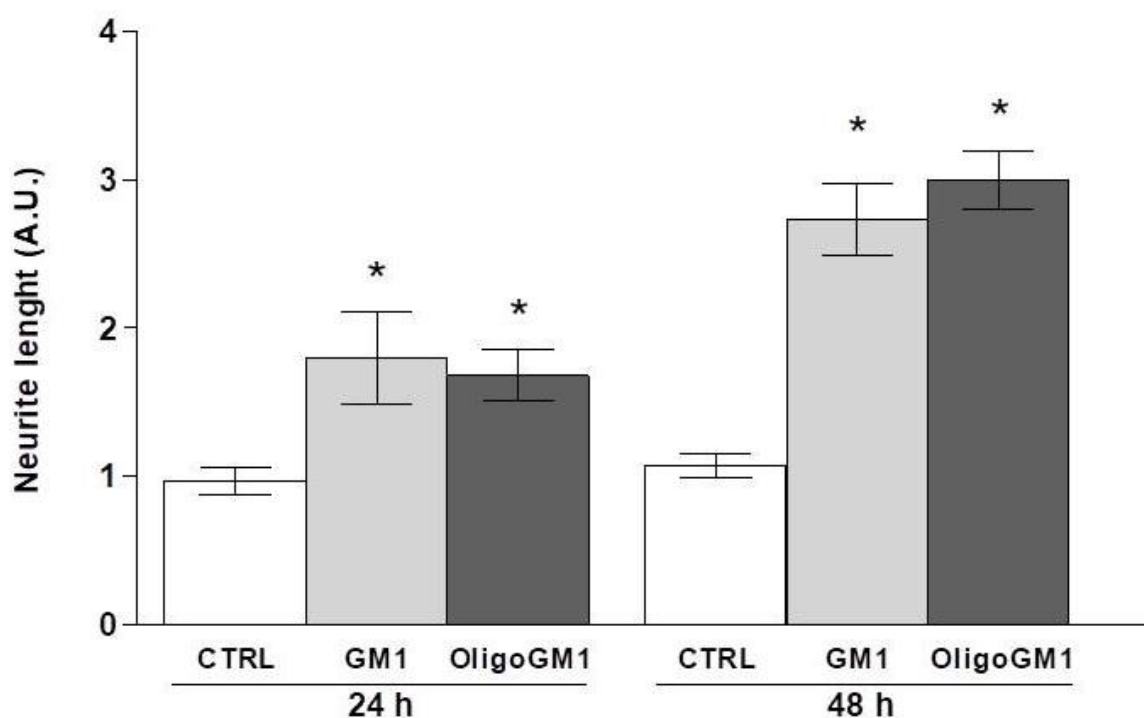


**Figure R5: Evaluation of neurite sprouting and elongation in N2a cells.** Neurite extensions were evaluated as the ratio between process length and cell body diameter after 24 and 48 hours treatment with 50  $\mu$ M GM1 or OligoGM1. The bars show the mean values  $\pm$  SEM from 5 different experiments ( $n = 5$ , \* = statistical significant difference,  $p < 0.01$ , Student's  $t$ -test vs CTRL).

### **Biochemical characterization**

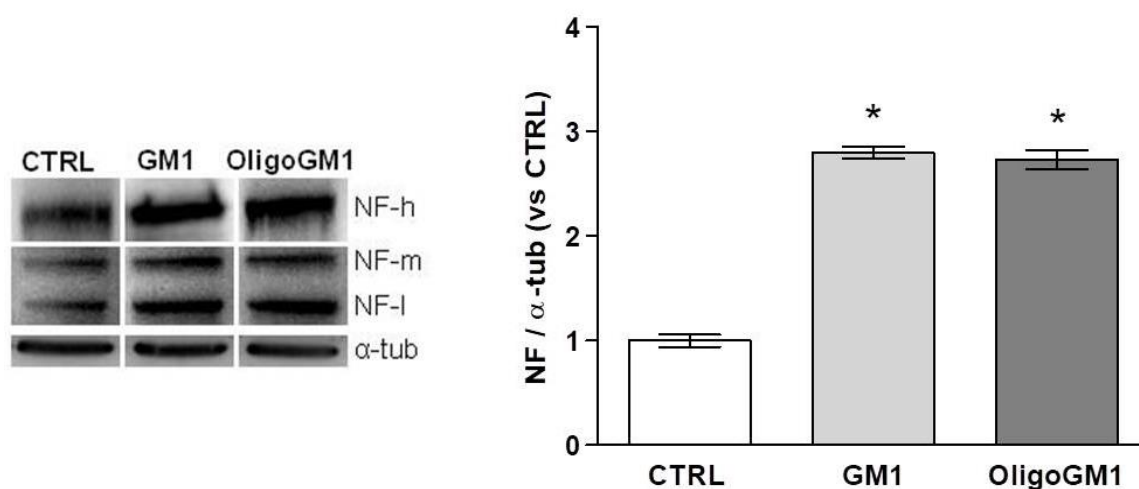
The level of intracellular neurofilament protein expression was evaluated as a biochemical marker of neurodifferentiation. Neurofilament is the major component of cytoskeleton supporting the axonal construction (Mao *et al.* 2000; Wang *et al.* 2004; Fukuda *et al.* 2014).

Immunoblotting analysis highlighted a significant increase in the expression of heavy, medium and light NF subunits (NF-h, NF-m, and NF-l) after 24 hours treatment with both GM1 and OligoGM1 (Chiricozzi *et al.* 2017), (figure R6a).

The result was qualitatively supported by the immunofluorescence assays (Chiricozzi *et al.* 2017) (figure R6b).

Since the presence of cell extensions, characterized by NF proteins expression, is considered marker of neurodifferentiation, the oligosaccharide portion of GM1 is allowable to promote neuritogenesis in N2a cells, analogously to GM1.

a.



b.



**Figure R6: Neurofilament protein expression in N2a:**

**a. Western Blotting analysis.** Immunoblotting for NF-h, NF-m, NF-l was performed after 24 hour treatment with 50  $\mu$ M GM1 or OligoGM1. The proteins are revealed by the specific antibody and visualized by chemiluminescence. *Left:* immunoblotting images. Blots are representative of 3 independent experiments. *Right:* semi-quantitative analysis of NF proteins amount.  $\alpha$ -tubulin was used for normalization. The bars represent the mean  $\pm$  SEM values of 3 different experiments expressed as the fold increase over CTRL ( $n = 3$ , \* = statistical significant difference,  $p < 0.01$ , Student's  $t$ -test vs CTRL).

**b. Immunofluorescence staining.** Neurofilament was detected using the specific antibody after 24 hours treatment with 50  $\mu$ M GM1 or OligoGM1. Cells were visualized by fluorescent microscopy at 400X magnification. Images are representative of 3 independent experiments ( $n = 3$ ).

## OligoGM1 interaction with N2a cells

Discovering the interaction between OligoGM1 and N2a cells represented the starting point to investigate about OligoGM1 targets in promoting neurodifferentiation. The fate of OligoGM1 was established using a procedure described to search for gangliosides administered to cells in culture (Chigorno *et al.* 1985). The experimental approach allows to search for three different modalities of OligoGM1 association to cells: *i.* weakly to the cell surface, *ii.* covalently to the cell surface, *iii.* internalized by cells.

Isotopic tritium labeled OligoGM1, [Gal-6-<sup>3</sup>H]OligoGM1, (figure M2b), was administered to N2a cells. Radioactivity allowed the recognition and the quantification of the molecule. After 0.5, 1, 6 and 24 hour treatments, cells were subjected to 10% serum-containing medium cell wash in order to remove and check the quantity of oligosaccharide weakly associated to the cells surface (serum labile fraction, SL). Subsequently, cells were treated with low-concentrated trypsin solution, searching for the oligosaccharide covalently bonded on PM protein extracellular domains (trypsin labile fraction, TL). Finally, cells were lysed in order to trace internalized OligoGM1 (trypsin stabile fraction, TS). About 99% of collected OligoGM1 was found in the serum fraction at each time point as shown in figure R7 (Chiricozzi *et al.* 2017).

The finding suggested that the oligosaccharide portion of GM1 does not enter into the cells neither in the PM, but it exerts its function interacting in a non-covalent manner with the cell surface.

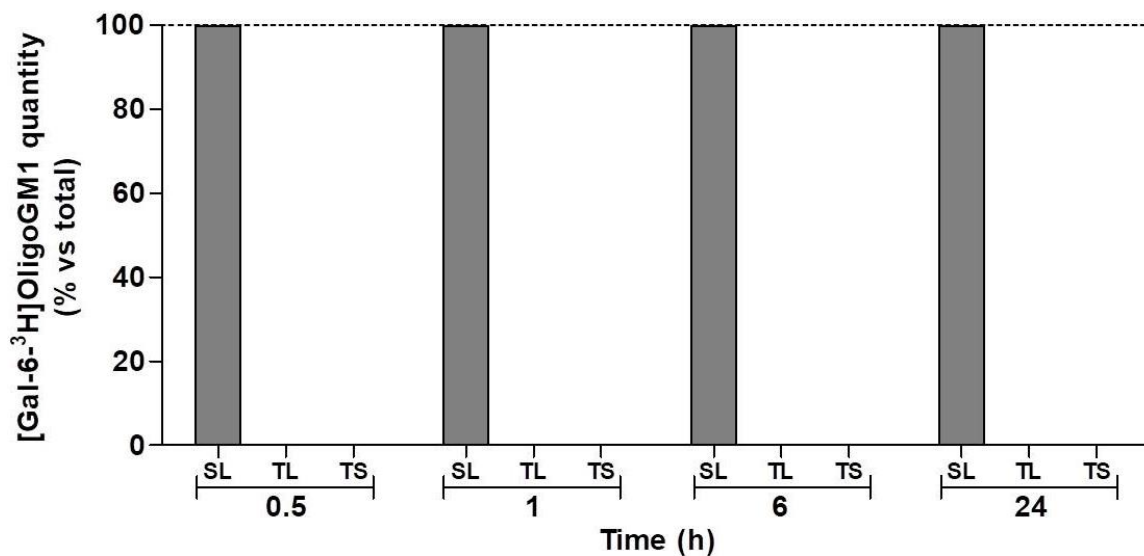


**Figure R7: Association of OligoGM1 to N2a cells.** N2a cells were incubated with 50  $\mu$ M [Gal-6-<sup>3</sup>H]OligoGM1 for 0.5, 1, 6 and 24 hours. After pulse, cells were washed with medium containing 10% FBS to collect the serum labile fraction (SL). Then cells were treated with 0.1% trypsin-EDTA solution to obtain the trypsin labile fraction (TL). Finally, cells were lysed to obtain the trypsin stable fraction (TS). The radioactivity associated with each fraction was determined by liquid scintillation counting. Data are expressed as percentage of total detected radioactivity. The bars express the mean  $\pm$  SEM values of three different experiments ( $n = 3$ ).

## **OligoGM1 effect on TrkA receptor pathway**

On the basis of TrkA-mediated neurodifferentiation promoted by GM1 amplifying NGF activity (Farooqui *et al.* 1997; Singleton *et al.* 2000; Duchemin *et al.* 2002; Da Silva *et al.* 2005; Mocchetti 2005; Zakharova *et al.* 2014), TrkA pathway was chosen as the subject of the study in order to investigate the molecular mechanism responsible for OligoGM1-induced neuritogenesis.

Particular attention was focused on the phosphorylation of the tyrosine 490 (Tyr490) that is relevant for differentiation pathway activation (Cordon-Cardo *et al.* 1991; Lavenius *et al.* 1995; Eggert *et al.* 2000; Damani *et al.* 2003; Biarc *et al.* 2012; Biarc *et al.* 2013). Furthermore, the activation of MAP Kinases Erk 1 and 2 (Erk1/2) was checked as downstream actor in the signaling cascade (Chao. 1992; Cowley *et al.* 1994; Lavenius *et al.* 1995; Fukuda *et al.* 1995; Sweatt, 2001; Vaudry *et al.* 2002).

### ***TrkA receptor activation***

A significant activation of TrkA receptor detected as the increase in Tyr490 phosphorylation level was highlighted both in GM1-treated cells and in OligoGM1-treated cells by immunoblotting analysis after 24 hours from the beginning of the treatment (Chiricozzi *et al.* 2017), (figure R8).

Checking the activation of MAP kinases, an important augmenting in ERK1/2 phosphorylation was also found in treated cells at the same time point (Chiricozzi *et al.* 2017), (figure R9).



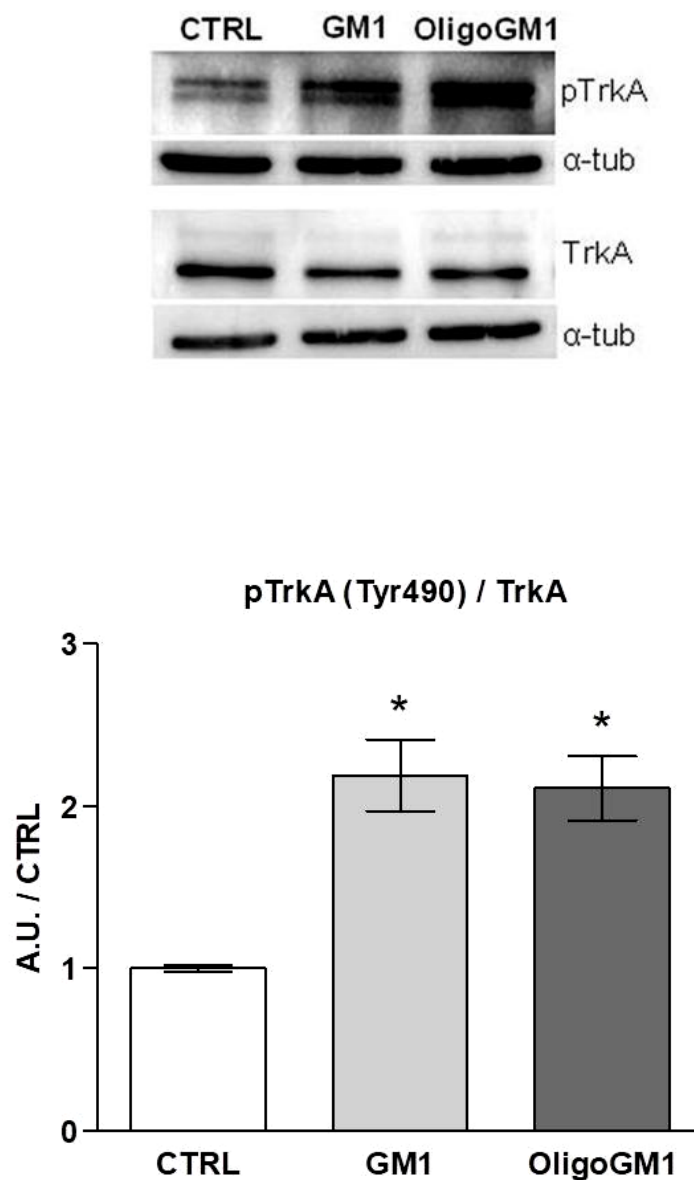


**Figure R8: GM1 and OligoGM1 effect on TrkA activation.** N2a cells were treated with 50  $\mu$ M GM1 or OligoGM1 for 24 hours. Immunoblotting for pTrkA (Tyr490), TrkA and  $\alpha$ -tub expression is revealed by specific antibodies and visualized by chemiluminescence. *Top*: immunoblotting images. Blots are representative of 8 independent experiments. *Bottom*: semi-quantitative analysis of pTrkA (Tyr490) related to the total TrkA level.  $\alpha$ -tub was used to normalizing. The bars represent the mean  $\pm$  SEM values of 8 different experiments, expressed as the fold increase over CTRL ( $n = 8$ , \* = statistical significant difference,  $p < 0.05$ , Student's  $t$ -test vs CTRL).

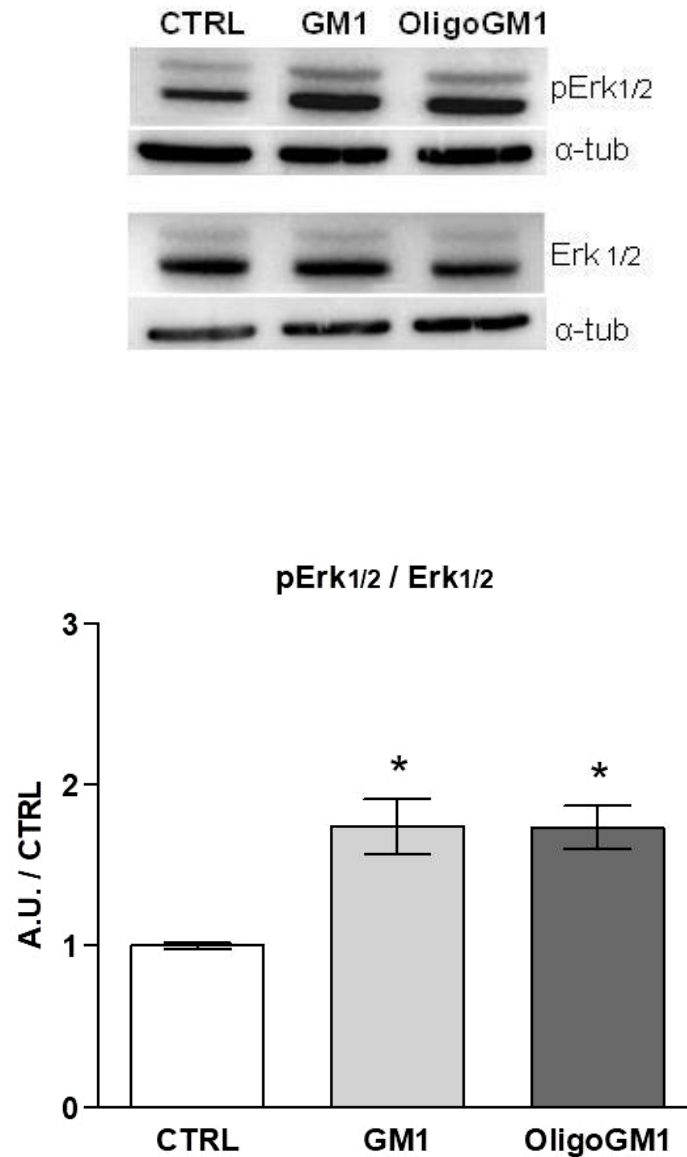


**Figure R9: GM1 and OligoGM1 effect on MAPK activation.** N2a cells were treated with 50  $\mu$ M GM1 or OligoGM1 for 24 hours. Immunoblotting for pErk1/2, Erk1/2 and  $\alpha$ -tub expression is revealed by specific antibodies and visualized by chemiluminescence. *Top*: immunoblotting images. Blots are representative of 8 independent experiments. *Bottom*: semi-quantitative analysis of pErk1/2 related to the total Erk1/2 level.  $\alpha$ -tub was used to normalizing. The bars represent the mean  $\pm$  SEM values of 8 different experiments, expressed as the fold increase over CTRL ( $n = 8$ , \* = statistical significant difference,  $p < 0.05$ , Student's  $t$ -test vs CTRL).

### ***Time course changing in TrkA-Erk signaling pathway***

In order to examine time course of TrkA-Erk pathway induction caused by GM1 and OligoGM1, the phosphorylation levels of TrkA (Tyr490) and Erk1/2 were evaluated over the duration of the treatments by western blot analysis.

As shown in figure R10, GM1 and OligoGM1 caused a rapid elevation of TrkA phosphorylation on Tyr490 that was significantly maintained over the 12 hours time course.

The enhancement in MAPK phosphorylation appeared successively, getting significant after 6 hours from GM1 and OligoGM1 administration (figure R11).

The results revealed that, following GM1 and OligoGM1 treatment, Tyr490-TrkA phosphorylation was increased within 30 minutes and Erk1/2 after 3 hours and both remained elevated throughout 24 hours, in parallel to morphological differentiation outcomes.

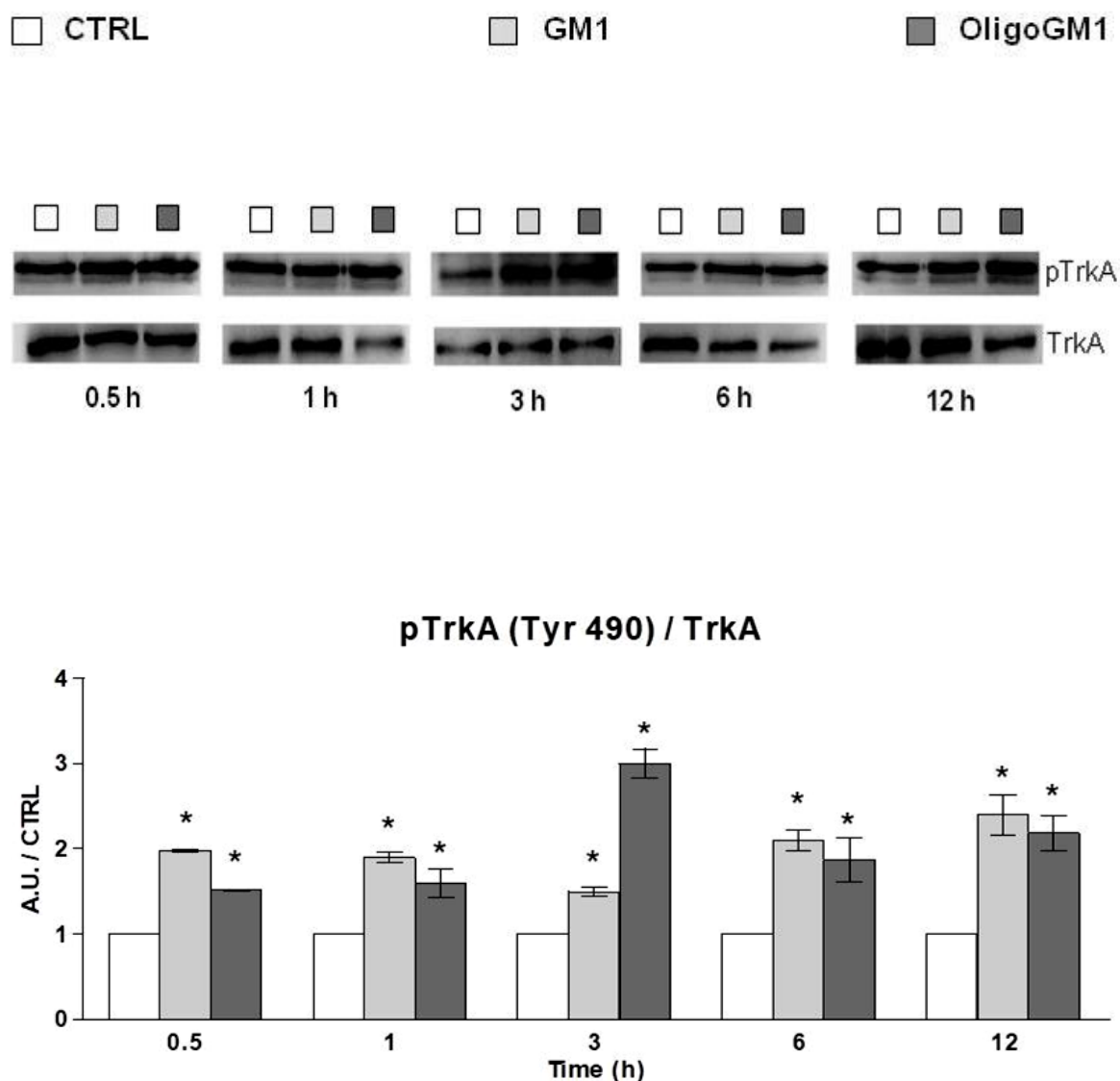


**Figure R10: Time course of Tyr 490-TrkA phosphorylation.** N2a cells were treated with 50  $\mu$ M GM1 or OligoGM1 up to 12 hours. The figure shows analysis for pTrkA (Tyr490) and TrkA expression performed after 0.5, 1, 3, 6 and 12 hours treatment. Immunoblotting was revealed by specific antibodies and visualized by chemiluminescence. *Top*: immunoblotting images. Blots are representative of 3 independent experiments. *Bottom*: semi-quantitative analysis of pTrkA (Tyr490) related to the total TrkA level. The bars represent the mean  $\pm$  SEM values of 3 different experiments, expressed as the fold increase over CTRL ( $n = 3$ , \* = statistical significant difference,  $p < 0.05$ , Student's  $t$ -test vs CTRL).

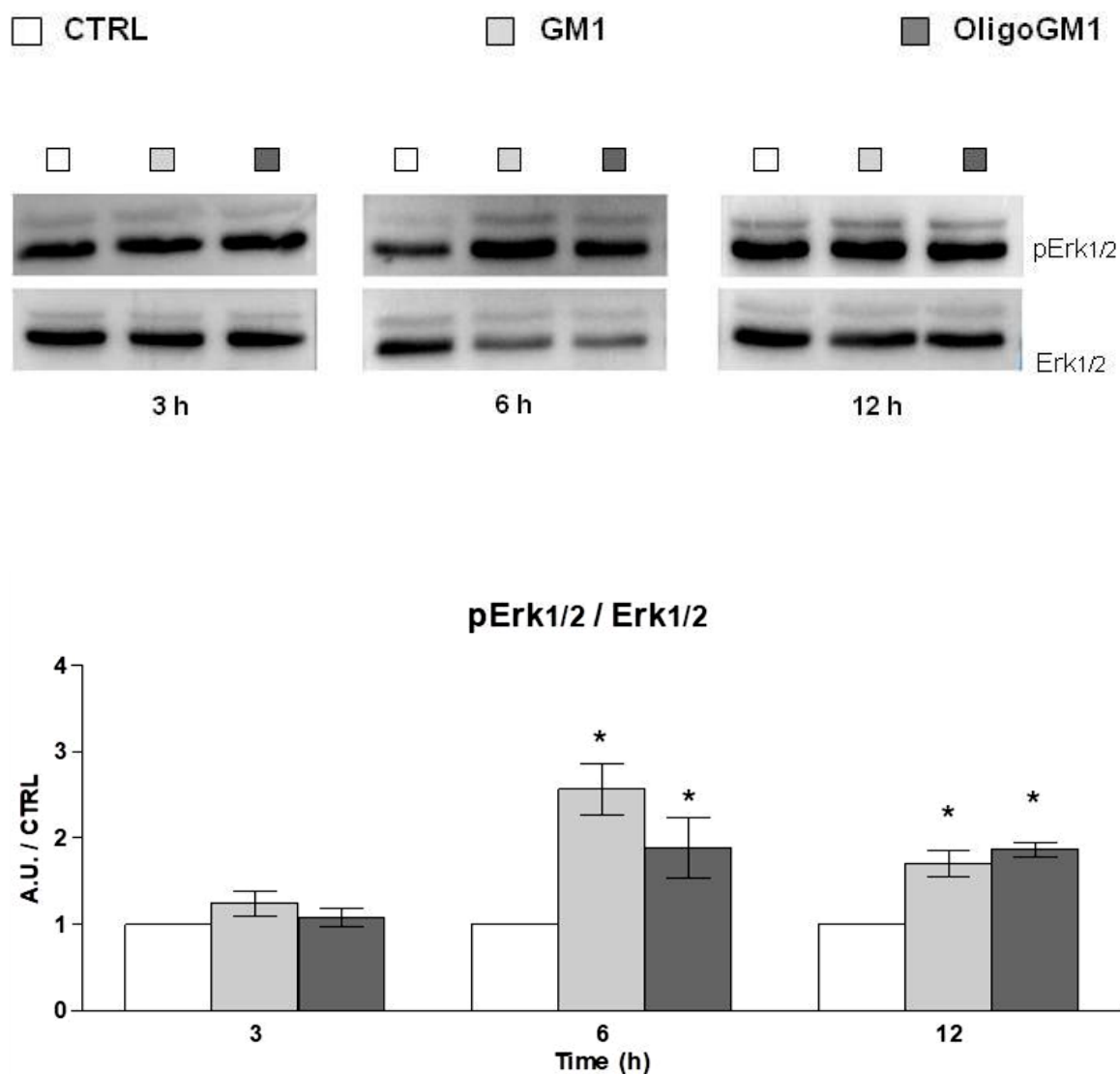


**Figure R11: GM1 Time course of Erk1/2 phosphorylation.** N2a cells were treated with 50  $\mu$ M GM1 or OligoGM1 up to 12 hours. The figure shows analysis for pErk1/2 and Erk1/2 expression performed after 3, 6 and 12 hours treatment. Immunoblotting was revealed by specific antibodies and visualized by chemiluminescence. *Top*: immunoblotting images. Blots are representative of 3 independent experiments. *Bottom*: semi-quantitative analysis of pErk1/2 related to the total Erk1/2 level. The bars represent the mean  $\pm$  SEM values of 3 different experiments, expressed as the fold increase over CTRL ( $n = 3$ , \* = statistical significant difference,  $p < 0.05$ , Student's  $t$ -test vs CTRL).

### ***TrkA receptor inhibition***

To prove that GM1 or OligoGM1 effect in N2a neurodifferentiation induction is properly mediated by TrkA-Erk pathway, TrkA activation was blocked using a specific inhibitor, able to fit the ATP pocket, preventing its consumption (Segal *et al.* 1996; D'Ambrosi *et al.* 2001; Wood *et al.* 2004; Lemmon & Schlessinger, 2010).

A specific inhibitor for TrkA receptor was employed in combination to GM1 and OligoGM1 treatments in order to prove that neuritogenic effect is properly mediated by TrkA-ERK pathway. The addition of TrkA inhibitor together with GM1 or OligoGM1 impeded phosphorylation processes in the signaling cascade of both Tyr490 and Erk p44/42 (Chiricozzi *et al.* 2017), (figure R12 a and b).

Blocking TrkA activity, the neurite elongation is arrested even in presence of GM1 and OligoGM1 for 24 hours (Chiricozzi *et al.* 2017), (figure R13).

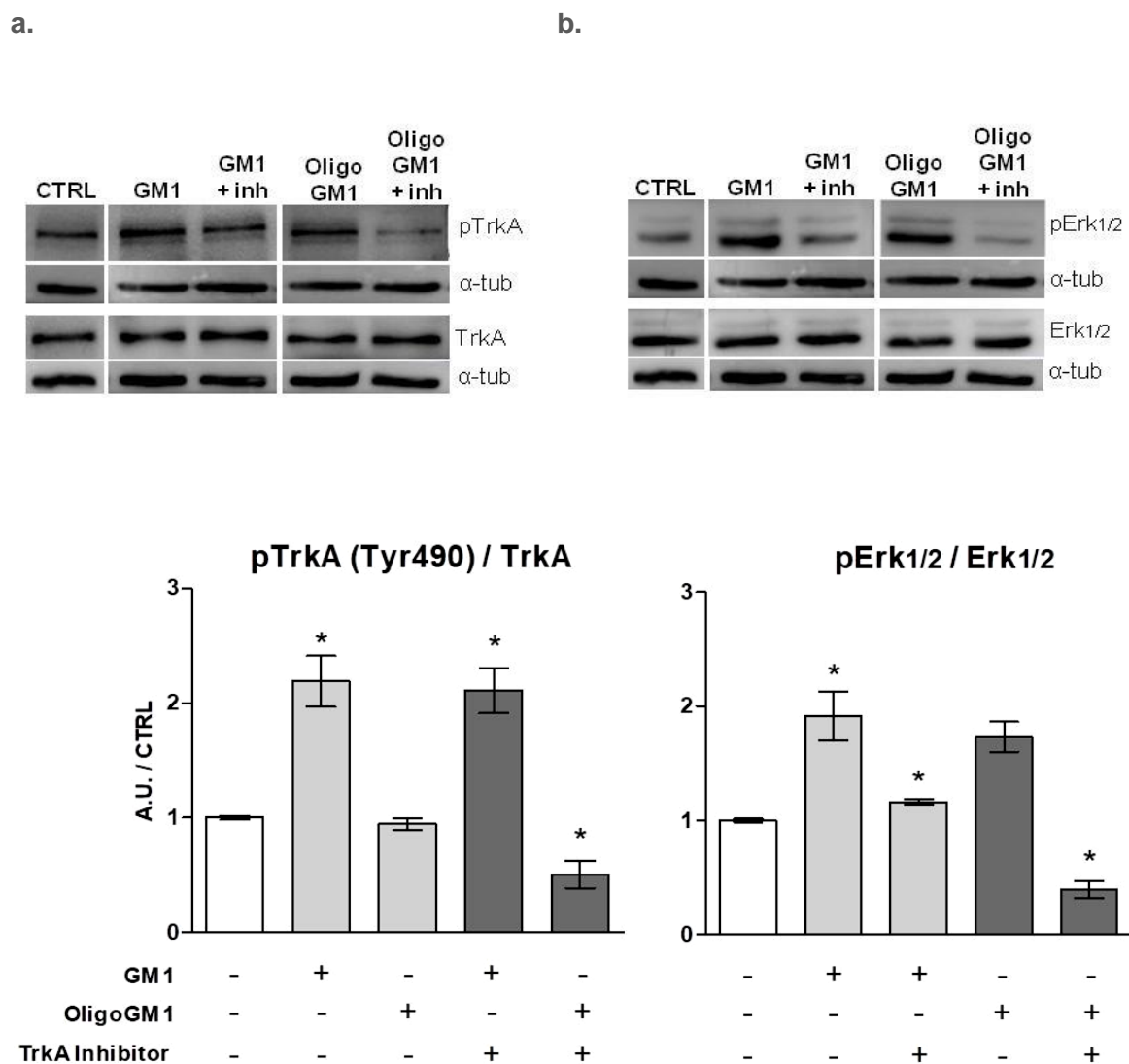


**Figure R12: Effect of TrkA chemical inhibition.** N2a cells were treated with 50  $\mu$ M GM1 or OligoGM1 for 24 hours in presence or in absence of a specific inhibitor for TrkA (120 nM). The figure shows analysis of TrkA (a) and Erk1/2 (b) activation. Immunoblotting for pTrkA (Tyr490), TrkA, pErk1/2, and Erk1/2 expression is revealed by specific antibodies and visualized by chemiluminescence. *Top*: immunoblotting images. Blots are representative of 5 independent experiments. *Bottom*: semi-quantitative analysis of pTrkA (a) and pErk1/2 (b) related to the total TrkA and Erk1/2 levels respectively.  $\alpha$ -tub was used to normalizing. The bars represent the mean  $\pm$  SEM values of 5 different experiments, expressed as the fold increase or decrease over CTRL ( $n = 5$ , \* = statistical significant difference,  $p < 0.05$ , Student's  $t$ -test vs CTRL).

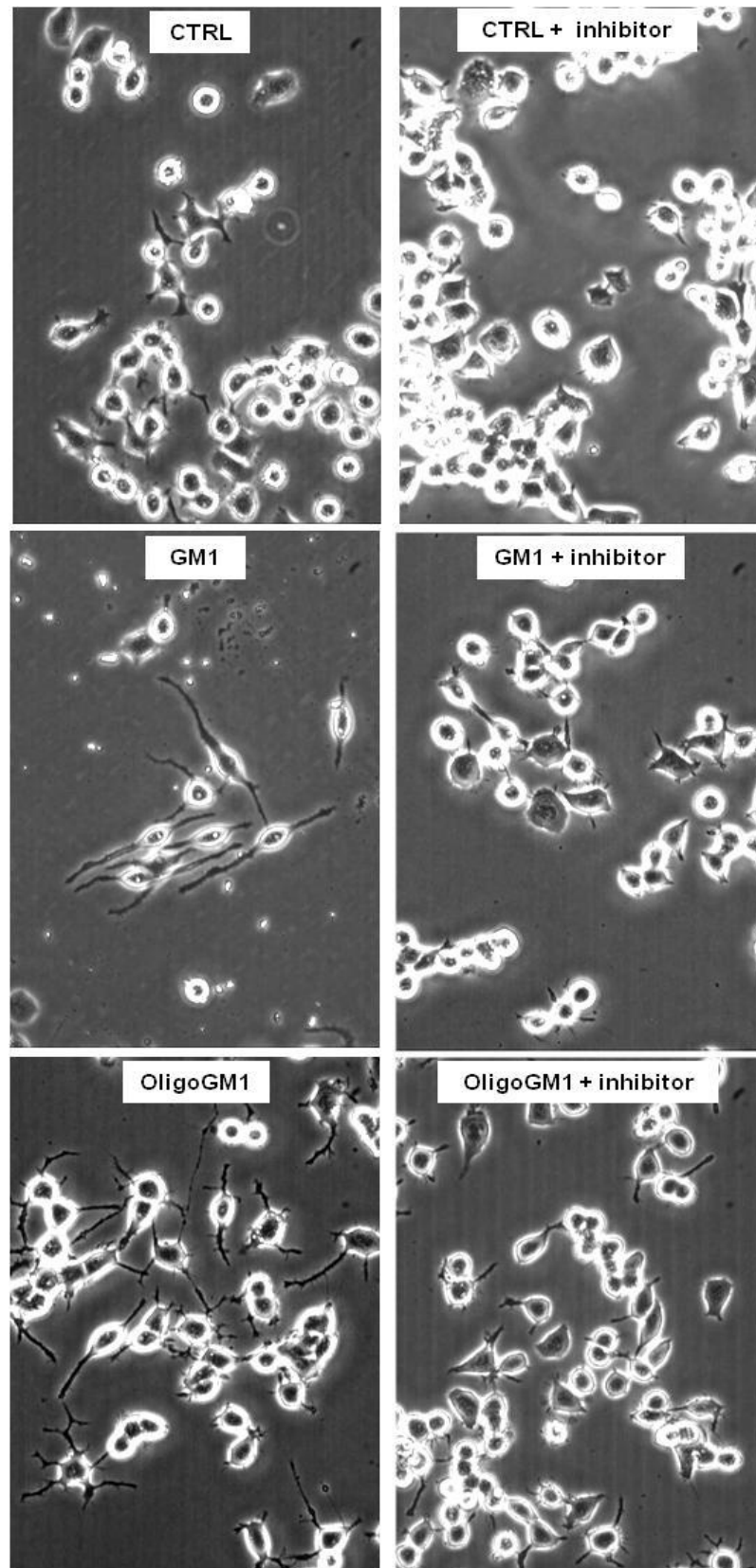


**Figure R13: Morphological outcomes of N2a cells after TrkA inhibition.** After 24 hours incubation with TrkA inhibitor in combination with 50  $\mu$ M GM1 or OligoGM1 cells were analyzed with phase contrast microscopy with 200X magnification. Images are representative of 5 independent experiments ( $n = 5$ ).



### ***TrkA receptor expression silencing***

In addition to the chemical inhibition, TrkA receptor expression was also knocked down by siRNA transfection. The approach offered the possibility to demonstrate the unavoidable implication of TrkA receptor in GM1 and OligoGM1-promoted neuritogenesis. Control cells were transfected by scramble siRNA. Silenced cells, resulting in a 70% reduction of TrkA expression, as evidenced in figure R14 were incubated with GM1 or OligoGM1 for 24 hours (Chiricozzi *et al.* 2017).

As shown by immunoblotting analysis, TrkA silencing prevented Erk1/2 phosphorylation due to GM1 and OligoGM1 in N2a cells (figure R14), that at the same time didn't undergo to differentiation (Chiricozzi *et al.* 2017), (figure R15).

a.

b.

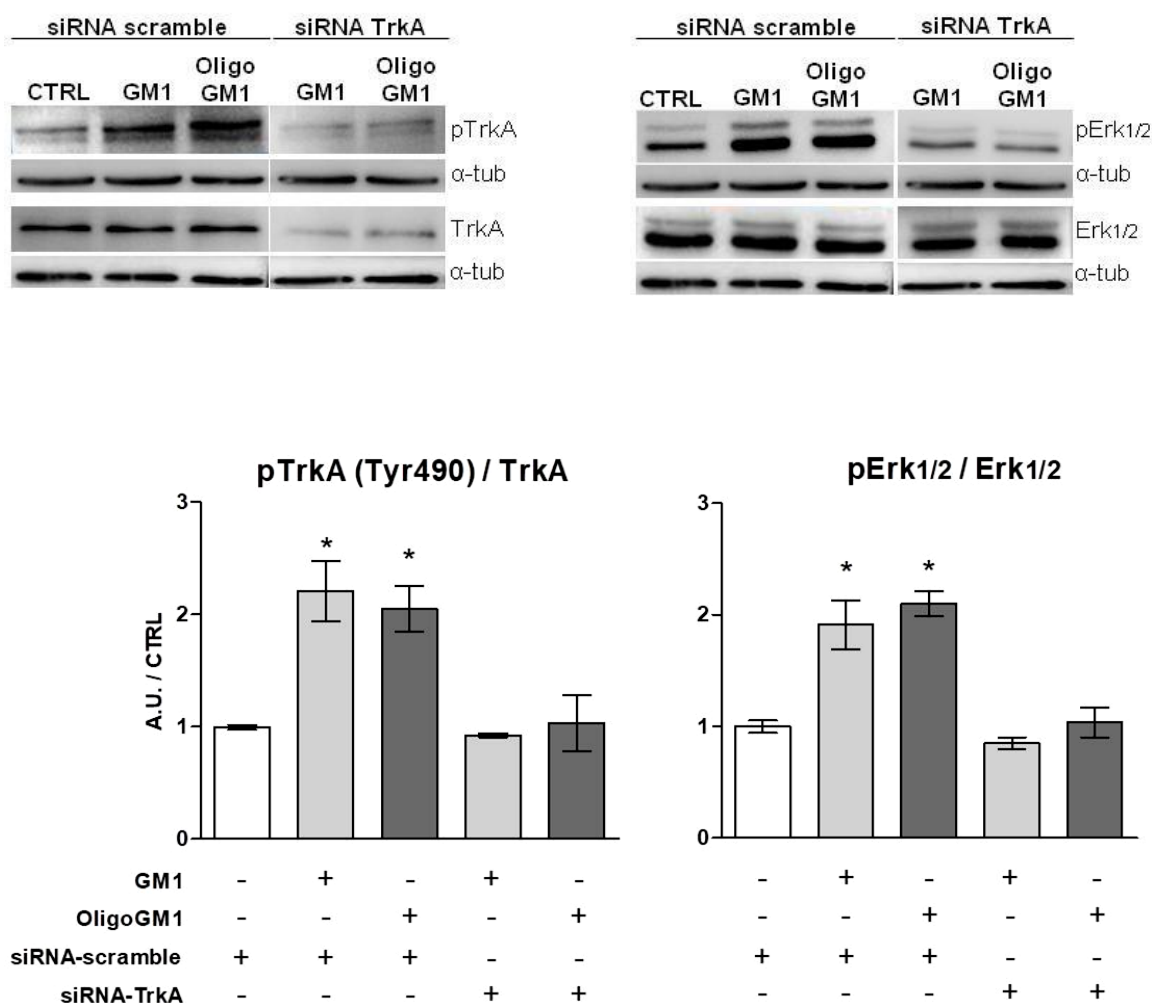


**Figure R14: Effect of silencing TrkA expression.** N2a cells were transfected with siRNA against TrkA (50nM). Control cells were transfected with scramble siRNA. 24 hours after transfection cells were exposed to 50  $\mu$ M GM1 or OligoGM1 for 24 hours. The figure shows the evaluation of TrkA (a) and Erk1/2 (b) phosphorylation. Immunoblotting for pTrkA (Tyr490), TrkA, pErk1/2, and Erk1/2 expression is revealed by specific antibodies and visualized by chemiluminescence. *Top*: immunoblotting images. Blots are representative of 3 independent experiments. *Bottom*: semi-quantitative analysis of pTrkA (a) and pErk1/2 (b) related to the total TrkA and Erk1/2 levels respectively.  $\alpha$ -tub was used to normalizing. The bars represent the mean  $\pm$  SEM values of 3 different experiments, expressed as the fold increase or decrease over untreated CTRL ( $n = 3$ , \* = statistical significant difference,  $p < 0.05$ , Student's  $t$ -test vs untreated CTRL).

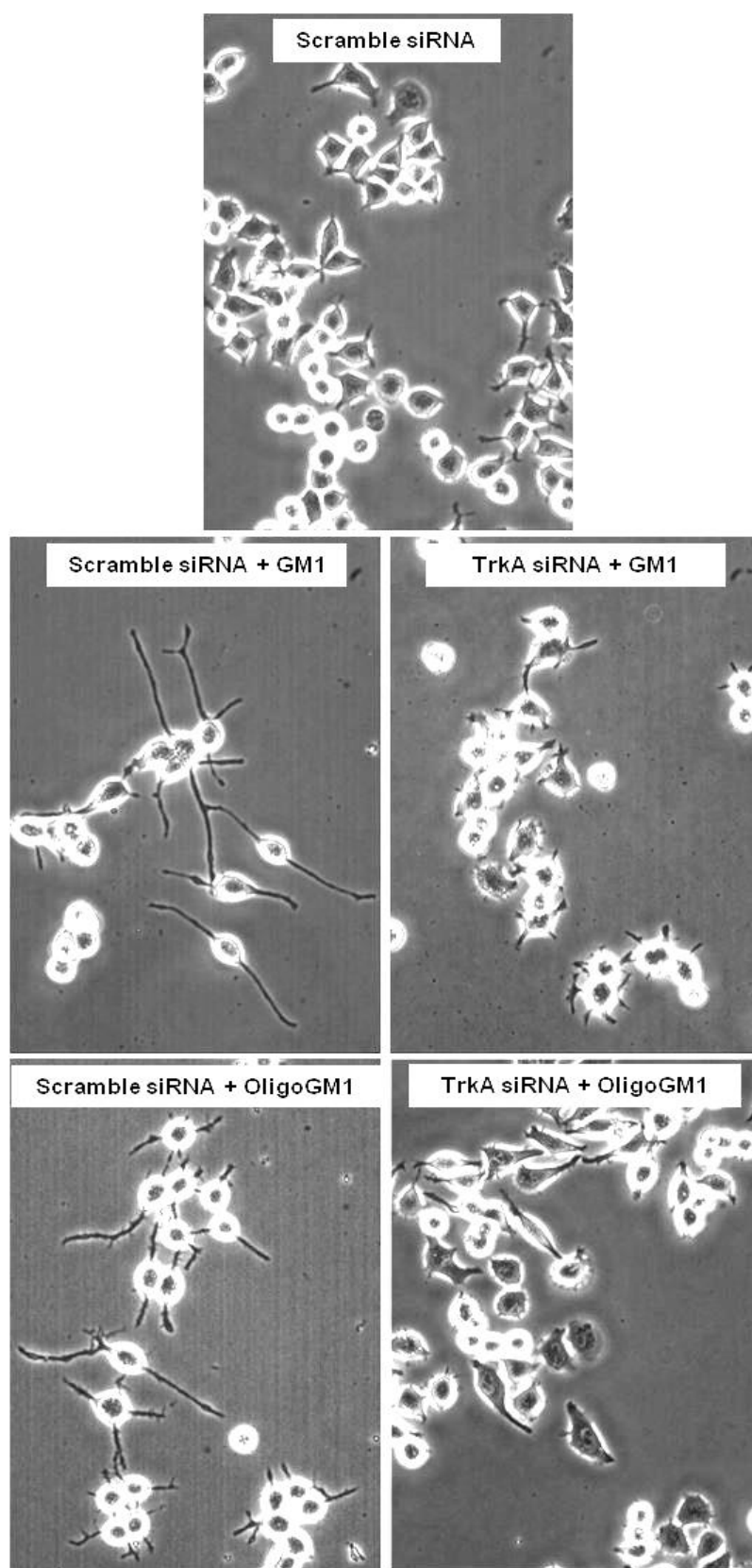


**Figure R15: Morphological outcomes of N2a cells after TrkA expression silencing.** After transfection with TrkA or scramble siRNA, N2a cells were treated for 24 h with 50  $\mu$ M GM1 or OligoGM1 and analyzed with phase contrast microscopy with 200X magnification. Images are representative of 3 independent experiments ( $n = 3$ ).

## Interaction between OligoGM1 and TrkA receptor

### ***Covalent cross-linking interaction by photolabeling***

In order to study the interaction between the oligosaccharide chain of GM1 and TrkA receptor, radioactive and photoactivable GM1 derivatives, [Gal-6-<sup>3</sup>H]GM1(Cer-N<sub>3</sub>), [Sph-3-<sup>3</sup>H]GM1(Gal-N<sub>3</sub>) and [Gal-6-<sup>3</sup>H]OligoGM1(Glc-N<sub>3</sub>) were prepared according to the procedure shown in M section.

The use of photoactivable radiolabeled derivatives allows to identify the interaction between the exogenous molecules and cell proteins. According to this approach, the azide, contained in the photoactivable group, is activated after UV illumination and becomes a nitrene. The nitrene is a very unstable intermediate that immediately generates a covalent bond with the adjacent molecules. So, in this way, proteins that interact with the azide-modified molecules were linked to the photoactivable group and at the same time recognizable by the radiolabeling (Sonnino *et al.* 1989).

N2a cells were incubated for 3 hours at 37 °C with the photosensitive derivatives under dark conditions. After pulse, cells were illuminated by UV-light for 40 minutes to induce covalent cross-linking between cell proteins and the radioactive derivatives. Target proteins were separated by SDS-PAGE, blotted on a PVDF membrane and visualized by digital autoradiography. Among the entire N2a protein pattern (figure R16, line 2), only few radioactive bands were detected on PVDF of every sample (figure R16, line 1). The radioactive tracks corresponded to specific proteins that, after the illumination, are covalently bond interacting with the derivatives, suggesting a specific association between GM1-derivatives and N2a proteins. After the radioimaging the same PVDF membranes were immunostained for TrkA: a specific radiolabeled band at 140 kDa overlapping TrkA signaling was found in [Sph-3-<sup>3</sup>H]GM1(Gal-N<sub>3</sub>) and [Gal-6-<sup>3</sup>H]OligoGM1(Glc-N<sub>3</sub>) treated samples (figure R18 and R19). No correspondence of TrkA signal with radioactive track was found out from the PVDF related to [Gal-6-<sup>3</sup>H]GM1(Cer-N<sub>3</sub>) treated sample (figure R17).

The results suggested that TrkA is directly connected to the oligosaccharide portion of GM1 ganglioside.

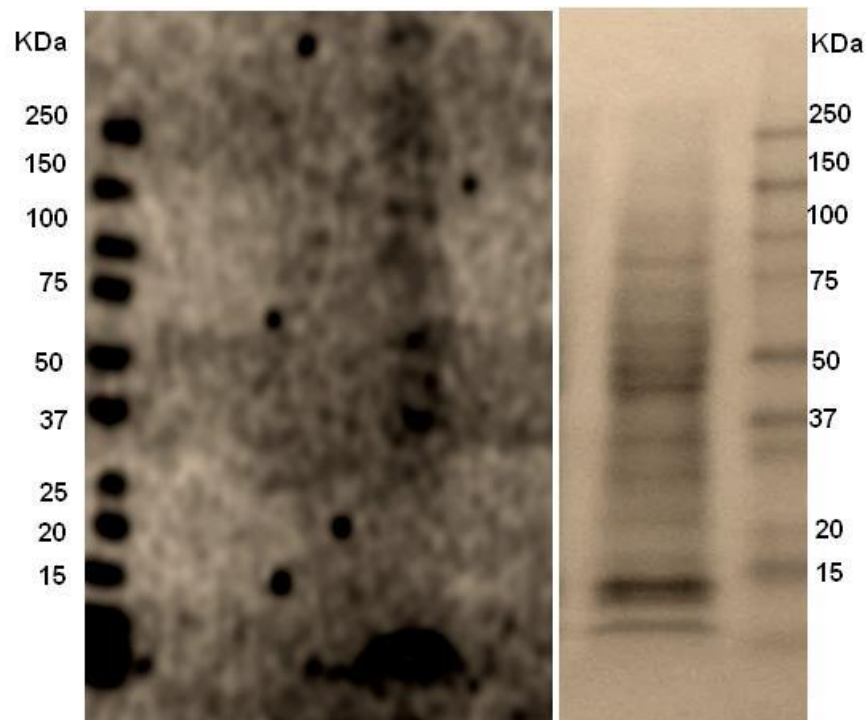


**Figure R16: N2a protein patterns.** *Line 1:* radioactive track on PVDF membrane of OligoGM1-interacting N2a proteins obtained using [Gal-6-<sup>3</sup>H]OligoGM1(Glc-N<sub>3</sub>) and acquired by digital autoradiography. *Line 2:* entire N2a protein pattern marked by Red Ponceau PVDF staining.

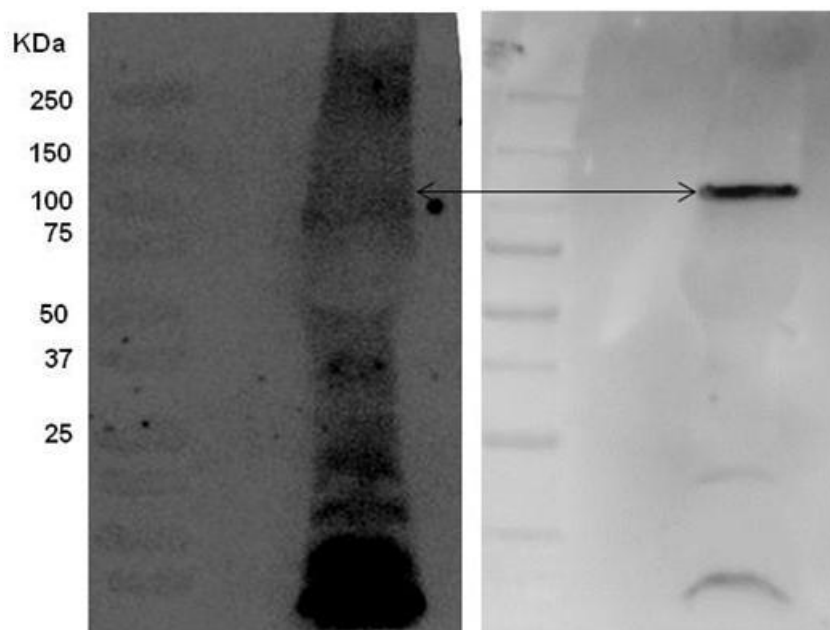


**Figure R17: Interaction between TrkA and GM1 in N2a cells.** [Gal-6- $^3\text{H}$ ]GM1(Cer- $\text{N}_3$ ) was added to N2a cells and cells were then illuminated. Cell lysate was submitted to 4–20% SDS–polyacrylamide gel electrophoresis, blotted on a PVDF membrane and visualized by digital autoradiography for 96 hours. TrkA receptor signal was visualized on the same PVDF by western blotting using specific antibody. The images are representative of three different experiments.

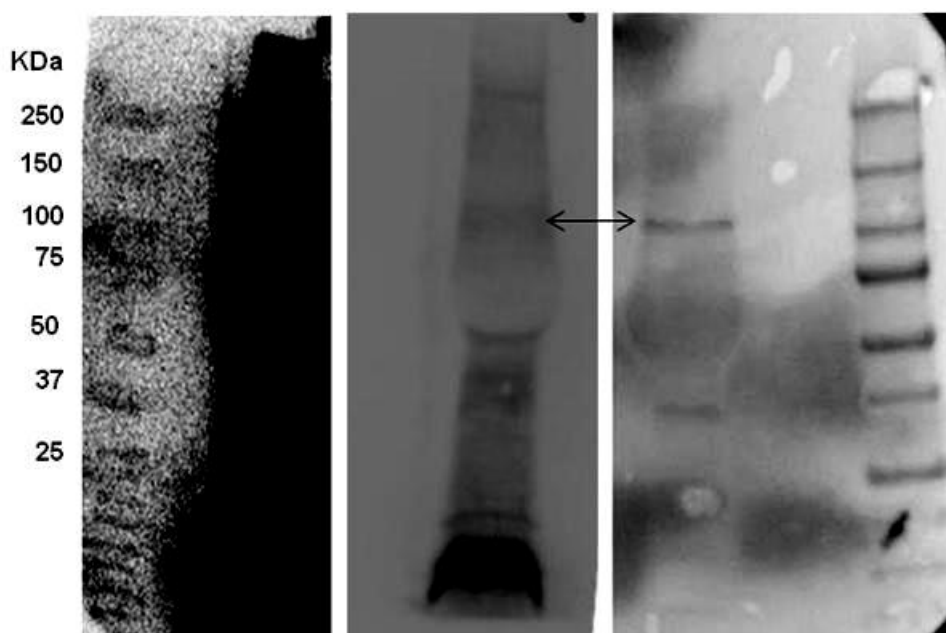


**Figure R18: Interaction between TrkA and GM1 in N2a cells.** [Sph-3- $^3\text{H}$ ]GM1(Gal- $\text{N}_3$ ) was added to N2a cells and cells were then illuminated. Cell lysate was submitted to 4–20% SDS–polyacrylamide gel electrophoresis, blotted on a PVDF membrane and visualized by digital autoradiography for 96 hours. TrkA receptor signal was visualized on the same PVDF by western blotting using specific antibody. The are images representative of three different experiments.

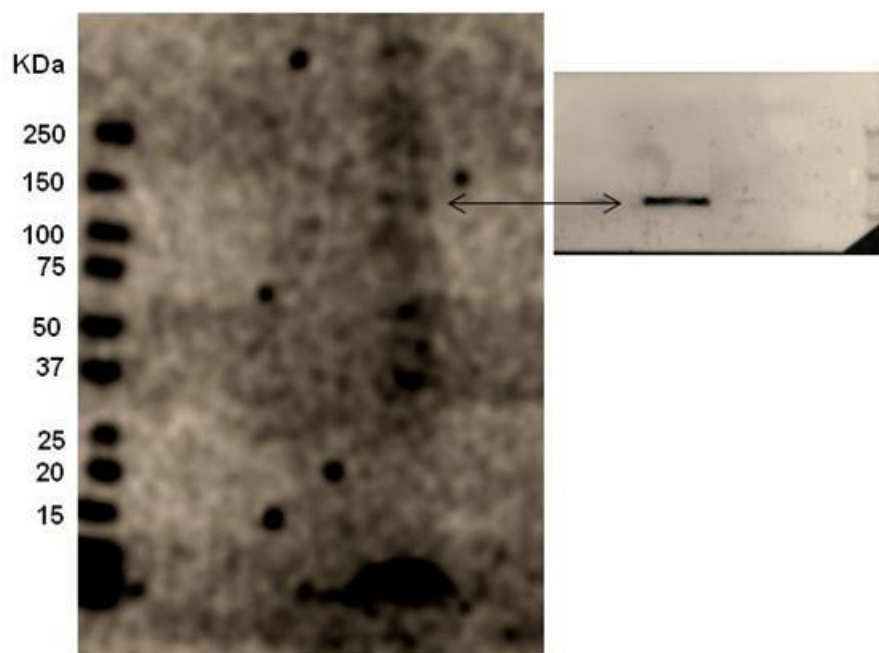


**Figure R19: Interaction between TrkA and OligoGM1 in N2a cells.** [Gal-6-<sup>3</sup>H]OligoGM1(Glc-N<sub>3</sub>) was added to N2a cells and cells were then illuminated. Cell lysate was submitted to 4–20% SDS–polyacrylamide gel electrophoresis, blotted on a PVDF membrane and visualized by digital autoradiography for 96 hours. TrkA receptor signal was visualized on the same PVDF by western blotting using specific antibody. The images are representative of three different experiments (Chiricozzi *et al.* 2017).

### ***Dynamic calculations for the TrkA-OligoGM1 complex***

The availability of the crystallographic structure of human TrkA extracellular segment in complex with NGF allowed bioinformatics analysis to support biochemical data.

The molecular docking of OligoGM1, purposely performed by exploring the interaction interface between TrkA and NGF, revealed that OligoGM1 is able to fit a space present between NGF and TrkA, tightly binding both simultaneously (figure R20).

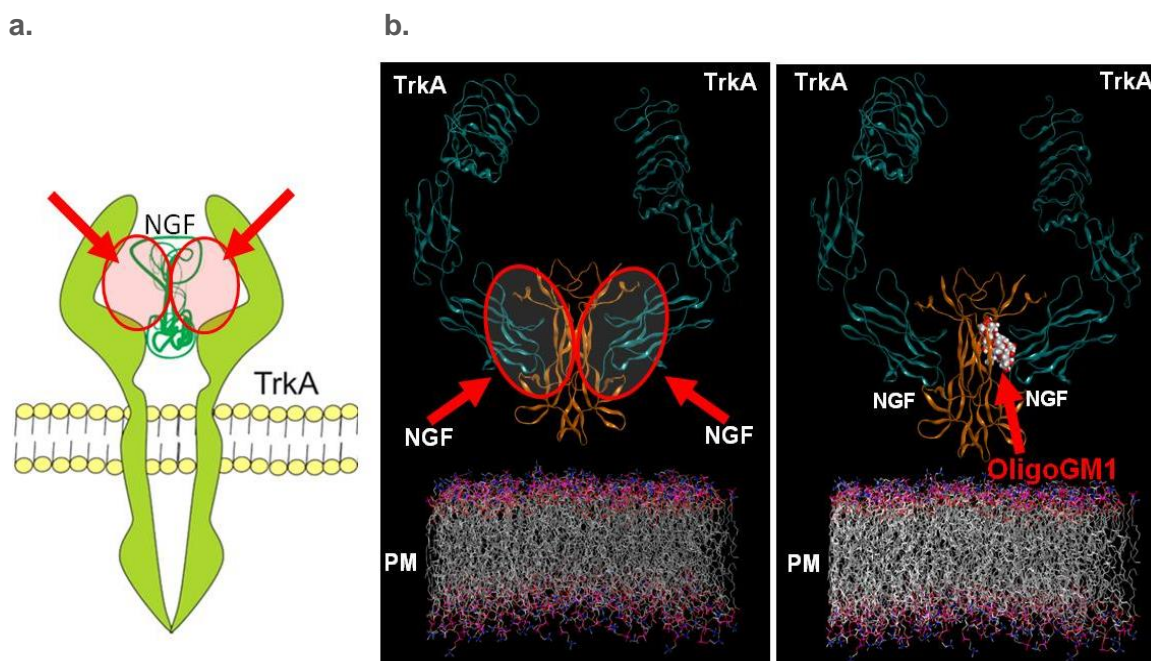


**Figure R20: prediction of OligoGM1-TrkA interaction.**

**a. Cartoon of TrkA-NGF complex.** TrkA receptor structure is resolved as a dimer in the presence of NGF, its natural ligand. A space occupied by water is circled in red.

**b. Crystallized structure of TrkA-NGF complex.** TrkA-NGF interaction is characterized by the presence of a space occupied by water (red circles). *In silico* analysis revealed that OligoGM1 fits perfectly within this space.



The presence of the oligosaccharide portion of GM1 into the TrkA-NGF complex changes the binding free energy from -7 kcal/mol (TrkA-NGF) to -11.3 kcal/mol (TrkA-OligoGM1-NGF) (Chiricozzi *et al.* 2017), (figure R21).

Obtained data suggested that the presence of OligoGM1 into the complex could stabilize the interaction among TrkA and NGF.

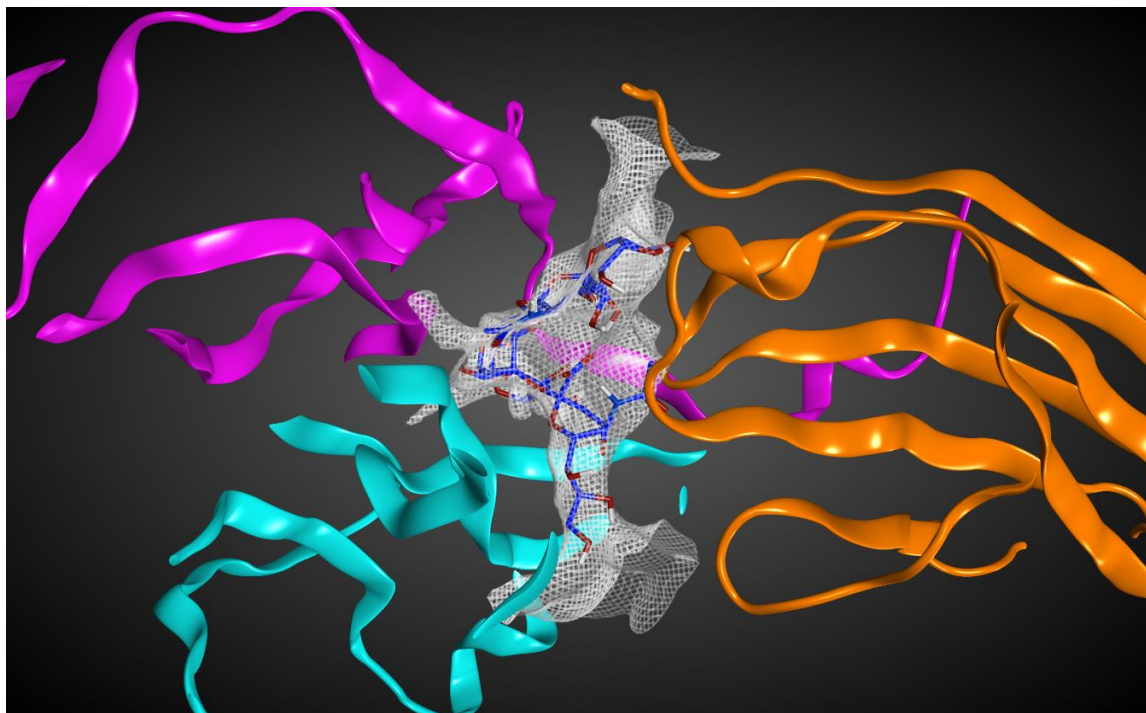


**Figure R21: Molecular dynamic calculations for the complex TrkA–nerve growth factor (NGF)–OligoGM1.** Top-scoring docking pose of OligoGM1 in the TrkA-NGF crystallographic complex. TrkA in orange ribbons; two NGF molecules: one in cyan ribbons and one in magenta ribbons. OligoGM1 is represented in sticks, with blue color for carbon atoms and red color for oxygen atoms. Van der Waals interaction surface between OligoGM1 and proteins is represented as a white mesh map.

The figure R22 shows the points of contact between NGF/TrkA and OligoGM1 as weakly bonds.

This findings further supported the results previously obtained regarding the not-covalent association of OligoGM1 to the cell surface.

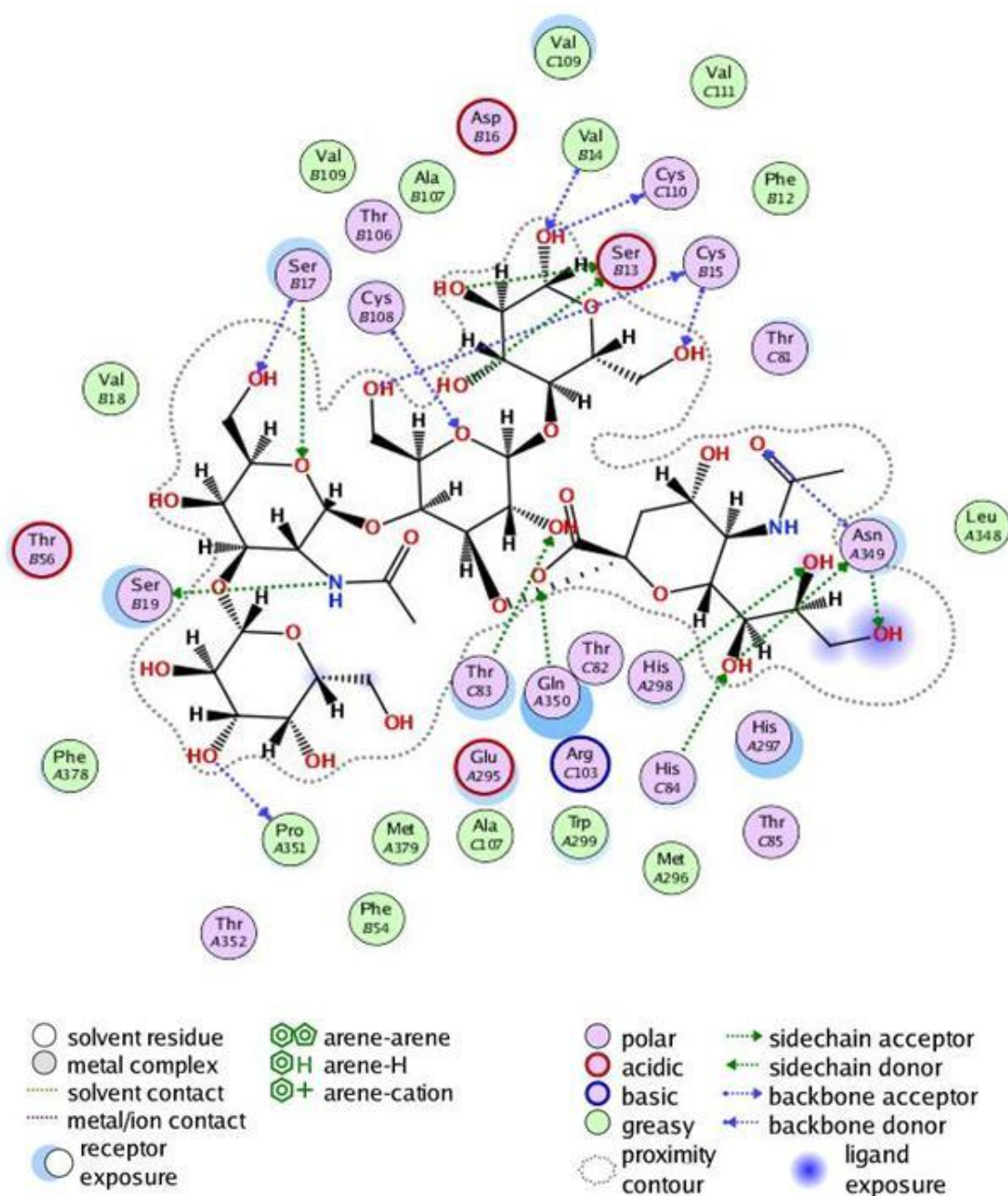


Figure R22: Points of contact between TrkA-NGF and OligoGM1. The weak bonds between OligoGM1 and TrkA-NGF complex.

# *Discussion*

Gangliosides are a large family of glycosphingolipids prevailing in nervous system cells representing averagely about one-sixth of the total lipid content of plasma membranes. They are components only of the outer membrane leaflet inserting through the hydrophobic ceramide within the lipid layer and protruding with the sialic acid-containing hydrophilic glycosidic chain in cell surrounding environment.

Gangliosides amphiphilicity and distinctiveness in elevated ratio between bulky sugar head and packed lipid moiety give them important constitutional features that allow their remarkable participation in lipid rafts separation and organization. The quantitative and qualitative specificity of lateral segregation of plasma membrane elements in lipid rafts is peculiarly related to the complexity of participating gangliosides affected in turn by the geometric properties of oligosaccharide chain.

Ganglioside structural influence on the assessment of plasma membrane microdomains, and in particular on protein recruitment, makes them also unavoidable players and mediators in cell signaling and regulatory pathways. The ceramide portion maintains and stabilizes ganglioside insertion in the core of lipid rafts, establishing hydrophobic interactions and providing a lateral functional dynamicity. The oligosaccharide facing toward the extracellular environment allowing specific side-to-side and head-to head recognition sites, favoring ganglioside-protein interactions, which lead to cell function modulation.

GM1 ganglioside has been abundantly studied and continually estimated because of its biological potential and attitude in modulation of neuronal activities. It is proved and described to be implicated in processes of cell differentiation, adhesion, migration, axon guidance and to take part in neurotrophic factor signaling, synaptic transmission, myelin genesis, and neuron–glia interactions (Schengrund 2015; Ledeen & Wu 2015; Aureli *et al.* 2016).

GM1-mediated neurodifferentiation has been investigated by *in vitro* and *in vivo* experiments (Facci *et al.* 1984; Lipartiti *et al.* 1991; Abad-Rodriguez *et al.* 2001; Da Silva *et al.* 2005; Mocchetti, 2005), but its proper molecular mechanism of action is still unclear.

The implication of oligosaccharide chain in physiological GM1-promoted neurodifferentiation have been hypothesized observing the neuritogenesis onset originated by two opposed experimental situations, enhancing or silencing Neu3 activity (Abad-Rodriguez *et al.* 2001; Da Silva *et al.* 2005; Valaperta *et al.* 2007). Moreover, the amplification of GM1 effects obtained with LIGA20, optimizing its availability to biological system by modifying only the fatty acid, but without altering the hydrophilic group (Schneider & Di Stefano, 1995; Saito *et al.* 1999; Wu *et al.* 2005), let believe in the oligosaccharide chain essential potential. Together these evidences support the idea of a qualitative GM1 impact on TrkA signaling, supposing a glycol-sensitive response carried by the receptor depending on the characteristic feature of the oligosaccharide chain.

The present thesis offers a perspective on the specific role of GM1 oligosaccharide in the process of GM1-mediated neurite elongation in murine neuroblastoma N2a cells. According to a biological meaning, ceramide would act as an aglycone, dynamically moving within the membrane layer and allowing different carbohydrate–protein interactions that are dependent on ganglioside content and membrane organization.

To realize the study, the preliminary step consisted in the preparation of GM1, Fuc-GM1, asialoGM1, GM2, and OligoGM3 oligosaccharides, GM1 tritiated derivatives, and GM1 tritiated-and-photoactivable derivatives following the chemical procedures reported in Methods section. Chromatography and MS analyses showed that the reaction products were pure (data not show).

Tritiated OligoGM1, [Gal-6-<sup>3</sup>H]OligoGM1, was added to culture medium in order to recognize the modality of association of GM1 oligosaccharide chain to the cells, according to the experimental techniques previously employed to investigate on GM1 behavior (Chigorno *et al.* 1985).

At 50  $\mu$ M concentration, OligoGM1 interacting to the cell could be completely detached by a greater affinity to serum proteins (figure R7). No detectable amount of OligoGM1 was taken up by the cells and no time influence could be underlined, conversely to the time-dependent GM1 attitude (Chigorno *et al.* 1985). The result suggests that the OligoGM1 fraction associated with the cell surface

remains in equilibrium with the free soluble form and certainly does not establish covalent linkage with cell protein domains.

The labile association of OligoGM1 to N2a cells, however, is able to reduced cell proliferation rate, without provoking any toxic reactions or alteration in cell viability (figure R1). The parallelism with GM1 impact on cell proliferation and knowing its properties on cell differentiation, a comparable effect appeared attributable to the oligosaccharide fraction.

Morphological analysis confirms differentiative properties exerted by GM1 oligosaccharide chains on N2a cells. In fact, OligoGM1 produced neurite sprouting as well as GM1 (figure R2). The neurite elongation is accompanied by the increase in neurofilament protein expression (figure R5 and R6). Accounting that neuritogenesis, neurite outgrowth and neurofilament protein expression are considered markers of neuronal differentiation (Fukuda *et al.* 2014), the effect exerted by OligoGM1 on N2a cells can be overlapped to the previously reported for ganglioside GM1 (Facci *et al.* 1984).

Moreover, the structure-specificity of OligoGM1 effect was demonstrated. As a matter of fact, residues of the total structure, such as sialic acid, galactose, OligoGM3, OligoGM2 or asialo-OligoGM1 did not show neuritegenic property (figure R3), at least at the used concentration. On the other hand, fucosylated OligoGM1 induces neurite sprouting (figure R4), suggesting that the terminal  $\alpha$ -Fuc-(1-2)- $\beta$ -Gal linkage does not alter the glycosil conformation of oligosaccharide chain required by the cells to activate neurite outgrowth signaling. This evidence agrees with a previous data describing similar binding constant showed by GM1 and Fuc-GM1 for cholera toxin (Masserini *et al.* 1992).

The positive correlation between the presence of GM1-enriched membrane domains and nerve growth factor receptor TrkA activity and, inversely, the loosing in TrkA pathway-related functions due to the absence of ganglioside GM1 (Ferrari *et al.* 1995; Mutoh *et al.* 1995; Farooqui *et al.* 1997; Mutoh *et al.* 1998; Abad-Rodriguez *et al.* 2001; Bachis *et al.* 2002; Da Silva *et al.* 2005) have been above reported.

TrkA autophosphorylation at the level of tyrosine 490 residue induces the activation of downstream cascade effective in cell differentiation promotion (Huang & Reichardt, 2003; Brodeur *et al.* 2009). Previous finding revealed the GM1

influence in the activation of the TrkA-Erk1/2 pathway (Farooqui *et al.* 1997; Singleton *et al.* 2000; Duchemin *et al.* 2002; Zakharova *et al.* 2014).

Thus, the present study investigate the involvement of TrkA-Erk1/2 pathway in OligoGM1-mediated neurodifferentiation.

The TrkA-Erk1/2 pathway activation was determined evaluating phosphorylation levels following the addition of OligoGM1 to N2a cells. For the first time, OligoGM1 was proved to enhance the phosphorylation of Tyr490 of TrkA and of Erk1/2 leading to neurodifferentiation (figure R8 and R9). The supposed mechanism of action is shown in figure D1.

The examination of time course pathway phosphorylation revealed a correspondence in the signaling stimulation between OligoGM1 and GM1, evidencing the oligosaccharide portion as a necessary and sufficient condition to promote neurodifferentiation by TrkA activation (figure R10 and R11).

TrkA receptor activity is inhibited (figure R12) or its expression was silenced (figure R14) in order to verify the OligoGM1–TrkA interaction requirement for initiate differentiation process. In both experiments, the N2a feeding with OligoGM1 did not promote neurite sprouting nor reduced the cell proliferation (figure R13 and R15).

These result support that the debated GM1 neurodifferentiative impact is really mediated by an interaction with TrkA receptor, that, in particular, appears at the expense of the oligosaccharide portion.

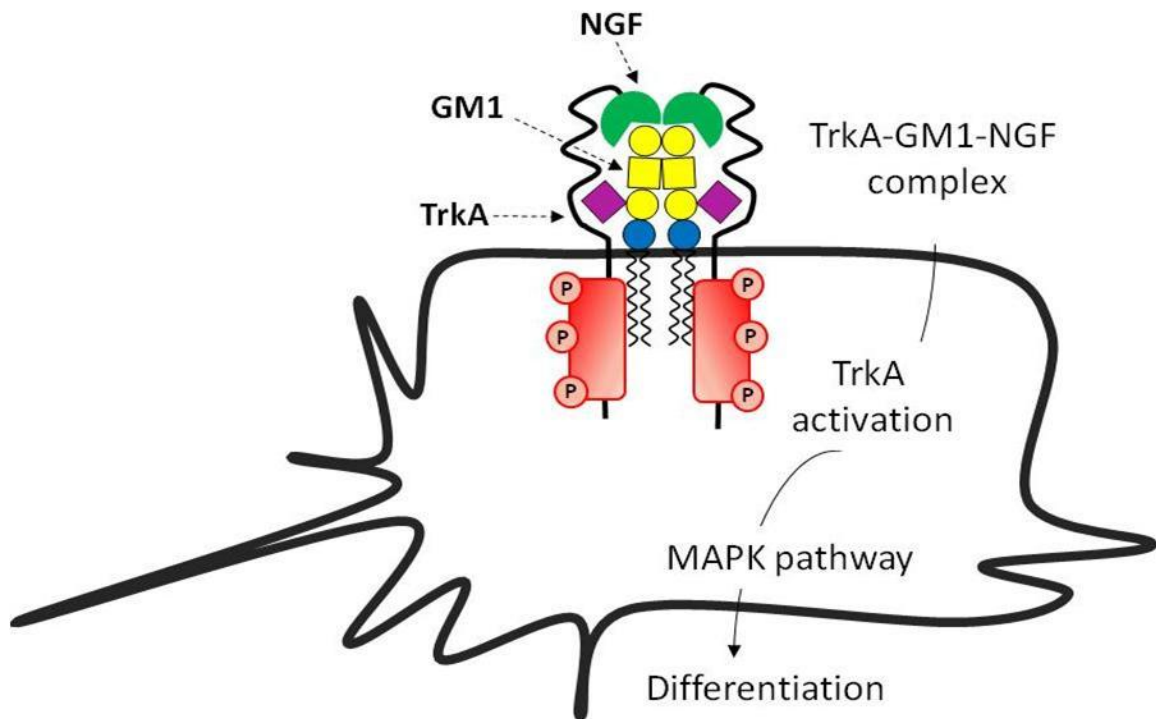


**Figure D1: Purposed mechanism for GM1-mediated neurodifferentiation in Neuro2a cells.** TrkA autophosphorylation is regulated by GM1-enriched receptor environment. GM1 modulates TrkA activity by stabilizing the TrkA-nerve growth factor (NGF) complex with its oligosaccharide portion. The TrkA-GM1 interaction is represented as a side-by-side interaction. GM1 triggers the phosphorylation of Tyr490 promoting the differentiation signaling.



In order to obtain a clarification about a possible direct interaction between the oligosaccharide portion of GM1 and TrkA receptor, different radiolabeled and photoactivable GM1 derivatives were employed to treat N2a cells. In particular, in addition to the azide-conjugated OligoGM1, [Gal-6-<sup>3</sup>H]OligoGM1(Glc-N<sub>3</sub>), two different GM1 derivatives, [Gal-6-<sup>3</sup>H]GM1(Cer-N<sub>3</sub>), photoactivable on sphingosine and [Sph-3-<sup>3</sup>H]GM1(Gal-N<sub>3</sub>), photoactivable on the last galactose residue, were employed to discriminate the N2a proteins interacting with the ceramide and with oligosaccharide chain respectively. In fact the photosensitive azide can be activated by UV radiation in nitrene, an unstable compound that covalently linked neighboring molecules. The used approach allows to identify proteins linked to these photoactivate compounds thanks to the simultaneously radiolabeling.

Photolabeling experiments with photoactivable glycosphingolipids were introduced several years ago (Loberto *et al.* 2003; Mauri *et al.* 2003) and permit to identify the interaction of glycosphingolipids with different proteins such as the insulin receptor (Kabayama *et al.* 2007), the receptor CD9 (Ono *et al.* 2001), the cytoskeleton tubulin (Palestini *et al.* 2000), the membrane protein caveolin 1 (Fra *et al.* 1995), the kinase Lyn (Chiricozzi *et al.* 2015), and the neuronal protein TAG1 (Loberto *et al.* 2003).

After incubation with the tritium-labeled photoactivable GM1 derivatives, cells were washed once with PBS to remove the non-cell-associated compound and following exposed to UV-light. According to the mechanism described above and recalling that the exogenous OligoGM1 does not become component of the cell membranes, any interaction of the [Gal-6-<sup>3</sup>H]OligoGM1(Glc-N<sub>3</sub>) with proteins yields to tritium-labeled OligoGM1-protein stable complexes that should involve the extracellular domain of transmembrane proteins or of GPI-anchored proteins. Regarding the interaction with GM1 derivatives and proteins, the difference in tritium-labeled GM1-protein stable complexes reflect the discriminate interaction of the ceramide and oligosaccharide with proteins. By SDS-PAGE separation, followed by radioimaging of the blotted material, few bands were recognized. For [Gal-6-<sup>3</sup>H]OligoGM1(Glc-N<sub>3</sub>) and [Sph-3-<sup>3</sup>H]GM1(Gal-N<sub>3</sub>) samples one of these bands showed a molecular mass of 140 KDa. A specific signal for TrkA was found overlapping the 140 KDa radiolabeled

band, in relation to the proteins derived from [Gal-6-<sup>3</sup>H]OligoGM1(Glc-N<sub>3</sub>) and [Sph-3-<sup>3</sup>H]GM1(Gal-N<sub>3</sub>) treated samples, suggesting a direct interaction between the oligosaccharide portion of GM1 and TrkA receptor (figure R18 and R19). On the other hand, no correspondence between a radiolabeled band and TrkA signal is revealed by the proteins of [Gal-6-<sup>3</sup>H]GM1(Cer-N<sub>3</sub>) treated sample (figure R17), supporting the idea that the portion of GM1 responsible of structural and functional association to TrkA is the oligosaccharide chain.

Over these experimental data, a molecular modeling tools was used to predict whether OligoGM1 can increase the TrkA-NGF complex stability, favoring their intermolecular interactions. Even if NGF is not expressed by N2a cells, it takes place in our experimental conditions since the culture medium contains serum (Leon *et al.* 1994).

The first step is the resolution of TrkA receptor crystallized structure, a dimer in the presence of NGF. The crystal structure of the TrkA-NGF complex is characterized by a pocket, which can be occupied by water molecules, as showed in crystallographic structure of the same complex (PDB ID: 1WWW), in figure R20a. *In silico* analysis revealed that OligoGM1 perfectly fits within this space (figure R21). Moreover, the energy associated to the TrkA-NGF complex, approx. 6.6 kcal/mol, becomes approx. 11.5 kcal/mol when OligoGM1 belongs to the complex.

The supposition expecting a OligoGM1 stabilization of the TrkA-NGF interaction, and a specific molecular recognition process between OligoGM1 and a specific extracellular domain of the TrkA receptor. According to weakly association of OligoGM1 to the cell surface, no covalent bounds between OligoGM1 and TrkA-NGF complex were found (figure R21).

Literature information clearly report that any experimental model capable to modify the local plasma membrane GM1 content, promotes N2a differentiation. GM1 is a natural amphiphilic compound with a structure that combines the ceramide lipid moiety with the soluble oligosaccharide chain. Altogether, the results obtained in this study, underlined GM1 oligosaccharide structural responsibility in enhancing neurodifferentiative properties exerted by GM1 (figure D1).

The GM1 oligosaccharide directly interacts with TrkA receptor resulting in TrkA-mediated neuritogenesis (Chiricozzi *et al.* 2017). Neuronal differentiation is characterized by an enhancement of several glycosyltransferases activity resulting in augmenting of PM ganglioside content (Aureli *et al.* 2011). According to reported findings, ceramide act physiologically as an aglycone essential for protrusion of glycan residues into the extracellular environment where interaction with functional proteins occurs. In this way, GM1 exhibits its oligosaccharide chain to the TrkA receptor. Molecular dynamic calculations confirm that the GM1 oligosaccharide perfectly fits with a TrkA domain stabilizing the TrkA-NGF interaction, allowing a rapid auto phosphorylation of the receptor cytosolic portion.

Finally, rather than to a broad plasma membrane increase of GM1, OligoGM1-TrkA interaction is attributable to a plasma membrane reorganization, that originate a local GM1-enriched microdomains, among which TrkA is segregated and environment is suitable for the recognition.

# *References*

- Abad-Rodriguez J, Piddini E, Hasegawa H, Miyagi T, and Dotti CG (2001) Plasma membrane ganglioside sialidase regulates axonal growth and regeneration in hippocampal neurons in culture. *J Neurosci.* 21:8387–8395.
- Acquotti D, Poppe L, Dabrowski J, von der Lieth CW, Sonnino S, and Tettamanti G (1990) Three-dimensional structure of the oligosaccharide chain of ganglioside revealed by distance mapping procedure: a rotating and laboratory frame nuclear Overhauser enhancement investigation of native glycolipid in dimethyl sulfoxide and in water-dodecylphosphocholine solution. *J Am Chem Soc.* 112:7772–7778.
- Acquotti D, Cantù L, Ragg E, and Sonnino S (1994) Geometrical and conformational properties of ganglioside GalNAc-GD1a, IV4GalNAcIV3Neu5AcII3Neu5AcGgOse4Cer. *Eur J Biochem.* 225:271–288.
- Arita M, Tsuji S, Omatsu M, and Nagai Y (1984) Studies on Bioactive Gangliosides: II. Requirement of Ganglioside GD1a for Prolonged GQ1b-Drive Nerve Growth Promotion in Neuroblastoma Cell Lines. *J Neur Res.* 12:289–297.
- Atukorale PU, Yang YS, Bekdemir A, Carney RP, Silva PJ, Watson N, Stellacci F, and Irvine DJ (2015) Influence of the glycocalyx and plasma membrane composition on amphiphilic gold nanoparticle association with erythrocyte. *Nanoscale.* 7:11420–11432.
- Aureli M, Loberto N, Lanteri P, Chigorno V, Prinetti A, and Sonnino S (2011) Cell surface sphingolipid glycohydrolase in neuronal differentiation and aging in culture. *J Neurochem.* 116(5):891–899.
- Aureli M, Mauri L, Ciampa MG, Prinetti A, Toffano G, Secchieri C, and Sonnino S (2016) GM1 Ganglioside: Past Studies and Future Potential. *Mol Neurobiol.* 53:1824–1842.
- Bachis A, Rabin SJ, Del Fiacco M, and Mocchetti I (2002) Ganglioside prevent excitotoxicity through activation of TrkB receptor. *Neurotox Res.* 4:225–234.
- Barrat DG, Rogers JD, Sharom FJ, and Gran CWM (1978) Direct modification of the glycocalyx of a cultured muscle cell line by incorporation of foreign gangliosides and an integral membrane glycoprotein. *J Cell Biochem.* 8(1):119–128.
- Basu S & Basu M (1982) in *The Glycoconjugates*, ed. Horowitz M. (Academic, New York) 3:265–285.
- Berridge MV, Tan AS, McCoy KD, Kansara M, and Rudert F (1996) CD95 (Fas/Apo-1)-induced apoptosis results in loss of glucose transporter function. *J Immunol.* 156(11):4092–4099.
- Bertoli E, Masserini M, Sonnino S, Ghidoni R, Riccardo, Cestaro B, and G Tettamanti (1981) Electron paramagnetic resonance studies on the fluidity and surface dynamics of egg phosphatidylcholine vesicles containing gangliosides. *Biochem Biophys Acta.* 2(6):196–202.
- Biarc J, Chalkley RJ, Burlingame AL, and Bradshaw RA (2012) The Induction of Serine/Threonine Protein Phosphorylations by a PDGFR/TrkA Chimera in Stably Transfected PC12 Cells. *Mol Cell Proteomics.* 11(5):15–30.
- Biarc J, Chalkley RJ, Burlingame AL, and Bradshaw RA (2013) Dissecting the Roles of Tyrosines 490 and 785 of TrkA Protein in the Induction of Downstream Protein Phosphorylation Using Chimeric Receptors. *J Biol Chem.* 288(23):16606–16618.
- Borges AR, Wieczorek L, Johnson B, Benesi AJ, Brown BK, Kensinger RD, Krebs FC, Wigdahl B, Blumenthal R, Puri A, FE McCutchan, DL Birx, VR Polonis, and CL Schengrund (2010) Multivalent dendrimeric compounds containing carbohydrates

- expressed on immune cells inhibit infection by primary isolates of HIV-1. *Viol.* 408(1):80–88.
- Brocca P, Acquotti D and Sonnino S (1993)  $^1\text{H-NMR}$  study on ganglioside amide protons: evidence that the deuterium exchange kinetics are affected by the preparation of samples. *Glycoconj J.* 10(6):441–446.
- Brocca P, Berthault P, and Sonnino S (1998) Conformation of the Oligosaccharide Chain of GM1 Ganglioside in a Carbohydrate-Enriched Surface. *Biophys J.* 74(1):309–318.
- Brocca P, Bernardi A, Raimondi L, and Sonnino S (2000) Modeling ganglioside headgroups by conformational analysis and molecular dynamics. *Glycoconj J.* 17(5):283–299.
- Brodeur GM, Minturn JE, Ho R, Simpson AM, Iyer R, Varela CR, Light JE, Kolla V, and Evans AE Trk receptor expression and inhibition in neuroblastomas (2009) *Clin Cancer Res.* 15(10):3244-50. Cantù L, Corti M, Sonnino S, and Tettamanti G (1986) Light scattering measurements on gangliosides: dependence of micellar properties on molecular structure and temperature. *Chem Phys Lipids.* 41:315–328.
- Cantù L, Corti M, and Salina P (1991) Direct measurement of the formation time of mixed micelles. *J Phys Chem.* 95:5981–5983.
- Cantù L, Del Favero E, Sonnino S, and Prinetti A (2011) Gangliosides and the multiscale modulation of membrane structure. *Chem Phys Lipids.* 164:796–810.
- Chao MV (1992) Growth factor signaling: Where is the specificity? *Cell.* 68(6):995–997.
- Chigorno V, Pitto M, Cardace G, Acquotti D, Kirschner G, Sonnino S, Ghidoni R, and Tettamanti G (1985) Association of Gangliosides to Fibroblasts in Culture: A Study Performed with  $^{14}\text{C}$ -labelled at the Sialic Acid Acetyl Group. *Glycoconj J.* 2:279–291.
- Chigorno V, Valsecchi M, Acquotti D, Sonnino S, and Tettamanti G.(1990) Formation of a cytosolic ganglioside-protein complex following administration of photoreactive ganglioside GM1 to human fibroblasts in culture. *FEBS Lett.* 263:329–331.
- Chiricozzi E, Ciampa MG, Brasile G, Compostella F, Prinetti A, Nakayama H, Ekyalongo RC, Iwabuchi K, Sonnino S, and Mauri L (2015) Direct interaction, instrumental for signaling processes, between LacCer and Lyn in the lipid rafts of neutrophil-like cells. *J Lipid Res.* 56(1):129–141.
- Chiricozzi E, Pomè YD, Maggioni M, Di Biase E, Parravicini C, Palazzolo L, Loberto N, Eberini I, and Sonnino S (2017) Role of the GM1 Ganglioside Oligosaccharide portion in the TrkA-dependent neurite sprouting in neuroblastoma cells. *J Neurochem.* 143(6):645–659.
- Cordon-Cardo C, Tapley P, Jing S, Nanduri V, O'Rourke E, Lamballe F, Kovary K, Klein R, Jones KR, Reichardt LF, and Barbacid M (1991) The trk Tyrosine Protein Kinase Mediates the Mitogenic Properties of Nerve Growth Factor and Neurotrophin-3. *Cell.* 66(1):173–183.
- Coskun U & Simons K (2011) Cell membranes: the lipid perspective. *Structure.* 19(11):1543–1548.
- Cowley S, Paterson H, Kemp P, and Marshall CJ. (1994) Activation of MAP kinase is necessary and sufficient for PC12 differentiation and for transformation of NIH 3T3 cells. *Cell.* 77(6):841–852.
- D'Ambrosi N, Murra B, Cavaliere F, Amadio S, Bernardi G, Burnstock G, and Volonté C. (2001) Interaction between ATP and nerve growth factor signalling in the survival and neuritic outgrowth from PC12 cells. *Neurosci.* 108(3):527–534.

- Da Silva JS, Hasegawa T, Miyagi T, Dotti CG, and Abad-Rodriguez (2005) Asymmetric membrane ganglioside sialidase activity specifies axonal fate. *Nat Neurosci.* 8(5):606–615.
- Damani KP, Barone S, Mundy WR (2003) Methylmercury decreases NGF-induced TrkA autophosphorylation and neurite outgrowth in PC12 cells. *Brain Res Dev Brain Res.* 141:71–81.
- Denham DA, Dennis DT, Ponnudurai T, Nelson GS, and Guy F (1971) Comparison of a counting chamber and thick smear methods of counting microfilariae. *Trans R Soc Trop Med Hyg.* 65(4):521–526.
- Dietrich C, Bagatolli LA, Volovyk ZN, Thompson NL, Levi M, Jacobson K, and Gratton E (2001) Lipid rafts reconstituted in model membranes. *Biophys J.* 80(3):1417–1428.
- Dong L, Liu Y, Colberg-Poley AM, Kaucic K, and Ladisch S (2002) Induction of GM1a/GD1b synthase triggers complex ganglioside expression and alters neuroblastoma cell behavior; a new tumor cell model of ganglioside function. *Glyconj J.* 28:137–147.
- Duchemin AM, Ren Q, Mo L, Neff NH, and Hadjiconstantinou M (2002) GM1 ganglioside induces phosphorylation and activation of Trk and Erk in brain. *J Neurochem.* 81(4):696–707.
- Eggert A, Ikegaki N, Liu X, Chou TT, Lee VM, Trojanowski JQ, and Brodeur GM (2000) Molecular dissection of TrkA signal transduction pathways mediating differentiation in human neuroblastoma cells. *Oncogene.* 19(16):2043–2051.
- Ewers H, Römer W, Smith AE, Bacia K, Dmitrieff S, Chai W, Mancini R, Kartenbeck J, Chambon V, Berland L, Oppenheim A, Schwarzmann G, Feizi T, Schwille P, Sens P, Helenius A, and Johannes L. (2010) GM1 structure determines SV40-induced membrane invagination and infection. *Nat Cell Biol.* 12(1):11–18.
- Facci L, Leon A, Toffano G, Sonnino S, Ghidoni R, and Tettamanti G (1984) Promotion of Neuritogenesis in Mouse Neuroblastoma Cells by Exogenous Gangliosides. Relationship Between the Effect and the Cell Association of Ganglioside GM1. *J Neurochem.* 42(2):299–305.
- Fang Y, Wu G, Xie X, Lu ZH, and Ledeen RW (2000) Endogenous GM1 Ganglioside of the Plasma Membrane Promotes Neuritogenesis by Two Mechanisms. *Neurochem Res.* 25(7):931–940.
- Fantini J, Carlus D, Yahi N. (2011). The fusogenic tilted peptide (67–78) of  $\alpha$ -synuclein is a cholesterol binding domain. *Biochim Biophys Acta.* 1808:2343–2351.
- Fantini J, Yahi N, and Garmy N (2013) Cholesterol accelerates the binding of Alzheimer's  $\beta$ -amyloid peptide to ganglioside GM1 through a universal hydrogen-bond-dependent sterol tuning of glycolipid conformation. *Front Physiol.* 4:120.
- Farooqui T, Franklin T, Pearl DK, and Yates AJ (1997) Ganglioside GM1 enhances induction by nerve growth factor of a putative dimer of TrkA. *J Neurochem.* 68:2348–2355.
- Ferrari G, Anderson BL, Stephens RM, Kaplan DR, and Greene LA (1995) Prevention of apoptotic neuronal death by GM1 ganglioside. Involvement of Trk neurotrophin receptors. *J Biol Chem.* 270:3074–3080.
- Fra AM, Masserini M, Palestini P, Sonnino S, and Simons K (1995) A photo-reactive derivative of ganglioside GM1 specifically cross-links VIP21-caveolin on the cell surface. *FEBS Lett.* 375:11–14.

- Fueshko SM & Schengrund CL (1992) Identification of a GM1-binding protein on the surface of murine neuroblastoma cells. *J Neurochem.* 59(2):527–535.
- Fukuda M, Gotoh Y, Tachibana T, Dell K, Hattori S, Yoneda Y, and Nishida E (1995) Induction of neurite outgrowth by MAP kinase in PC12 cells. *Oncogene.* 11(2):239–244.
- Fukuda Y, Fukui T, Hikichi, C, Ishikawa T, Murate K, Adachi T, Imai H, Fukuhara K, Ueda A, Kaplan AP, and Mutoh T (2014) Neurotrophin promotes NGF signaling through interaction of GM1 ganglioside with Trk neurotrophin receptor in PC12 cells. *Brain Res.* 1596:13–21.
- Furukawa K, Ohmi Y, Ohkawa Y, Tokuda N, Kondo Y, Tajima O, and Furukawa K (2011) Regulatory mechanisms of nervous systems with glycosphingolipids. *Neurochem Res.* 36:1578–1586.
- Ghidoni R, Sonnino S, Tettamanti G, Wiegandt H, and Zambotti V (1976) On the structure of two new gangliosides from beef brain. *J Neurochem.* 27:511–515.
- Ghidoni R, Sonnino S, Masserini M, Orlando P, and Tettamanti G (1981) Specific tritium labeling of gangliosides at the 3-position of sphingosines. *J Lipid Res.* 22(8):1286–1295.
- Ghidoni R, Fiorilli A, Trinchera M, Venerando B, Chigorno V, and Tettamanti G (1989) Uptake, cell penetration and metabolic processing of exogenously administered GM1 ganglioside in rat brain. *Neurochem Int.* 4:455–465.
- Hakomori S (1983) Glycosphingolipids as receptors in *Handbook of Lipid Research*, ed. Kanfer JN & Hakomori S. (Plenum, New York) 3: 437–471.
- Hakomori S, Handa K, Iwabuchi K, Yamamura S, and Prinetti A (1998) New insights in glycosphingolipid function: 'glycosignaling domain', a cell surface assembly of glycosphingolipids with signal transducer molecules, involved in cell adhesion coupled with signaling. *Glycobiol.* 8(10) xi–xix.
- Hansson HA, Holmgren J, and Svennerholm L (1977) Ultrastructural localization of cell membrane GM1 ganglioside by cholera toxin. *PNAS.* 74(9):3782–3786.
- Hasegawa T, Yamaguchi K, Wada T, Takeda A, Itoyama Y, and Miyag T (2000) Molecular Cloning of Mouse Ganglioside Sialidase and Its Increased Expression in Neuro2a Cell Differentiation. *J Biol Chem.* 275:8007–8015.
- Holmgren J, Lonnroth I, and Svennerholm L (1973) Tissue receptor for cholera exotoxin: postulated structure from studies with GM1 ganglioside and related glycolipids. *Infect Immun.* 8:208–214.
- Huang EJ & Reichardt LF (2003) Trk receptors: roles in neuronal signal transduction. *Annu Rev Biochem.* 72:609–42.
- Ichikawa N, Iwabuchi K, Kurihara H, Ishii K, Kobayashi T, Sasaki T, Hattori, Mizuno Y, Hozumi K, Yamada Y, and Arikawa-Hirasawa E (2009) Binding of laminin-1 to monosialoganglioside GM1 in lipid rafts is crucial for neurite outgrowth. *J Cell Sci.* 8:208–214.
- Iglesias-Bartolomé R, Trenchi A, Comín R, Moyano AL, Nores GA, and Daniotti JL (2009) Differential endocytic trafficking of neuropathy-associated antibodies to GM1 ganglioside and cholera toxin in epithelial and neural cells. *Biochim Biophys Acta.* 1788(12):2526–2540.
- IUPAC-IUB Joint Commission on Biochemical Nomenclature (JCoBN, 1998). Nomenclature of glycolipids. Recommendations 1997. *Eur. J. Biochem.* 257:293–298.



- IUPAC-IUBMB JCoBN (1998) Nomenclature of glycolipids. *Carbohydr Res.* 312: 167–175.
- Kabayama K, Sato T, Saito K, Loberto N, Prinetti A, Sonnino S, Kinjo M, Igarashi Y, Inokuchi J (2007) Dissociation of the insulin receptor and caveolin-1 complex by ganglioside GM3 in the state of insulin resistance. *Proc Natl Acad Sci USA.* 104(34):13678–13683.
- Kaji R & Kimura J (1999) Facts and fallacies on anti-GM1 antibodies: physiology of motor neuropathies. *Brain.* 122(5):797–798.
- Kappagantula S, Andrews MR, Cheah M, Abad-Rodriguez J, Dotti CG, and Fawcett JW (2014) Neu3 sialidase-mediated ganglioside conversion is necessary for axon regeneration and is blocked in CNS axons. *J Neurosci.* 34(7):2477–2492.
- Karlsson KA (1970) On the chemistry and occurrence of sphingolipid long-chain bases. *Chem Phys Lipids.* 5(1):6–43.
- Kharlamov A, Guidotti A, Costa E, Hayes R, and Armstrong D (1993) Semisynthetic sphingolipids prevent protein kinase C translocation and neuronal damage in the perifocal area following a photochemically induced thrombotic brain cortical lesion. *J Neurosci.* 13:2483–2494.
- Khatun UL, Gayen A, and Mukhopadhyay C (2014). Capability of ganglioside GM1 in modulating interactions, structure, location and dynamics of peptides/proteins: biophysical approaches. *Glycoconj J.* 31:435–467.
- Kiarash A, Boyd B, Lingwood CA (1994). Glycosphingolipid receptor function is modified by fatty acid content. Verotoxin 1 and verotoxin 2c preferentially recognize different globotriaosyl ceramide fatty acid homologues. *J Biol Chem.* 269:11138–11146.
- Klenk E (1942) Über die Ganglioside, eine neue Gruppe von zuckerhaltigen Gehirnlipoiden. *Z Physiol Chem.* 273:76–86.
- Kolter T, Proia RL, Sandhoff K (2002) Combinatorial ganglioside biosynthesis. *J Biol Chem.* 277:25859–25862.
- Kolter T (2004) Glycosphingolipids in *Bioactive Lipids*, ed. Nicolaou A & Kokotos G. (The Oily, Bridgewater) 169–196.
- Kolter T (2012) Ganglioside Biochemistry. *ISRN Biochem.* 506160.
- Kraft ML (2013). Plasma membrane organization and function: moving past lipid rafts. *Mol Biol Cell.* 24:2765–2768.
- Kuhn R & Wiegandt H (1963) Die Konstitution der Ganglio-N-tetraose und des Gangliosids Gl. *Chem Ber.* 96(3):866–880.
- Kuziemko GM, Stroh M, and Stevens RC (1996) Cholera toxin binding affinity and specificity for gangliosides determined by surface plasmon resonance. *Biochem.* 35(20):6375–6384.
- Kwak DH, Yu K, Kim SM, Lee DH, Kim SM, Jung JU, Seo JW, Kim N, Lee S, Jung KY, You HK, Kim HA, and Choo YK (2006) Dynamic changes of gangliosides expression during the differentiation of embryonic and mesenchymal stem cells into neural cells. *Exp Mol Med.* 38:668–676.
- Ladisch S & Liu Y, (2014) Dynamic Aspects of Neural Tumour Gangliosides in *Glycobiology of the Nervous System*, ed. Schengrund CL & Yu R. (Springer, New York) 501–516.

- Lavenius E, Gestblom C, Johansson I, Nanberg E, and Pahlman S (1995) Transfection of TRK-A into human neuroblastoma cells restores their ability to differentiate in response to nerve growth factor. *Cell Growth Differ.* 6(6):727–736.
- Ledeen RW (1984) Biology of gangliosides: Neuritogenic and neuronotrophic properties. *J Neurosci Res.*
- Ledeen RW, Wu GS, Lu ZH, Kozireski-Chubak D, and Fang Y (1998) The role of GM1 and other gangliosides in neuronal differentiation - overview and new findings. *Ann NY Acad Sci.* 845:341–348.
- Ledeen RW & Wu G. (2009) Neurobiology meets glycosciences in *The Sugar Code. Fundamentals of glycosciences*, ed Gabius HJ. (Wiley-VCH, Weinheim) 495–516.
- Ledeen RW & Wu G (2015) The multi-tasked life of GM1 ganglioside, a true factotum of nature. *Trends Biochem Sci.* 40:407–418.
- Lemmon MA & Schlessinger J (2010) Cell Signaling by Receptor Tyrosine Kinases. *Cell.* 141(7):1117–1134.
- Leon A, Facci L, Toffano G, Sonnino S, Tettamanti G (1981) Activation of (Na<sup>+</sup>, K<sup>+</sup>)-ATPase by nanomolar concentrations of GM1 ganglioside. *J Neurochem.* 37(2):350–357.
- Leon A, Facci L, Benvegnù D, and Toffano G. (1982) Morphological and biochemical effects of gangliosides in neuroblastoma cells. *Dev Neurosci.* 5(1):108–114.
- Leon A, Buriani A, Dal Toso R, Fabris M, Romanello S, Aloe L, and Levi-Montalcini R (1994) Mast cells synthesize, store, and release nerve growth factor. *Proc Natl Acad Sci USA.* 91(9):3739–43.
- Levine JM & Flynn P (1986) Cell surface changes accompanying the neural differentiation of an embryonal carcinoma cell line. *J Neurosci.* 6(11):3374–3384.
- Linnartz B & Neumann H (2013) Microglial activatory (immunoreceptor tyrosine-based activation motif)- and inhibitory (immunoreceptor tyrosine-based inhibition motif) signaling receptors for recognition of the neuronal glycocalyx. *Glia.* 61(1):37–46.
- Linnarts-Gerlach B, Kopatz J, and Neumann H (2014) Siglec functions of microglia. *Glycobiol.* 24:794–799.
- Lingwood, CA (2000) A holistic approach to glycolipid function; is the lipid moiety important? *Trends Glycosci Glycotechnol.* 12:7–16.
- Lipartiti M, Lazzaro A, Zanoni R, Mazzari S, Toffano G, and Leon A (1991) Monosialoganglioside GM1 reduces NMDA neurotoxicity in neonatal rat brain. *Exp Neurol.* 113:301–305.
- Loberto N, Prioni S, Prinetti A, Ottico E, Chigorno V, Karagogeos D, and Sonnino S (2003) The adhesion protein TAG-1 has a ganglioside environment in the sphingolipid-enriched membrane domains of neuronal cells in culture. *J Neurochem.* 85(1):224–233.
- Lubineau A, Bouchain G, and Y Queneau (1995) Reactivity of the carbonyl group in water. Generation of azomethine ylides from aqueous formaldehyde: Michael addition versus dipolar trapping. *J Chem Soc.* 24:2433–2437.
- Maggio B, Cumar FA, Caputto R (1981) Molecular behaviour of glycosphingolipids in interfaces Possible participation in some properties of nerve membranes. *Biochim Biophys Acta.* 650:69–87.
- Malchiodi-Albedi F, Paradisi S, Matteucci A, Frank C, and Diociaiuti M (2011) Amyloid Oligomer Neurotoxicity, Calcium Dysregulation, and Lipid Rafts. *Int J Alzheimers Dis.* 2011:906964.

- Mao AJ, Bechberger J, Lidington D, Galipeau J, Laird DW, and Naus CG (2000) Neuronal Differentiation and Growth Control of Neuro-2a Cells After Retroviral Gene Delivery of Connexin43. *J Biol Chem.* 275:34407–34414.
- Masserini M, Freire E, Palestini P, Calappi E, and Tettamanti G (1992) Fuc-GM1 ganglioside mimics the receptor function of GM1 for cholera toxin. *Biochem.* 31:2422–2426.
- Mauri L, Prioni S, Loberto N, Chigorno V, Prinetti A, and Sonnino S (2003) Synthesis of radioactive and photoactivable ganglioside derivatives for the study of ganglioside-protein interactions. *Glycoconj J.* 20(1)11–23.
- Mehlen P, Mehlen A, Godet J, and Arrigo AP (1988) Hsp27 as a Switch between Differentiation and Apoptosis in Murine Embryonic Stem Cell. *J Biol Chem.* 272: 31657–31665.
- Merrill AH, (1991) Cell regulation by sphingosine and more complex sphingolipids. *J Bioenerg Biomembr.* 23:83–104.
- Merrill AH (2011) Sphingolipid and glycosphingolipid metabolic pathways in the era of sphingolipidomics. *Chem Rev.* 111:6387–6422.
- Merrill AH & Sandhoff K (2002) Sphingolipids: metabolism and cell signalling in *Biochemistry of Lipids, Lipoproteins and Membranes*, ed Vance DE & Vance J. (Elsevier, Amsterdam) 373–407.
- Milani D, Minozzi MC, Petrelli L, Guidolin D, Skaper SD, and Spoerri PE (1992) Interaction of ganglioside GM1 with the B subunit of cholera toxin modulates intracellular free calcium in sensory neurons. *J Neurosci Res.* 33:466–475.
- Miller-Podraza H & Fishman PH (1982) Translocation of newly synthesized gangliosides to the cell surface. *Biochem.* 21(14):3265–3270.
- Mitsuda T, Furukawa K, Fukumoto S, Miyazaki H, Urano T, Furukawa K (2002) Overexpression of ganglioside GM1 results in the dispersion of platelet-derived growth factor receptor from glycolipid-enriched microdomains and in the suppression of cell growth signals. *J Biol Chem.* 277(13):11239–11246.
- Miyagi T & Yamaguchi K (2012) Mammalian sialidases: physiological and pathological roles in cellular functions. *Glycobiol.* 22(7):880–896.
- Mocchetti I (2005) Exogenous gangliosides, neuronal plasticity and repair, and the neurotrophins. *Cell Mol Life Sci.* 62:2283–2294.
- Montell C (2004) Exciting trips for TRPs. *Nat Cell Biol.* 6:690–692.
- Monti E, Bassi MT, Papini N, Riboni M, Manzoni M, Venerando B, Croci G, Preti A, Ballabio A, Tettamanti G, and Borsani G (2000) Identification and expression of NEU3, a novel human sialidase associated to the plasma membrane. *Biochem J.* 349:343–351.
- Mosmann T (1983) Rapid colorimetric assay for cellular growth and survival: application to proliferation and cytotoxicity assays. *J Immunol Methods.* 65:55–63.
- Mutoh T, Tokuda A, Miyadai T, Hamaguchi M, and Fujiki N (1995) Ganglioside GM1 binds to the Trk protein and regulates receptor function. *PNAS.* 74(9):3782–3786.
- Mutoh T, Tokuda, A., Inokuchi, J. and Kuriyama, M. (1998). Glucosylceramide synthase inhibitor inhibits the action of nerve growth factor in PC12 cells. *J Biol Chem.* 273:26001–26007.

- Mutoh T, Hamano T, Yano S, Koga H, Yamamoto H, Furukawa K, and Ledeen RW. (2002) Stable Transfection of GM1 Synthase Gene into GM1-Deficient NG108-15 Cells, CR-72 Cells, Rescues the Responsiveness of TRK-Neurotrophin Receptor to Its Ligand, NGF. *Neurochem Res.* 27:801–806.
- Nagai Y (1985) Bioactive gangliosides: a proposal of the ganglioside-mediated bimodal modulation of cellular activity through cell membrane microdomain and the ganglioside cascade in *Glycoconjugates*, ed. Davidson EA *et al* (Prager Scientific, New York) 525–526.
- Nagai Y (1995) Functional roles of gangliosides in bio-signalling. *Behav Brain Res.* 66:99–104.
- Naïm M, Bhat S, Rankin KN, Dennis S, Chowdhury SF, Siddiqi I, Drabik P, Sulea T, Bayly CI, Jakalian A, Purisima EO (2007) Solvated interaction energy (SIE) for scoring protein-ligand binding affinities. 1. Exploring the parameter space. *J Chem Inf Model.* 47(1):122–33.
- Nishio M, Fukumoto S, Furukawa K, Ichimura A, Miyazaki H, Kusunoki S, Urano T, and Furukawa K (2004) Overexpressed GM1 Suppresses Nerve Growth Factor (NGF) Signals by Modulating the Intracellular Localization of NGF Receptors and Membrane Fluidity in PC12 Cells. *J Biol Chem.* 279:33368–33378.
- Nowycky M, Wu G, and Ledeen RW (2014). Glycobiology of Ion Transport in the Nervous System. *Adv Neurobiol.* 9:321–342.
- Ohmi Y, Ohkawa Y, Yamauchi Y, Tajima O, Furukawa K, and Furukawa K, (2012) Essential Roles of Gangliosides in the Formation and Maintenance of Membrane Microdomains in Brain Tissues. *Neurochem Res.* 6:1185–1191.
- Ono M, Handa K, Sonnino S, Withers DA, Nagai H, and Hakomori S (2001) GM3 ganglioside inhibits CD9-facilitated haptotactic cell motility: coexpression of GM3 and CD9 is essential in the downregulation of tumor cell motility and malignancy. *Biochem.* 40:6414–6421.
- Ozkök E, Cengiz S, and Güvener B (1999) Age-dependent changes in liver ganglioside levels. *J Basic Clin Physiol Pharmacol.* 10(4):337–344.
- Palestini P, Pitto M, Tedeschi G, Ferraretto A, Parenti M, Brunnerl J, and Massimo Masserini (2000) Tubulin Anchoring to Glycolipid-enriched, Detergent-resistant Domains of the Neuronal Plasma Membrane. *J Biol Chem.* 277:49466–49472.
- Patel DS, Park S, Wu EL, Yeom MS, Widmalm G, Klauda JB, and Im W (2016) Influence of Ganglioside GM1 Concentration on Lipid Clustering and Membrane Properties and Curvature. *Biophys J.* 111(9):1987–1999.
- Pavlov KV, Akimov SA, Bashkirov PV, Boldyrev IA, Telford WG, and Molotkovskaya IM (2009) Influence Of Ganglioside GM1 On Formation And Properties Of Rafts In Lipid Membranes. *Biophys J.* 96(3):448a.
- Prinetti A, Chigorno V, Mauri L, Loberto N, and Sonnino S (2007) Modulation of cell functions by glycosphingolipid metabolic remodeling in the plasma membrane. *J Neurochem.* 103(1):113–125.
- Prioni S, Mauri L, Loberto N, Casellato R, Chigorno V, Karagogeos D, Prinetti A, and Sonnino S (2004) Interactions between gangliosides and proteins in the exoplasmic leaflet of neuronal plasma membranes: A study performed with a tritium-labeled GM1 derivative containing a photoactivable group linked to the oligosaccharide chain. *Glycoconj J.* 21:461–470.
- Rabin SJ, Bachis A, and Mocchetti I (2002) Gangliosides Activate Trk Receptors by Inducing the Release of Neurotrophins. *J Biol Chem.* 277:49466–49472.



- Robert KY, Yi-Tzang T, Toshio A, and Makoto Y (2011) Structures, Biosynthesis, and Functions of Gangliosides-an Overview. *J Oleo Sci* 60.(10):537–544.
- Roisen FJ, Bartfeld H, Nagele R, Yorke G (1981) Ganglioside stimulation of axonal sprouting in vitro. *Science*. 214(4520):577–578.
- Rösner H, Wiegandt H, Rahmann H (1973) Sialic acid incorporation into gangliosides and glycoproteins of the fish brain. *J Neurochem*. 21(3):655–665.
- Rother J, van Echten G, Schwarzmann G, and Sandhoff, K. (1992) Biosynthesis of sphingolipids: dihydroceramide and not sphinganine is desaturated by cultured cells. *Biochem Biophys Res Commun*. 189:14–20.
- Russo D, Parashuraman S, and D'Angelo G (2016) Glycosphingolipid–Protein Interaction in Signal Transduction. *Int J Mol Sci*. 17(10):1732.
- Saqr HE, Pearl DK, and Yates AJ (1993) A Review and Predictive Models of Ganglioside Uptake by Biological Membranes. *J Neurochem*. 61(2):395–441.
- Saito M, Saito M, Berg MJ, Guidotti A, and Marks N (1999) Gangliosides attenuate ethanol-induced apoptosis in rat cerebellar granule neurons. *Neurochem Res*. 24:1107–1115.
- Saito M & Sugiyama K (2000) Specific ganglioside changes in extraneural tissues of adult rats with hypothyroidism. *Biochim Biophys Acta*. 1523:230–235.
- Sandhoff K & Kolter T (2003) Biosynthesis and degradation of mammalian glycosphingolipids. *Phil Trans R Soc Lond B*. 358:847–861.
- Sato C, Matsuda T, and Kitajima K (2002) Neuronal Differentiation-dependent Expression of the Disialic Acid Epitope on CD166 and Its Involvement in Neurite Formation in Neuro2A Cells. *J Biol Chem*. 277:45299–45305.
- Schaal H, Wille C, and Wille W. (1985) Changes of ganglio-side pattern during cerebellar development of normal and staggerer mice. *J Neurochem*. 45:544–551.
- Schauer R (1982) Sialic Acid-Chemistry, Metabolism and Functions, ed Schauer R (Springer, New York).
- Schengrund CL & Garrigan OW (1969) A comparative study of gangliosides from the brains of various species. *Lipids*. 4(6):488–495.
- Schengrund CL & Prouty C (1988) Oligosaccharide portion of GM1 enhances process formation by S20Y neuroblastoma cells. *J Neurochem*. 51(1):277–282.
- Schengrund CL & Ringler NJ (1989) Binding of Vibrio cholera toxin and the heat-labile enterotoxin of Escherichia coli to GM1, derivatives of GM1, and nonlipid oligosaccharide polyvalent ligands. *J Biol Chem*. 264(22):13233–13237.
- Schengrund, (1990) The role(s) of gangliosides in neuronal differentiation and repair: a prospective. *Brain Res Bull*. 24:131–141.
- Schengrund CL & Mummert CM (1998) Exogenous gangliosides. How do they cross the blood-brain barrier and how do they inhibit cell proliferation. *Ann N Y Acad. Sci*. 845:278–284.
- Schengrund CL (2015) Gangliosides: glycosphingolipids essential for normal neural development and function. *Trends Biochem Sci*. 40(7):397–406.
- Schnaar RL, Gerardy-Schahn R, and Hildebrandt (2014) Sialic Acids in the Brain: Gangliosides and Polysialic Acid in Nervous System Development, Stability, Disease, and Regeneration. *Physiol Rev*. 94(2):461–518.

- Schneider JS & Di Stefano L (1995) Response of the damaged dopamine system to GM1 and semisynthetic gangliosides: effects of dose and extent of lesion. *Neuropharmacol.* 34:489–493.
- Schwarzmann G & Sandhoff K (1990) Metabolism and intracellular transport of glycosphingolipids. *Biochem.* 29(49):10865–10871.
- Segal RA, Bhattacharyya A, Rua LA, Alberta JA, Stephens RM, Kaplan DR, and Stiles CD (1996) Differential Utilization of Trk Autophosphorylation Sites. *J Biol Chem.* 271(33):20175–20181.
- Senn HJ, Orth M, Fitzke E, Wieland H, and Gerok W. (1989) Gangliosides in normal human serum. Concentration, pattern and transport by lipoproteins. *Eur J Biochem.* 181(3):657–662.
- Sharom FJ & Grant CWM (1978) A model for ganglioside behaviour in cell membranes. *Biochem Biophys Acta.* 507(2):280–293.
- Shen KF & Crain SM (1990) Cholera toxin-B blocks opioid excitatory effects on sensory neuron action potentials indicating that GM-1 ganglioside may regulate Gs-linked opioid receptor functions. *Brain Res.* 531:1–7.
- Simons K & Ikonen E (1997) Functional rafts in cell membranes. *Nature.* 387(6633):569–572.
- Simons K & Sampaio JL (2011) Membrane organization and lipid rafts. *Cold Spring Harb Perspect Biol.* 3(10):a004697.
- Singleton DW, Lu CL, Colella R, and Roisen FJ (2000) Promotion of neurite outgrowth by protein kinase inhibitors and ganglioside GM1 in neuroblastoma cells involves MAP kinase ERK1/2. *Int J Develop Neurosci.* 18(8):797–805.
- Sonnino S, Chigorno V, Acquotti D, Pitto M, Kirschner G, and Tettamanti G (1989) A photoreactive derivative of radiolabeled GM1 ganglioside: preparation and use to establish the involvement of specific proteins in GM1 uptake by human fibroblasts in culture. *Biochem.* 28:77–84.
- Sonnino S, Chigorno V, Valsecchi M, Pitto M, and Tettamanti G (1992) Specific ganglioside–cell protein interactions: a study performed with GM1 ganglioside derivative containing photoactivable azide and rat cerebellar granule cells in culture. *Neurochem Int.* 20:315–321.
- Sonnino S, Cantù L, Corti M, Acquotti D, and Venerando B (1994) Aggregative properties of gangliosides in solution, *Chem Phys Lipids.* 71:21–45.
- Sonnino S, Prinetti A, Mauri L, Chigorno V, and Tettamanti G (2006) Gangliosides as components of lipid membrane domains. *Chem. Rev.* 106(6):2111–2125.
- Sonnino S, Mauri L, Chigorno V, and Prinetti A (2007) Dynamic and Structural Properties of Sphingolipids as Driving Forces for the Formation of Membrane Domains *Glycobiol.* 17(1):1–13.
- Sonnino S & Prinetti A (2010) Lipids and membrane lateral organization. *Front Physiol.* 1:153.
- Sonnino S, Aureli M, Loberto N, Chigorno V, Prinetti A, (2010) Fine tuning of cell functions through remodeling of glycosphingolipids by plasma membrane-associated glycohydrolases. *FEBS Lett.* 584(9):1914–1922.
- Sonnino S, Chigorno V, Aureli M, Masilamani AP, Valsecchi M, Loberto N, Prioni S, Mauri L, and Alessandro Prinetti (2011) Role of Gangliosides and Plasma Membrane-Associated Sialidase in the Process of Cell Membrane Organization in *The Molecular*

- Immunology of Complex Carbohydrates-3. Advances in Experimental Medicine and Biology*, ed Wu A (Springer, Boston) 705.
- Sonnino S & Prinetti A (2013) Membrane domains and the "lipid raft" concept. *Curr Med Chem.* 20(1):4–21.
- Sribney M (1966) Enzymatic synthesis of ceramide. *Biochim Biophys Acta.* 125(3):542–547.
- Strober W (2001) Trypan blue exclusion test of cell viability. *Curr Protoc Immunol.* 3:B
- Svennerholm L (1964) The gangliosides. *J Lipid Res.* 5:145–155.
- Svennerholm L & Fredman P (1980) A procedure for the quantitative isolation of brain gangliosides. *Biochim Biophys Acta.* 617(1):97–109.
- Svennerholm L, Boström K, Fredman P, Jungbjer B, Lekman A, Månsson JE, Rynmark BM (1994) Gangliosides and allied glycosphingolipids in human peripheral nerve and spinal cord. *Biochim Biophys Acta.* 1214(2):115–123.
- Sweatt D T (2001) The neuronal MAP kinase cascade: a biochemical signal integration system subserving synaptic plasticity and memory. *J Neurochem.* 76(1):1–10.
- Taylor BV, Gross L, Windebank AJ (1996) The sensitivity and specificity of anti-GM1 antibody testing. *Neurol.* 47(4):951–955.
- Tettamanti G, Bonali F, Marchesini S, Zambotti V (1973) A new procedure for the extraction and purification of brain ganglioside *Biochim Biophys Acta.* 296:160–170.
- Tettamanti G, Sonnino S, Ghidoni R, Masserini M, and Veberando B (1985) Chemical and functional properties of gangliosides. Their possible implication in the membrane mediated transfer of information in *Physics and amphiphiles: micelles, vesicles and microemulsions*, ed. Degiorgio V & Corti M (North Holland Physics, Amsterdam) 160–170.
- Tettamanti G & Riboni L (1993) Gangliosides and modulation of the function of neural cells. *Adv Lipid Res.* 25:235–267.
- Thompson TE & Tillack TW (1985) Organization of Glycosphingolipids in Bilayers and Plasma Membranes of Mammalian Cells. *Ann Rev Biophys Biophys Chem.* 14:361–386.
- Tomasi M, Roda LG, Ausiello C, D'Agnolo G, Venerando B, Ghidoni R, Sonnino S, Tettamanti G. (1980) Interaction of GM1 ganglioside with bovine serum albumin: formation and isolation of multiple complexes. *Eur J Biochem.* (2):315–324.
- Ulrich-Bott B & Wiegandt H (1984) Micellar properties of glycosphingolipids in aqueous media. *J Lipid Res.* 25(11):1233-1245.
- Valaperta R, Valsecchi M, Rocchetta F, Aureli M, Prioni S, Prinetti A, Chigorno V, and Sonnino S (2007) Induction of axonal differentiation by silencing plasma membrane-associated sialidase Neu3 in neuroblastoma cells. *J Neurochem.* 100(3):708–719.
- Van Den Eijnden DH (1973) The subcellular localization of Cytidine 5'-Monophosphate-N-Acetylneuraminic Acid Synthetase in the Calf Brain *J Neurochem.* 21:949–958.
- Vaudry D, Stork PJ, Lazarovici P, and Eiden LE (2002) Signaling pathways for PC12 cell differentiation: making the right connections. *Science.* 296(5573):1648–1649.
- Venerando B, Goi GC, Preti A, Fiorilli A, Lombardo A, and Tettamanti G, (1982) Cytosolic sialidase in developing rat forebrain. *Neurochem Int.* 4:313–320.
- Vengris VE, Reynolds Jr FH, Hollenberg MD, and Pitha PM (1976) Interferon action: Role of membrane gangliosides. *Virology.* 2(15):486–493.

- Wang YP, Wang ZF, Zhang YC, Tian Q, and Wang JZ (2004) Effect of amyloid peptides on serum withdrawal-induced cell differentiation and cell viability. *Cell Res.* 14: 467–472.
- Watarai S, Kiura K, Shigeto R, Shibayama T, Kimura I, and Yasuda T (1994) Establishment of monoclonal antibodies specific for ganglioside GM1: detection of ganglioside GM1 in small cell lung carcinoma cell lines and tissues. *J Biochem.* 116:948–954.
- Wiegandt H & Bücking HW. (1970) Carbohydrate components of extraneuronal gangliosides from bovine and human spleen, and bovine kidney. *Eur J Biochem.* 15(2):287–292.
- Wood ER, Kuyper L, Petrov KG, Hunter RN, Harris PA, and Lackey K (2004) Discovery and in vitro evaluation of potent TrkA kinase inhibitors: oxindole and aza-oxindoles. *Bioorg Med Chem Lett.* 14(4):953–957.
- Wu G & Ledeen RW (1991) Stimulation of Neurite Outgrowth in Neuroblastoma Cells by Neuraminidase: Putative Role of GM1 Ganglioside in Differentiation. *J Neurochem.* 56(1):95–104.
- Wu G, Lu ZH, and Ledeen RW (1997) Interaction of the  $\delta$ -opioid receptor with GM1 ganglioside: conversion from inhibitory to excitatory mode. *Neurochem Res.* 44(2):341–346.
- Wu G, Fang Y, Lu ZH, and Ledeen RW (1998) Induction of axon-like and dendrite-like processes in neuroblastoma cells. *J Neurocytol.* 27:1–14.
- Wu G, Lu ZH, Wang J, Wang Y, Xie X, Meyenhofer MF, and Ledeen RW (2005) Enhanced susceptibility to kainite-induced seizures, neuronal apoptosis, and death in mice lacking ganglioside GM1: protection with LIGA 20, a membrane-permeant analog of GM1. *J Neurosci.* 25:11014–11022.
- Wu G, Lu ZH, Obukhov AG, Nowycky MC, and Ledeen RW (2007) Induction of Calcium Influx through TRPC5 Channels by Cross-Linking of GM1 Ganglioside Associated with  $\alpha 5\beta 1$  Integrin Initiates Neurite Outgrowth. *J Neurosci.* 27(28):7447–7458.
- Xie X, Wu G, Lu ZH, and RW Ledeen (2002) Potentiation of a sodium–calcium exchanger in the nuclear envelope by nuclear GM1 ganglioside. *J Neurochem.* 81(6): 1185–1195.
- Yu RK, Macala LJ, Taki T, Weinfeld HM, and Yu FS (1988) Developmental changes in ganglioside composition and synthesis in embryonic rat brain. *J Neurochem.* 50(6):1825–182.
- Yamakawa T & Nagai Y (1978) Glycolipids at the cell surface and their biological functions. *Trends Biochem Sci.* 3(2):128–131.
- Zakharova N, Kornienko V, Potapov A, Pronin I (2014) *Neuroimaging of Traumatic Brain Injury*, (Springer, New York).
- Zeng Y & Tarbell JM (2014) The Adaptive Remodeling of Endothelial Glycocalyx in Response to Fluid Shear Stress. *PLoS ONE.* 9(1):e86249.



ORIGINAL  
ARTICLERole of the GM1 ganglioside oligosaccharide  
portion in the TrkA-dependent neurite sprouting in  
neuroblastoma cellsElena Chiricozzi,<sup>\*1</sup>  Diego Yuri Pomè,<sup>\*1</sup> Margherita Maggioni,<sup>\*</sup>  
Erika Di Biase,<sup>\*</sup> Chiara Parravicini,<sup>†</sup> Luca Palazzolo,<sup>†</sup> Nicoletta Loberto,<sup>\*</sup>  
Ivano Eberini<sup>†</sup> and Sandro Sonnino<sup>\*1</sup> <sup>\*</sup>Department of Medical Biotechnology and Translational Medicine, University of Milano, Segrate,  
Milano, Italy<sup>†</sup>Department of Pharmacological and Biomolecular Sciences, University of Milano, Milano, Italy

## Abstract

GM1 ganglioside (II<sup>3</sup>NeuAc-Gg<sub>4</sub>Cer) is known to promote neurite formation in neuroblastoma cells by activating TrkA-MAPK pathway. The molecular mechanism by which GM1 is involved in the neurodifferentiation process is still unknown, however, *in vitro* and *in vivo* evidences have suggested that the oligosaccharide portion of this ganglioside could be involved. Here, we report that, similarly to the entire GM1 molecule, its oligosaccharide II<sup>3</sup>NeuAc-Gg<sub>4</sub>, rather than its ceramide (Cer) portion is responsible for the neurodifferentiation process by augmenting neurite elongation and increasing the neurofilament protein expression in murine neuroblastoma cells, Neuro2a. Conversely, asialo-GM1, GM2 and GM3 oligosaccharides are not effective in neurite elongation on Neuro2a cells, whereas the effect exerted by the Fuc-GM1 oligosaccharide (IV<sup>2</sup>αFucII<sup>3</sup>Neu5Ac-Gg<sub>4</sub>) is similar

to that exerted by GM1 oligosaccharide. The neurotrophic properties of GM1 oligosaccharide are exerted by activating the TrkA receptor and the following phosphorylation cascade. By photolabeling experiments performed with a nitrophenylazide containing GM1 oligosaccharide, labeled with tritium, we showed a direct interaction between the GM1 oligosaccharide and the extracellular domain of TrkA receptor. Moreover, molecular docking analyses confirmed that GM1 oligosaccharide binds the TrkA-nerve growth factor complex leading to a binding free energy of approx. -11.5 kcal/mol, acting as a bridge able to increase and stabilize the TrkA-nerve growth factor molecular interactions.

**Keywords:** differentiation, GM1 ganglioside, GM1 oligosaccharide chain, neuronal development, plasma membrane signaling, TrkA neurotrophin receptor.

*J. Neurochem.* (2017) <https://doi.org/10.1111/jnc.14146>

Gangliosides, glycosphingolipids containing sialic acid, constitute a wide family whose components differ in the structure of both the oligosaccharide and lipid chains (Sonnino *et al.* 2006). They are typical components of neuronal membranes taking place with a 10-fold higher amount than in non-neuronal cells and presenting oligosaccharide chains that contain up to five residues of sialic acid. Their change in concentration during brain development suggests specific roles in the nervous system (Allende and

<sup>1</sup>These authors contributed equally to this work.

Ganglioside nomenclature is in accordance with IUPAC-IUBB recommendations (IUPAC-IUBMB 1998).

**Abbreviations used:** AGM1, tetrahexosylceramideGg<sub>4</sub>; DMEM, Dulbecco's modified Eagles' medium; ERK1/2, extracellular signal-regulated protein kinases 1 and 2; FBS, fetal bovine serum; Fucosylated GM1 oligosaccharide, IV<sup>2</sup>αFucII<sup>3</sup>Neu5Ac-Gg<sub>4</sub>; GM1 oligosaccharide, II<sup>3</sup>Neu5Ac-Gg<sub>4</sub>; GM1, II<sup>3</sup>Neu5Ac-Gg<sub>4</sub>Cer; β-Gal-(1-3)-β-GalNAc-(1-4)-[α-Neu5Ac-(2-3)]-β-Gal-(1-4)-β-Glc-Cer; GM2 oligosaccharide, II<sup>3</sup>Neu5Ac-Gg<sub>3</sub>; GM3 oligosaccharide, sialyllactose; HPTLC, high-performance silica gel thin-layer chromatography; MAPK, mitogen-activated protein kinase; MTT, 3-(4,5-dimethylthiazole-2-yl)-2,5-diphenyltetrazolium bromide; N2a, Neuro2a cells; NF, neurofilament; NGF, nerve growth factor; PBS, phosphate-buffered saline; p-ERK1/2, phosphorylated ERK1/2; PM, plasma membrane; p-TrkA, phosphorylated TrkA; PVDF, polyvinylidene difluoride; siRNA, short interfering RNA; Trk, neurotrophin tyrosin kinase receptor; Tyr490, tyrosine 490; α-tub, α-tubulin.

Received May 24, 2017; revised manuscript received July 12, 2017; accepted August 2, 2017.

Address correspondence and reprint requests to Prof. Sandro Sonnino, Via Fratelli Cervi 93, 20090 Segrate (MI), Italy. E-mail: [sandro.sonnino@unimi.it](mailto:sandro.sonnino@unimi.it)

Panzetta 1994; Wu *et al.* 1995; Kwak *et al.* 2005; Yu *et al.* 2009; Aureli *et al.* 2011). Particular attention has been devoted to ganglioside GM1,  $\text{II}^3\text{NeuAc-Gg}_4\text{Cer}$  (Ledeen and Wu 2015; Schengrund 2015; Aureli *et al.* 2016), structurally characterized by the oligosaccharide chain  $\text{II}^3\text{NeuAc-Gg}_4$ ,  $\beta\text{-Gal-(1-3)-}\beta\text{-GalNAc-(1-4)-}[\alpha\text{-Neu5Ac-(2-3)}]\text{-}\beta\text{-Gal-(1-4)-}\beta\text{-Glc-}$  (Kuhn and Wiegandt 1963). *In vitro* and *in vivo* approaches highlighted the neurotrophic and neurodifferentiative functions of ganglioside GM1 (Roisen *et al.* 1981; Facci *et al.* 1984; Chigorno *et al.* 1985; Lipartiti *et al.* 1991; Rodriguez *et al.* 2001; Da Silva *et al.* 2005; Mochetti 2005; Schneider *et al.* 2010; Sonnino *et al.* 2011; Miyagi and Yamaguchi 2012). The effects exerted by GM1 occur when its plasma membrane (PM) content increases in membrane lipid micro-domains (Hakomori *et al.* 1998). The membrane local enrichment causes (i) the GM1 content-dependent membrane reorganization, which alters membrane properties and ensures the physical parameters required for proper protein function or (ii) the GM1 oligosaccharide-protein direct interactions, which modify the protein conformation and function (Coskun and Simons 2011).

The plasma membrane increase of GM1 is responsible for the activities of several membrane enzyme and receptor (Tettamanti 1986; Zoli *et al.* 1990). In fact, membrane-associated proteins, including neurotrophin receptors, opioid receptors, integrins and calcium transporter, have been proposed as interactor partners of GM1 (Ledeen and Wu 2015). In particular, interaction between GM1 and the neurotrophin tyrosin kinase receptor (Trk) has been claimed for modulation of neuritogenesis (Ferrari *et al.* 1995; Mutoh *et al.* 1995; Farooqui *et al.* 1997; Bachis *et al.* 2002). As described by different authors, plasma membrane increase of GM1 and formation of a GM1 enriched platform leads to membrane reorganization triggering to the dimerization of Trk, followed by its autophosphorylation (Rodriguez *et al.* 2001; Da Silva *et al.* 2005).

In spite of many papers, connect the neurite elongation with GM1 plasma membrane content and with modulation of the Trk activity, the precise GM1 mechanism of action remains elusive. Opposite experimental approaches, such as the PM sialidase NEU3 over-expression, but also its inhibition, led to think that changes in oligosaccharidic chains of plasma membrane gangliosides could affect the fine tuning of the processes through the plasma membrane (Rodriguez *et al.* 2001; Valperta *et al.* 2007). However, only few data concerning the relationship between ganglioside oligosaccharide and neuritogenesis processes have been reported so far (Schengrund and Prouty 1988). For this reason, we decided to investigate the role played by the oligosaccharide chain of GM1 and we found out that the GM1 oligosaccharide is able to promote the TrkA-dependent neurite sprouting in mouse neuroblastoma cells.

## Methods

### Materials

Commercial chemicals were of the highest purity available, common solvents were distilled before use and water was doubly distilled in a glass apparatus.

Cell culture plates and Transfectagro™ reduced serum medium were from Corning (Corning, NY, USA). Mouse neuroblastoma Neuro2a (N2a) cells (RRID: CVCL\_0470), phosphate-buffered saline (PBS), Paraformaldehyde, Triton X-100, sodium dodecyl sulfate (SDS), 2-propanol, Formic acid, 3-(4,5,-dimethylthiazole-2yl)-2,5-diphenyltetrazolium bromide (MTT), Trypan blue, Galactose, Sialic Acid, anti-rabbit FITC conjugate, and mouse  $\alpha$ -tubulin antibodies were from Sigma-Aldrich (St. Louis, MO, USA). Dulbecco's modified Eagle's high glucose medium, fetal bovine serum (FBS), L-glutamine (L-Glut), Penicillin (10.000 U/mL), Streptomycin and 30% acrylamide were from EuroClone (Paignton, UK). Gibco™ OptiMEM™ I reduced serum medium, Lipofectamine® 2000 and goat anti-mouse IgG (H+L) antibody (RRID: AB\_228307) were from Thermo Fischer Scientific (Waltham, MA, USA). TrkA inhibitor (CAS 388626-12-8) was from Merck Millipore (Billerica, MA, USA). The short interfering RNAs (siRNAs) were from Qiaagen (Velno, Netherlands). Rabbit anti-TrkA (RRID: AB\_10695253), rabbit anti-phospho-TrkA (tyrosine 490, Tyr490) (RRID: AB\_10235585), rabbit anti-p44/42 MAPK (Erk1/2) (RRID: AB\_390779), rabbit anti-phospho-p44/42 MAPK (pErk1/2) (Thr202/Tyr204) (RRID: AB\_2315112) and anti-rabbit IgG (RRID: AB\_2099233) antibodies were from Cell Signaling Technology (Danvers, MA, USA). Rabbit anti-pan Neurofilament (NF) antibody (RRID: AB\_10539699) was from Biomol International (Plymouth Meeting, PA, USA). Chemiluminescent kit for western blot was from Cyanagen (Bologna, Italy). Ultima gold was from Perkin Elmer (Waltham, MA, USA). DC protein assay kit was from BioRad (Hercules, CA, USA). High-performance thin-layer chromatography (HPTLC) was from Merck Millipore (Frankfurt, Germany). Polyvinylidene difluoride (PVDF) membrane was from GE Healthcare Life Sciences (Chigago, IL, USA).

### Preparation of gangliosides and their oligosaccharides

Fuc-GM1 (Ghidoni *et al.* 1976), GM1 and GM2 gangliosides were purified from the total ganglioside mixture extracted from pig brains (Tettamanti *et al.* 1973), submitted to sialidase hydrolysis (Acquotti *et al.* 1994). Desialylated GM1 (AGM1, asialo-GM1) was prepared by acid hydrolysis of GM1 and chromatographic purification (Ghidoni *et al.* 1976). GM1 containing tritium at position 6 of external galactose was prepared by enzymatic oxidation with galactose oxidase followed by reduction with sodium borotritide (Sonnino *et al.* 1996). The oligosaccharides  $\text{Gg}_4$ ,  $\text{II}^3\text{Neu5Ac-Lac}$ ,  $\text{II}^3\text{Neu5Ac-Gg}_3$ ,  $\text{II}^3\text{Neu5Ac-}[\text{H}]\text{Gg}_3$ ,  $\text{II}^3\text{Neu5Ac-Gg}_4$ ,  $\text{II}^3\text{Neu5Ac-}[\text{H}]\text{Gg}_4$ , and  $\text{IV}^2\alpha\text{FucII}^3\text{Neu5Ac-Gg}_4$ , were prepared by ozonolysis followed by alkaline degradation (Wiegandt and Bucking 1970), from tetrahexosylceramide, GM3, GM2,  $[\text{H}]\text{GM2}$ , GM1,  $[\text{H}]\text{GM1}$ , and Fuc-GM1, respectively. Altogether, NMR, MS, HPTLC, and autoradiographic analyses showed a homogeneity over 99% for all the prepared gangliosides and oligosaccharides (data not shown).

Tritium-labeled and photoactivable GM1 oligosaccharide,  $\text{II}^3\text{Neu5Ac-}[\text{H}]\text{Gg}_4\text{-N}_3$ , was prepared from  $\text{II}^3\text{Neu5Ac-}[\text{H}]\text{Gg}_4$ , according to the scheme reported in Fig. 1.

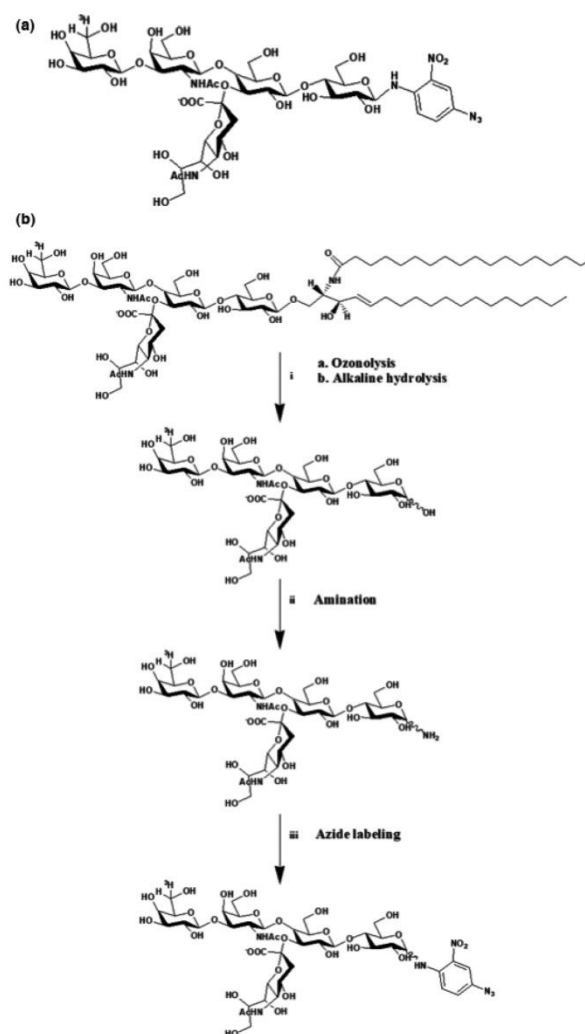


**Fig. 1**  $11^3\text{Neu5Ac-}[\text{}^3\text{H}]\text{Gg}_4\text{-N}_3$  structure and chemical synthesis. (a) Structure of  $11^3\text{Neu5Ac-}[\text{}^3\text{H}]\text{Gg}_4\text{-N}_3$ . (b) Scheme of the synthetic process for the preparation of  $11^3\text{Neu5Ac-}[\text{}^3\text{H}]\text{Gg}_4\text{-N}_3$ . Reagents and conditions: (i) a.  $\text{O}_3$ ,  $\text{CH}_3\text{OH}$ ,  $23^\circ\text{C}$ , 30 min.; (b) triethylamine,  $23^\circ\text{C}$ , 18 h; (ii)  $\text{NH}_4\text{HCO}_3$ ,  $\text{NH}_4\text{OH}$  33%,  $40^\circ\text{C}$ , 48 h; (iii) 2-nitro-4-fluorophenylazide,  $\text{Bu}_3\text{N}$ , DMF/dimethylsulfoxide,  $80^\circ\text{C}$ , 18 h. Final yield, 45%.

An amount of 52  $\mu\text{moles}$  of  $11^3\text{Neu5Ac-}[\text{}^3\text{H}]\text{Gg}_4$  (0.5 Ci/mmol) were dissolved in 33% ammonia and treated with 1 mg of ammonium hydrogen carbonate. The reaction was maintained under stirring for 48 h at  $40^\circ\text{C}$ . The solution was then immediately freeze-dried (Lubineau *et al.* 1995).

The crude amino- $11^3\text{Neu5Ac-}[\text{}^3\text{H}]\text{Gg}_4$  was dissolved in 0.5 mL of dry dimethylformamide, then 1 mg of 2-nitro-4-fluorophenylazide

and 1  $\mu\text{L}$  of tributylamine in 25  $\mu\text{L}$  of dry dimethylsulfoxide were added under dark conditions. Maintaining dark conditions for all the process, the reaction mixture was stirred overnight at  $80^\circ\text{C}$ . After solvent evaporation, the photoactivable  $11^3\text{Neu5Ac-}[\text{}^3\text{H}]\text{Gg}_4\text{-N}_3$  was purified by flash chromatography using chloroform/methanol/2-propanol/water 60 : 35 : 5 : 5 as eluent (Mauri *et al.* 2004).  $11^3\text{Neu5Ac-}[\text{}^3\text{H}]\text{Gg}_4\text{-N}_3$  solubilized in methanol was stored at  $4^\circ\text{C}$ .



HPTLC analyses were performed using the solvent system chloroform/methanol/0.2% CaCl<sub>2</sub>, 60 : 35 : 8 by vol. Bound sialic acid was determined by the resorcinol-HCl method (Svennerholm 1957; Takki-Luukkainen and Miettinen 1959), pure Neu5Ac being used as the reference standard.

#### Cell cultures

N2a cells were cultured and propagated as monolayer in Dulbecco's modified Eagle's medium-High Glucose medium supplemented with 10% heat inactivated FBS, 1% L-glutamine and 1% penicillin/streptomycin, at 37°C in a humidified atmosphere of 95% air/5% CO<sub>2</sub>. Cells were subcultured to a fresh culture when growth reached the 80–90% confluence (i.e. every 3–4 days).

#### Cell treatments

N2a cells were plated at  $5 \times 10^3/\text{cm}^2$  and incubated for 24 h to allow cells attachment and recovery in complete medium before all treatments. Control cells were incubated under identical conditions but omitting any addition.

#### Ganglioside and oligosaccharide treatments

To induce differentiation, growth medium was removed and cells were pre-incubated in pre-warmed (37°C) Transfectagro medium containing 2% FBS, 1% L-glutamine, 1% penicillin/streptomycin, for 30 min at 37°C. Cell treatments were performed in serum reduced culture medium, in order to minimize interactions between serum components and exogenous gangliosides or their oligosaccharides. Subsequently, cells were incubated at 37°C up to 48 h in the presence of 50  $\mu\text{M}$  gangliosides, oligosaccharides, galactose, or sialic acid.

#### TrkA chemical inhibition experiments

In order to block TrkA activity in N2a cells, the TrkA inhibitor (120 nM) was added to the incubation medium 1 h before the addition of GM1 or II<sup>3</sup>Neu5Ac-Gg<sub>4</sub> (Wood *et al.* 2004).

#### siRNA mediated RNA interference experiments

TrkA knockdown was achieved by RNA interference applying siRNA. Three distinct siRNAs were used to silence TrkA: Mm\_Ntrk1\_1 (sense 5'-CCAUCAUAAUAGCAAUAUATT-3', antisense 5'-AUAAUUGCUAAUUAUGGAT-3'); Mm\_Ntrk1\_5 (sense 5'-GGUGGCUGCUGGUAUGGUATT-3', antisense 5'-UACCAUACCAGCAGCCACC TG-3'); and Mm\_Ntrk1\_6 (sense 5'-CCUUCUUGUCUCAACAAATT-3', antisense 5'-UUUGUUGAGCACAAGAAGGAG-3'). As a negative control, non-silencing siRNA with no homology to any known mammalian gene was used (sense 5'-UUCUUCGAACGUGU CACGUdTdT-3', antisense 5'-ACGUGACACGUUCGGAGAA dTdT-3'). Transfection was performed after 24 h from cell plating in antibiotic and serum free culture media with solution containing 25% OptiMEM, 0.25% Lipofectamine 2000 and 50 nM siRNA (16.7 nM of each siRNA). After 6 h, the transfection medium was changed to culture medium containing antibiotic and serum. After 24 h from the silencing, cells were treated with GM1 or II<sup>3</sup>Neu5Ac-Gg<sub>4</sub> as above.

#### Photolabeling experiments

Cells were incubated with 50  $\mu\text{M}$  II<sup>3</sup>Neu5Ac-[<sup>3</sup>H]Gg<sub>4</sub>-N<sub>3</sub> for 3 h at 37°C. After incubation, medium was removed and cells were illuminated for 40 min under UV light ( $\lambda = 360 \text{ nm}$ ) on ice to induce photo-activation. All the procedures before exposure to UV

light were performed under red safelight. The cells were lysed and subjected to 4–20% sodium dodecyl sulfate–polyacrylamide gel electrophoresis (SDS–PAGE) and blotted on PVDF membrane. Digital autoradiography of the PVDF membrane was performed with Beta-Imager 2000 (Biospace, Paris, France). PVDF membrane was then incubated with anti-TrkA antibody (Sonnino *et al.* 1989, 1992; Chigorno *et al.* 1990; Loberto *et al.* 2003; Chiricozzi *et al.* 2015).

#### Determination of cell viability

Cell viability was determined by Trypan blue exclusion and by MTT assays after 12, 24 and 48 h treatment with gangliosides and oligosaccharides. The number of living and death cells has been determined by counting cells after Trypan blue staining, as previously described (Mehlen *et al.* 1988; Aureli *et al.* 2011). Proliferation was determined by the MTT method (Mosmann 1983). Briefly, at the end of incubation, 2.4 mM MTT (4 mg/mL in PBS) were added to each well and plates were re-incubated for 4 h at 37°C. Medium was carefully removed and replaced with 2-propanol: formic acid, 95 : 5 (v/v). Plates were gently agitated prior to read the absorbance at 570 nm with a microplate spectrophotometer (Wallac 1420 VICTOR2™; Perkin Elmer).

#### Morphological analysis and neurite outgrowth evaluation

Cultured cells treated with ganglioside GM1 or different oligosaccharides were observed by phase contrast microscopy (Olympus BX50 microscope; Olympus, Tokyo, Japan). The neurite-like length was measured on bidimensional images and expressed as the ratio between neurite length and cell body diameter (Schengrund and Prouty 1988). Five random fields were examined from each well, giving a total cell count of at least 200 cells per well.

#### Immunofluorescence analysis

Treated or not treated cells were fixed in 4% paraformaldehyde for 20 min at 23°C. Cells were permeabilized with 0.1% Triton X-100 for 30 min and then treated with a blocking solution for 1 h at 23°C. Cells were incubated with rabbit polyclonal antibody anti-NF for 2 h at 23°C. After washing with PBS, cells were incubated 1 h with secondary anti-rabbit antibody FITC-conjugated. Fluorescence microscopy was carried out using an Olympus U-RFL-T EPI Fluorescence Microscope (Olympus) and the images processing were performed with ImageJ software.

#### Fate of II<sup>3</sup>Neu5Ac-Gg<sub>4</sub> added to the cells

Fate of II<sup>3</sup>Neu5Ac-Gg<sub>4</sub> administered to cells was determined using tritium-labeled II<sup>3</sup>Neu5Ac-Gg<sub>4</sub>. After the cell administration with 50  $\mu\text{M}$  II<sup>3</sup>Neu5Ac-[<sup>3</sup>H]Gg<sub>4</sub> for different times, the medium was removed and the following treatments were performed sequentially: (i) cells were washed five times with 10% FBS-medium to remove the amount of II<sup>3</sup>Neu5Ac-Gg<sub>4</sub> weakly associated to the cells — serum removable fraction; (ii) cells were treated with 0.1% trypsin solution to evaluate the II<sup>3</sup>Neu5Ac-Gg<sub>4</sub> strongly linked to extracellular domain of PM proteins — trypsin removable fraction; (iii) cells were lysed in order to evaluate the quantity of II<sup>3</sup>Neu5Ac-Gg<sub>4</sub> internalized — trypsin stable fraction. The procedure was established previously to determine the fate of gangliosides administered to cells in culture (Chigorno *et al.* 1985).

**Protein analysis**

Equal amounts of proteins derived from treated and untreated cells were denatured, separated on 7.5% polyacrylamide gels, and transferred to PVDF membranes. The presence of NF, TrkA, p-TrkA, extracellular signal-regulated protein kinases 1 and 2 (ERK1/2) and p-ERK1/2 was determined by specific primary antibodies, followed by reaction with secondary horseradish peroxidase-conjugated antibodies.  $\alpha$ -tubulin was used as loading control. The data acquisition and analysis were performed using Alliance Uvitec (Eppendorf, Germany).

**Molecular modeling**

Crystallographic structure of the extracellular segment of human TrkA in complex with nerve growth factor (NGF) (RCSB PDB ID: 2IFG) was used for molecular docking calculations. Protein complex was submitted to the Molecular Operating Environment 2016.0802 (MOE) Structure Preparation application, in order to fix all issues and to prepare structures for subsequent computational analyses.

The  $\text{II}^3\text{Neu5Ac-Gg}_4$  structure was built with the MOE Carbohydrate Builder and a geometry optimization was carried out with MOPAC7 and the PM6 basis set.

Molecular docking was carried out through the MOE Dock program, setting as receptor the complex between TrkA and NGF, as ligand the optimized  $\text{II}^3\text{Neu5Ac-Gg}_4$  structure. The binding site was identified at the interface between the two proteins. Before placement procedure, 20 000 rotamers of the ligand was generated, exploring all the molecule rotatable bonds. Alpha PMI placement algorithm, specifically developed for tight binding pocket, was selected. The London dG empirical scoring function was used for sorting the poses. The 30 top-scoring poses was refined through molecular mechanics, considering the receptor as a rigid body, and the refined complexes were scored through the GBVI/WSA dG empirical scoring function, keeping the five top-scoring poses.

The top-scoring pose from the docking procedure was refined by using the MOE QuickPrep procedure aimed at relaxing and refining the complex before calculating the approx. binding free energy via the GBVI/WSA dG empirical scoring function (Naim *et al.* 2007).

**Statistical analysis**

Data are expressed as mean  $\pm$  SEM and were analyzed for significance by Student's *t*-test or two-way ANOVA test. The analysis was performed with Prism software (GraphPad Software, Inc. La Jolla, CA, USA).

**Other analytical methods**

NMR spectra were recorded with a Bruker AVANCE-500 spectrometer at a sample temperature of 298 K. NMR spectra were recorded in CDCl<sub>3</sub> or CD<sub>3</sub>OD and calibrate using the TMS signal as internal reference.

Mass spectrometric analysis were performed in positive or negative ESI-MS. MS spectra were recorded on a Thermo Quest Finnigan LCQTM DECA ion trap mass spectrometer, equipped with a Finnigan ESI interface; data were processed by Finnigan Xcalibur software system (Thermo Fischer Scientific, Waltham, MA, USA).

All reactions were monitored by TLC on silica gel 60 plates (Merck).

Radioactivity associated with cells and trypsin and serum labile cell fractions was determined by liquid scintillation counting. Digital autoradiography of the PVDF membranes was performed with a Beta-Imager 2000 (Biospace).

Any randomization or blinding procedures were performed for our experiments. Institutional approval was not needed.

**Results****N2a cell viability upon treatments with ganglioside GM1 and its oligosaccharide**

Trypan blue assay, performed on N2a cells treated with 50  $\mu\text{M}$  GM1 ganglioside or its oligosaccharide up to 48 h, showed a viability overlapping to that of control cells and over 94% (Fig. 2a). On the other hand, we observed a reduction in cell proliferation starting from 12 h of treatment (Fig. 2b).

**Neurite sprouting by administration to N2a cells of  $\text{II}^3\text{Neu5Ac-Gg}_4$** 

Incubation of N2a cells with  $\text{II}^3\text{Neu5Ac-Gg}_4$  induced a neuron-like morphology after 24 (Fig. 3) and 48 h (Figure S1), pointing out the sprouting and elongation of neurites, which are almost absent in round-shaped control cells. A similar result was obtained in cells treated with GM1, confirming previous data (Facci *et al.* 1984; Rabin *et al.*

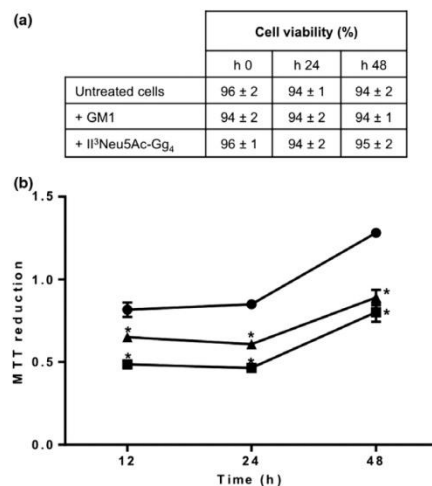


**Fig. 2** Effect of GM1 and  $\text{II}^3\text{Neu5Ac-Gg}_4$  on Neuro2a (N2a) cell viability. N2a cells were induced to differentiate in the presence or absence of 50  $\mu\text{M}$  GM1 or  $\text{II}^3\text{Neu5Ac-Gg}_4$  up to 48 h. (a) The number of living and death cells was determined by Trypan blue exclusion assay. Values represent the percentage mean of living cells  $\pm$  SEM for three different culture preparations ( $n = 3$ ). (b) Cell proliferation was evaluated by 3-(4,5-dimethylthiazole-2-yl)-2,5-diphenyltetrazolium bromide (MTT) reduction assay on N2a cells grown in the absence (●) or presence of GM1 (□) or  $\text{II}^3\text{Neu5Ac-Gg}_4$  (▲). Results are expressed as mean of absorbance values at 570 nm  $\pm$  SEM for three different culture preparations (\* $p < 0.05$  vs. CTRL, two-way ANOVA,  $n = 3$ ).

2002). N2a cells were treated with Gg<sub>4</sub>, II<sup>3</sup>Neu5Ac-Gg<sub>3</sub>, sialyllactose, galactose, or sialic acid in order to clarify the minimal structure required to promote neurite elongation. None of these compounds induced cell morphological changes (Fig. 3 and Figure S1), suggesting that the whole structure of the II<sup>3</sup>Neu5Ac-Gg<sub>4</sub> is necessary to block cell proliferation and to induce neurite sprouting. In addition, cells were treated with fucosylated II<sup>3</sup>Neu5Ac-Gg<sub>4</sub>, which induces neurite sprouting and reduction of cell proliferation in a similar way as II<sup>3</sup>Neu5Ac-Gg<sub>4</sub>. This result suggests that the neurite sprouting process requires specifically the β-Gal-(1-3)-β-GalNAc-(1-4)-[α-Neu5Ac-(2-3)]-β-Gal-(1-4)-Glc structure and that the addition to it of an α-fucose at position 2 of the external galactose is irrelevant for the processes (Fig. 3 and Figure S1).

Neurite extensions, observed after 24 h treatment with II<sup>3</sup>Neu5Ac-Gg<sub>4</sub>, were measured as the ratio between the length of processes and the diameter of cell body (Fig. 4a). This ratio resulted at least two fold higher compared to the control and similar to GM1-treated cells.

Expression of heavy, medium, and light intracellular NF subunits (NF-H, NF-M and NF-L), considered markers of neurodifferentiation (Fukuda *et al.* 2014), was evaluated by immunoblotting. NF proteins are considered the major components of cytoskeleton supporting axonal construction. NF expression increased significantly after 24 h treatment with both GM1 and II<sup>3</sup>Neu5Ac-Gg<sub>4</sub> (Fig. 4b), resulting quite evident by immunofluorescence (Fig. 4c).

#### Fate of the II<sup>3</sup>Neu5Ac-Gg<sub>4</sub> added to N2a cells

Isotopic tritium-labeled II<sup>3</sup>Neu5Ac-Gg<sub>4</sub> was administered to the N2a cells. After 0.5, 1, 6, and 24 h treatment, cells were treated according to a procedure previously developed (Chigomo *et al.* 1985). At the end of the incubation, cells were washed with culture medium containing 10% serum in order to evaluate the quantity of oligosaccharide weakly associated to the cells surface (serum labile). Successively cells were treated with trypsin to evaluate a possible portion strongly bond to the extracellular domain of PM proteins (trypsin labile). At the end, cells were lysed in order to evaluate the quantity of internalized II<sup>3</sup>Neu5Ac-Gg<sub>4</sub> (trypsin stabile). At each time point analyzed, about 99% of II<sup>3</sup>Neu5Ac-Gg<sub>4</sub> was found in the serum labile form as shown in Fig. 5. This suggests that the II<sup>3</sup>Neu5Ac-Gg<sub>4</sub> is not taken up by the cells and that it is associated to PM proteins.

#### TrkA-dependent neuritogenesis induced by II<sup>3</sup>Neu5Ac-Gg<sub>4</sub>

It was previously reported that GM1 promotes neurite elongation by amplifying the effect exerted by NGF on TrkA (Farooqui *et al.* 1997; Singleton *et al.* 2000;

Duchemin *et al.* 2002; Da Silva *et al.* 2005; Mocchetti 2005; Zakharova *et al.* 2014). We checked the activation of TrkA receptor in N2a cells treated with the II<sup>3</sup>Neu5Ac-Gg<sub>4</sub>, to verify the role of II<sup>3</sup>Neu5Ac-Gg<sub>4</sub> in the GM1-promoted TrkA activation. In detail, we focused on phosphorylation of Tyr490, which leads to the activation of the neuronal differentiation pathway (Singleton *et al.* 2000; Duchemin *et al.* 2002; Huang and Reichardt 2003; Zakharova *et al.* 2014). By immunoblotting analysis, we highlighted the activation of TrkA receptor revealed by the increase in the phosphorylation of Tyr490 either in GM1-treated cells and in cells that received II<sup>3</sup>Neu5Ac-Gg<sub>4</sub> (Fig. 6a). In the treated cells, we also checked the activation of MAP kinases finding an increase of ERK1/2 phosphorylation (Fig. 6a). To prove that the neuritogenic effect exerted by the GM1 or its oligosaccharide was directly mediated by TrkA-ERK pathway, we blocked the TrkA receptor by chemical inhibition, using a specific TrkA inhibitor, able to fit in the ATP pocket (Wood *et al.* 2004). The addition of TrkA inhibitor together with the GM1 or the II<sup>3</sup>Neu5Ac-Gg<sub>4</sub> prevented the phosphorylation processes (Fig. 6a) and the neurite elongation (Fig 6b).

Furthermore, to prove the necessary requirement of TrkA in II<sup>3</sup>Neu5Ac-Gg<sub>4</sub>-mediated neuritogenesis, TrkA was knocked down using the siRNA approach. Control cells were transfected with scramble-siRNA. Silenced cells, resulting in a 70% reduction of TrkA expression (Fig. 7a), were incubated with GM1 or II<sup>3</sup>Neu5Ac-Gg<sub>4</sub> for 24 h and no differentiation, nor the phosphorylation of Erk1/2 (Fig. 7b and c) could be observed.

#### II<sup>3</sup>Neu5Ac-Gg<sub>4</sub>-TrkA interaction in N2a cells

To study the interaction between the oligosaccharide chain of GM1 and TrkA, we prepared, according to the scheme in Fig. 1, a radioactive and photoactivable II<sup>3</sup>Neu5Ac-Gg<sub>4</sub> derivative, II<sup>3</sup>Neu5Ac-[<sup>3</sup>H]Gg<sub>4</sub>(N<sub>3</sub>).

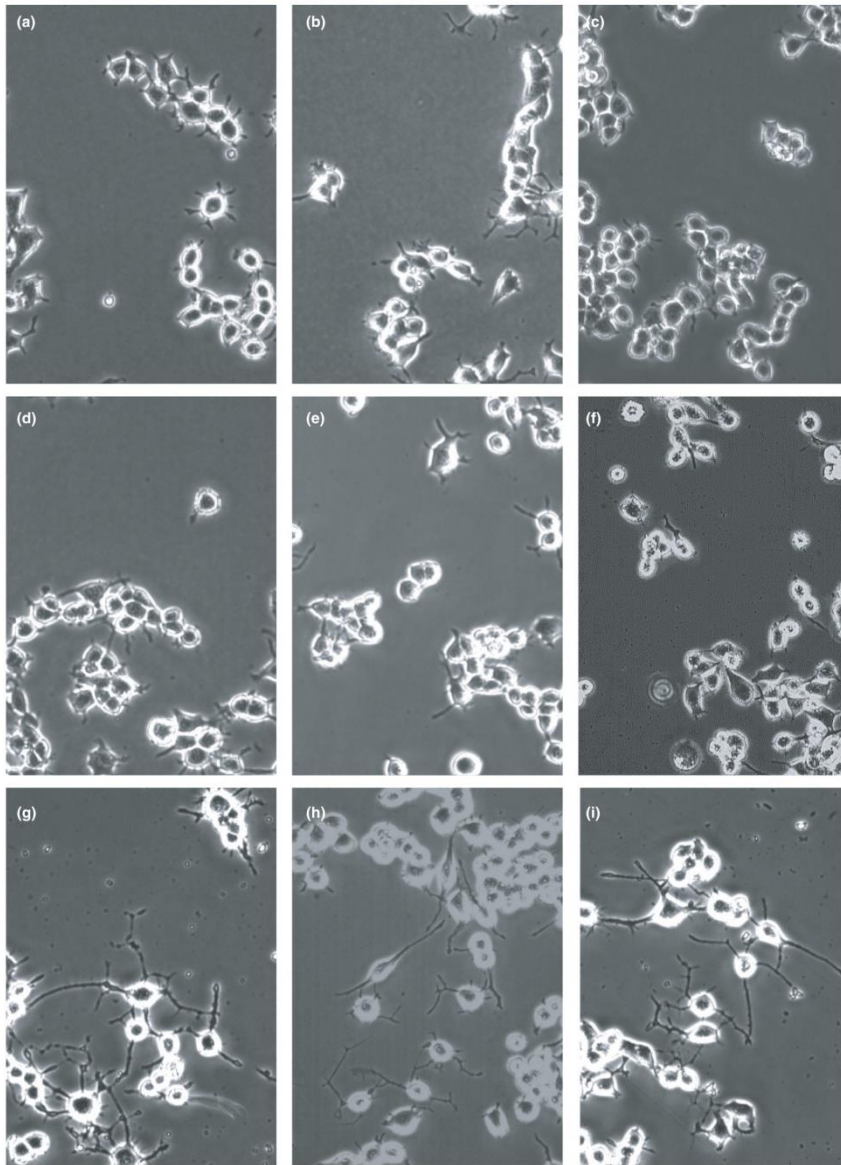
N2a cells were incubated with II<sup>3</sup>Neu5Ac-[<sup>3</sup>H]Gg<sub>4</sub>(N<sub>3</sub>) under dark conditions. After pulse, cells were illuminated under UV-light to induce covalent cross-linking between cell surface proteins and the radioactive GM1 oligosaccharide derivative. Proteins were separated by SDS-PAGE, blotted on a PVDF membrane and the radioactive bands visualized by digital autoradiography. In comparison to N2a protein pattern, few radioactive bands were detected. They correspond to specific proteins that, after the illumination, are covalently bond with II<sup>3</sup>Neu5Ac-Gg<sub>4</sub> (Fig. 8). After radioimaging, the PVDF membrane was incubated with TrkA antibody and we could detect a specific TrkA signal co-migrating with the radioactive band at 140 kDa visualized by the digital autoradiography (Fig. 8).

**Fig. 3** Effect of GM1, a series of oligosaccharides and saccharides on the morphology of Neuro2a (N2a) cells. N2a cells in the absence (a) or presence of 50 μM galactose (b), sialic acid (c), sialyllactose (d), II<sup>3</sup>Neu5Ac-Gg<sub>3</sub> (e), Gg<sub>4</sub> (f), II<sup>3</sup>Neu5Ac-Gg<sub>4</sub> (g), IV<sup>2</sup>FuclI<sup>3</sup>Neu5Ac-Gg<sub>4</sub>

(h) and GM1 (i). After 24 h incubation, cells were analyzed with phase contrast microscopy with 200× magnification. Images are representative of ten independent experiments (n = 10).



Appendix I



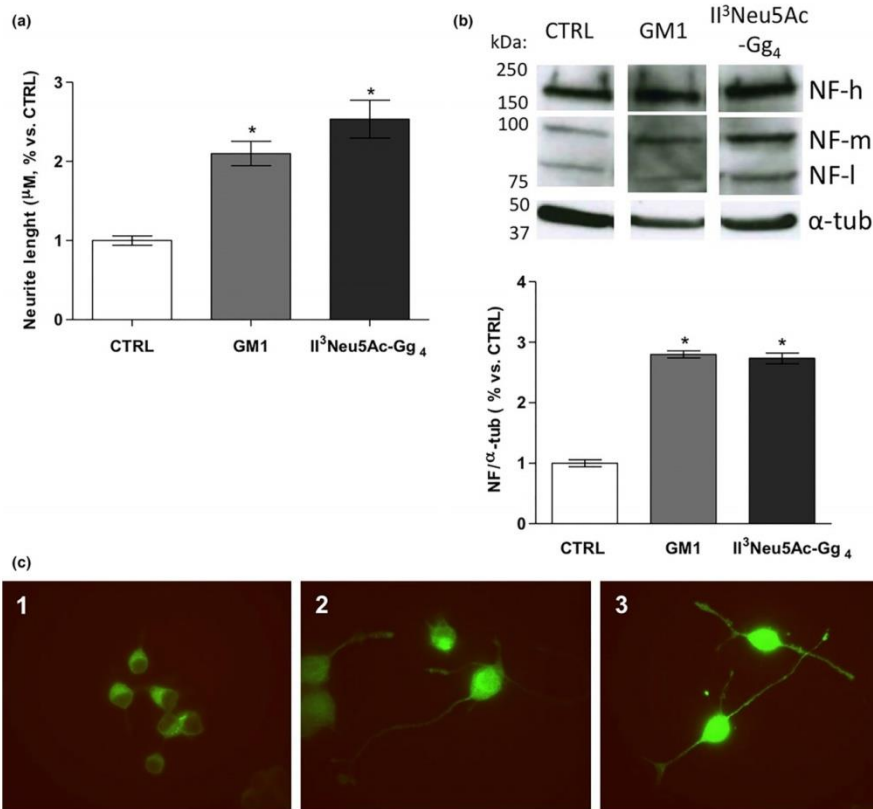


**Fig. 4** Characterization of the neurite sprouting in Neuro2a cells following administration of GM1 and II<sup>3</sup>Neu5Ac-Gg<sub>4</sub>. (a) Neurite length was measured as the ratio between the length of extensions and cell body diameter. Values are expressed as fold increase over CTRL of mean ± SEM from five different experiments (\**p* < 0.01, Student's *t*-test, *n* = 5); (b) Immunoblotting for neurofilament (NF)-h, NF-m, NF-l expression is revealed by specific antibodies and visualized by chemiluminescence. Top: immunoblotting images. Blots are

representative of three independent experiments. Bottom: semi-quantitative analysis of NF proteins amount. α-tubulin (α-tub) was used as internal normalizer. Data are expressed as fold increase over CTRL of mean ± SEM from three different experiments (\**p* < 0.01, Student's *t*-test, *n* = 3); (c) Immunofluorescence staining of NF proteins (400× Magnification), 1, CTRL; 2, GM1; 3, II<sup>3</sup>Neu5Ac-Gg<sub>4</sub>. Images are representative of three independent experiments (*n* = 3).

**Dynamic calculations for the TrkA-II<sup>3</sup>Neu5Ac-Gg<sub>4</sub> complex**

The availability of the crystallographic structure of the extracellular segment of human TrkA in complex with NGF allowed us to support biochemical data with bioinformatics. The molecular docking of II<sup>3</sup>Neu5Ac-Gg<sub>4</sub>, specifically carried out exploring the interaction interface between TrkA and NGF, showed that II<sup>3</sup>Neu5Ac-Gg<sub>4</sub> is able to tightly bind both TrkA and NGF contemporarily, producing only one

very stable pose, with an approximative binding free energy of -11.3 kcal/mol (Fig. 9).

**Discussion**

Gangliosides are components of the external layer of plasma membranes where they represent about one-sixth of the total lipid content. In addition to their structural role, they are



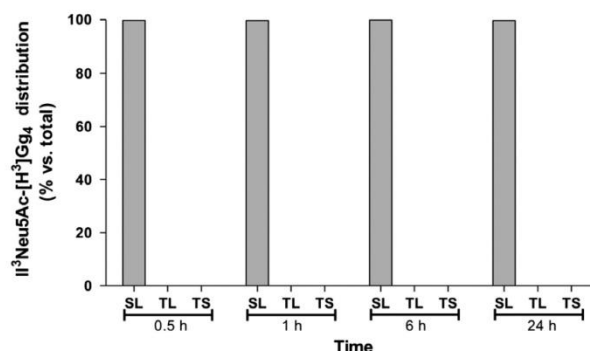


**Fig. 5** Association of  $\text{II}^3\text{Neu5Ac-}[\text{H}^3]\text{Gg}_4$  to Neuro2a (N2a) cells. N2a cells were incubated with  $50 \mu\text{M}$   $\text{II}^3\text{Neu5Ac-}[\text{H}^3]\text{Gg}_4$  for 0.5, 1, 6 and 24 h. After pulse, cells are washed with medium containing 10% fetal bovine serum to obtain the serum labile fraction (SL). Then cells are treated with low concentrated trypsin to obtain the trypsin labile fraction

(TL). Finally, cells are lysed to obtain the trypsin stable fraction (TS) corresponding to the fraction of compound taken up by the cells. The radioactivity associated with each fraction was determined by liquid scintillation counting. Data are expressed as percentage mean of total radioactivity  $\pm$  SEM of three different experiments ( $n = 3$ ).

considered players in signaling and regulatory pathways. The chemical structure of gangliosides makes them ideal mediators of information across the plasma membrane: the ceramide portion allows hydrophobic interactions inside the membrane core, the ceramide amide linkage leads to the formation of a net of hydrogen bonds at the water–lipid interface and the oligosaccharide facing toward the extracellular environment provides specific side-to-side and head-to-head recognition sites. These properties favor formation of lipid rafts, segregation of proteins and ganglioside–protein interactions, which lead to cell function modulation.

GM1 is the best-studied neuronal ganglioside. Its properties, such as modulation of differentiation, adhesion, migration, neurotrophic factor signaling, axon guidance, synaptic transmission, myelin genesis, and neuron–glia interactions have been described, and continue to be confirmed in several papers (see recent reviews Schengrund 2015; Ledeen and Wu 2015; Aureli *et al.* 2016).

GM1-mediated neurodifferentiation has been studied by *in vitro* and *in vivo* experiments (Facci *et al.* 1984; Lipartiti *et al.* 1991; Rodriguez *et al.* 2001; Da Silva *et al.* 2005; Mocchetti 2005), but the precise molecular mechanism by which GM1 exerts its neurotrophic action is still unclear. Anyhow, the increase of GM1 within the plasma membrane seems to be necessary for TrkA-mediated neurodifferentiative processes; in fact the lack of GM1 caused unresponsiveness of the TrkA protein to NGF (Facci *et al.* 1984; Mutoh *et al.* 1998).

Here, we presented a specific role of GM1 oligosaccharide, a part from the entire ganglioside, in the process of neurite elongation in murine neuroblastoma N2a cells. This line of evidence suggests that ceramide acts as an aglycone, dynamically moving within the membrane layer and

allowing different carbohydrate–protein interactions that are dependent on ganglioside content and membrane organization.

For our experiments, we prepared the GM1 oligosaccharide, its tritiated form and its tritiated-and-photoactivable form. The GM1 oligosaccharide was prepared by chemical ozonolysis of pure GM1 followed by alkaline fragmentation according to an old procedure capable to give very high yield (Wiegandt and Bucking 1970). Chromatography and MS analyses showed that the GM1 oligosaccharide was pure and devoid of GM1 (Figure S2). The same procedure was applied to a GM1 carrying tritium at the C6 position of external galactose to obtain  $\text{II}^3\text{Neu5Ac-}[\text{H}^3]\text{Gg}_4$ , part of which was derivatized with nitro-phenyl-azide to prepare a tritium-labeled and photoactivable  $\text{II}^3\text{Neu5Ac-Gg}_4$  (Fig. 1).

$\text{II}^3\text{Neu5Ac-Gg}_4$  was added to cell culture medium to obtain a  $50 \mu\text{M}$  concentration. The  $\text{II}^3\text{Neu5Ac-Gg}_4$  associated to the cell surface could be completely detached from the cells by washing cells with protein solutions (Fig. 5). No detectable amount of  $\text{II}^3\text{Neu5Ac-Gg}_4$  was taken up by the cells. This suggests that the  $\text{II}^3\text{Neu5Ac-Gg}_4$  associated with the surface remains in equilibrium with the free soluble form. The association of  $\text{II}^3\text{Neu5Ac-Gg}_4$  to N2a cells reduced cell proliferation, with no changes in cell viability (Fig. 2), and rapidly produced neurite sprouting (Fig. 3 and Figure S1). The neurite elongation goes together with the increase of neurofilament protein expression (Fig. 4). The neurite sprouting and the expression of neurofilaments are markers of neuronal differentiation (Fukuda *et al.* 2014), and we conclude that the effect exerted by  $\text{II}^3\text{Neu5Ac-Gg}_4$  on N2a cells overlaps to that previously reported for ganglioside GM1 (Facci *et al.* 1984). Moreover, we demonstrated that the effect exerted by  $\text{II}^3\text{Neu5Ac-Gg}_4$  was structure-specific.

## Appendix I

10 | E. Chiricozzi *et al.*

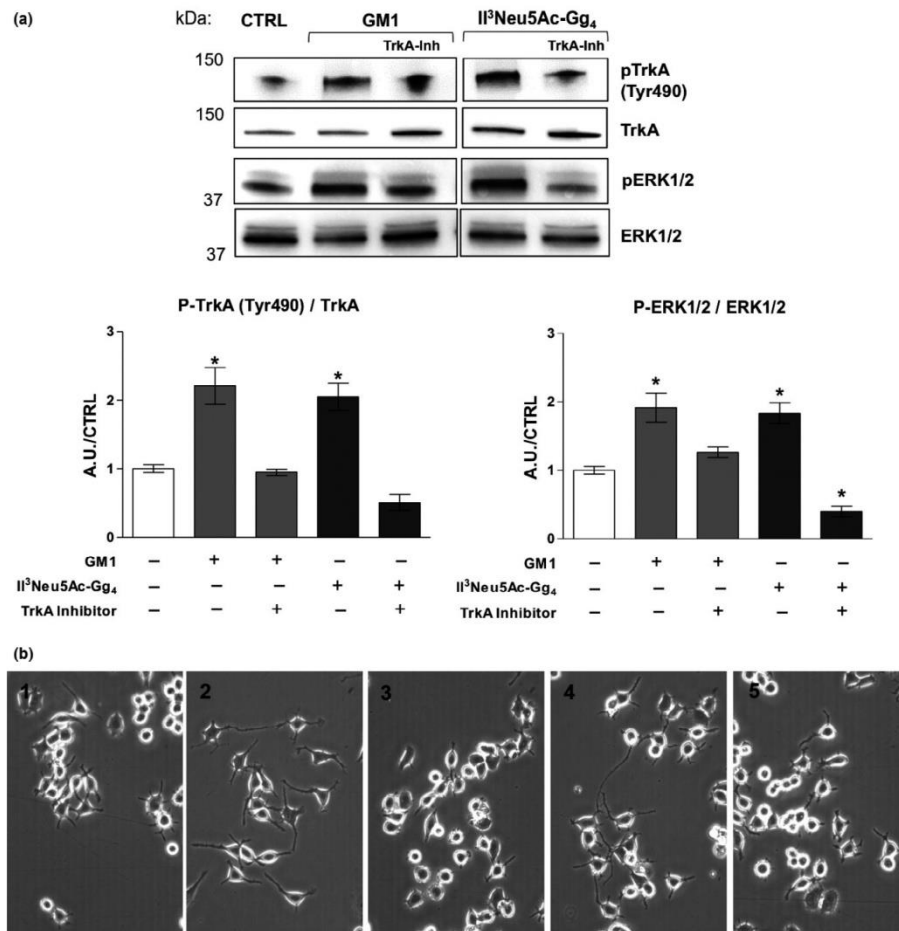
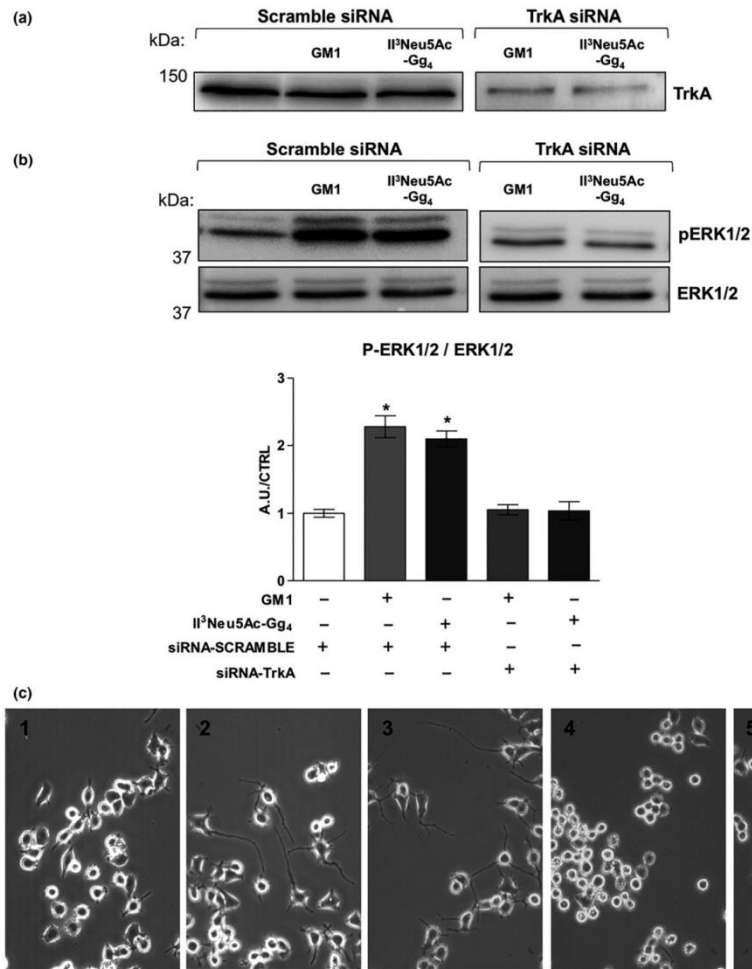


**Fig. 6** GM1 and II<sup>3</sup>Neu5Ac-Gg<sub>4</sub> effect on TrkA pathway. Neuro2a (N2a) cells were treated with 50  $\mu$ M GM1 and II<sup>3</sup>Neu5Ac-Gg<sub>4</sub> for 24 h. Where indicated, the TrkA receptor inhibitor (120 nM) was added to the N2a cells as mentioned in Methods section. (a) Expression of TrkA, phosphorylated TrkA (tyrosine 490, Tyr490), total extracellular signal-regulated protein kinases 1 and 2 (ERK1/2) and phosphorylated ERK1/2 in cell lysate by means of specific antibodies and revealed by enhanced chemiluminescence. Top: immunoblotting images are shown. Bottom: Semi-

quantitative analysis of phosphorylated TrkA and ERK1/2 related to total level of TrkA and ERK1/2, respectively. Data are expressed as fold increase over control of the mean  $\pm$  SEM from five different experiments ( $*p < 0.05$ , Student's *t*-test,  $n = 5$ ). (b) Morphological analysis of N2a cells. 1, control; 2, GM1; 3, TrkA-Inh + GM1; 4, II<sup>3</sup>Neu5Ac-Gg<sub>4</sub>; 5, TrkA-Inh + II<sup>3</sup>Neu5Ac-Gg<sub>4</sub>. Following 24 h incubation, cells were evaluated with phase contrast microscopy with 200 $\times$  magnification. Images are representative of ten independent experiments ( $n = 10$ ).

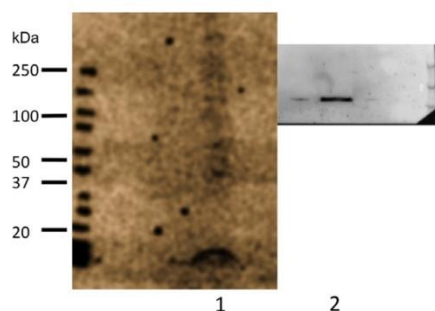
In fact, residues of the total structure, such as sialic acid, galactose, sialyllactose, Neu5Ac-Gg<sub>3</sub> and Gg<sub>4</sub>, did not show neuritogenic properties, at least at the used concentration (Fig. 3 and Figure S1). On the other hand, fucosylated

II<sup>3</sup>Neu5Ac-Gg<sub>4</sub> showed the same effect of II<sup>3</sup>Neu5Ac-Gg<sub>4</sub> suggesting that the terminal  $\alpha$ -Fuc-(1-2)- $\beta$ -Gal linkage does not change the conformation of the Neu5Ac-Gg<sub>4</sub> necessary for the activation of the sprouting process (Fig. 3 and



**Fig. 7** Effect of GM1 and II<sup>3</sup>Neu5Ac-Gg<sub>4</sub> on Neuro2a (N2a) cells following silencing of TrkA. N2a cells were transfected with siRNA against TrkA (50 nM) as described in Methods section. Control cells were transfected with scramble-siRNA. 24 h after transfection cells were exposed to 50 μM GM1 or II<sup>3</sup>Neu5Ac-Gg<sub>4</sub> for 24 h. (a) Western blotting representative image for TrkA expression in siRNA treated cells. (b) Expression of total extracellular signal-regulated protein kinases 1 and 2 (ERK1/2) and phosphorylated ERK1/2 by specific antibodies and revealed by enhanced chemiluminescence. Top: representative

immunoblotting images. Bottom: Semi-quantitative analysis of phosphorylated ERK1/2 related to ERK 1/2 total level. Data are expressed as fold increase over control of the mean ± SEM from five different experiments (\**p* < 0.05, Student's *t*-test, *n* = 5). (c) Morphological analysis of N2a cells 1, scramble-siRNA; 2, scramble-siRNA + GM1; 3, scramble-siRNA + II<sup>3</sup>Neu5Ac-Gg<sub>4</sub>; 4, siRNA-TrkA + GM1; 5, siRNA-TrkA + II<sup>3</sup>Neu5Ac-Gg<sub>4</sub>. Following 24 h incubation, cells were evaluated with phase contrast microscopy with 200× magnification. Images are representative of ten independent experiments (*n* = 10).

12 | E. Chiricozzi *et al.*

**Fig. 8** Interaction between TrkA and  $\text{II}^3\text{Neu5Ac-Gg}_4$  in Neuro2a (N2a) cells. Photoactivable  $\text{II}^3\text{Neu5Ac-}[\text{H}]\text{Gg}_4\text{-N}_3$  was added to N2a cells and cells were then illuminated. Cell lysate was submitted to 4–20% sodium dodecyl sulfate–polyacrylamide gel electrophoresis, blotted on a polyvinylidene difluoride (PVDF) membrane and visualized by digital autoradiography for 96 h (lane 1). The same PVDF was visualized by western blotting using specific antibody anti-TrkA (lane 2). The image is representative of three different experiments.

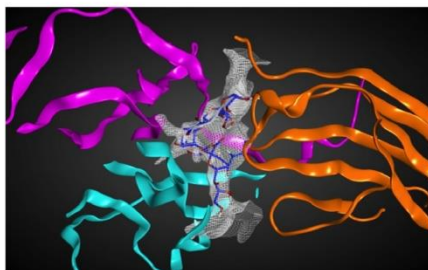


**Fig. 9** Molecular dynamic calculations for the complex TrkA–nerve growth factor (NGF)– $\text{II}^3\text{Neu5AcGg}_4$ . Top-scoring docking pose of  $\text{II}^3\text{Neu5Ac-Gg}_4$  in the TrkA–NGF crystallographic complex. TrkA in orange ribbons; two NGF molecules: one in cyan ribbons and one in magenta ribbons.  $\text{II}^3\text{Neu5AcGg}_4$  is represented in sticks, with blue color for carbon atoms and red color for oxygen atoms. Van der Waals interaction surface between  $\text{II}^3\text{Neu5AcGg}_4$  and proteins is represented as a white mesh map.

Figure S1). This evidence agrees with the previous information reporting that GM1 and Fuc-GM1 show similar binding constant for cholera toxin (Masserini *et al.* 1992).

It has been reported that nerve growth factor receptor TrkA requires the presence of GM1-enriched membrane to be active, while the absence of ganglioside GM1 is negatively correlated with TrkA function (Ferrari *et al.* 1995; Mutoh *et al.* 1995, 1998; Farooqui *et al.* 1997; Rodriguez *et al.* 2001; Bachis *et al.* 2002; Da Silva *et al.* 2005). TrkA phosphorylation at Tyr490 residue induces the

phosphorylation cascade as shown in Fig. 10 (Huang and Reichardt 2003; Brodeur *et al.* 2009). Previous finding revealed the activation of the TrkA–Erk1/2 pathway by ganglioside GM1 (Farooqui *et al.* 1997; Singleton *et al.* 2000; Duchemin *et al.* 2002; Zakharova *et al.* 2014). Thus, we studied the TrkA–Erk1/2 pathway following the addition of  $\text{II}^3\text{Neu5Ac-Gg}_4$  to N2a. For the first time, we showed that,  $\text{II}^3\text{Neu5Ac-Gg}_4$  enhances the phosphorylation of Tyr490 of TrkA and of Erk1/2 leading to neurodifferentiation (Fig. 6). To confirm that the GM1–TrkA interaction triggers the differentiation, we silenced or inhibited TrkA. In both experiments, the addition of  $\text{II}^3\text{Neu5Ac-Gg}_4$  to the cells did not promote neurite sprouting nor reduced the cell proliferation (Figs 6 and 7).

These findings support that the well-known GM1 neurotrophic effects are mediated by TrkA receptor, which could be considered an  $\text{II}^3\text{Neu5Ac-Gg}_4$  target.

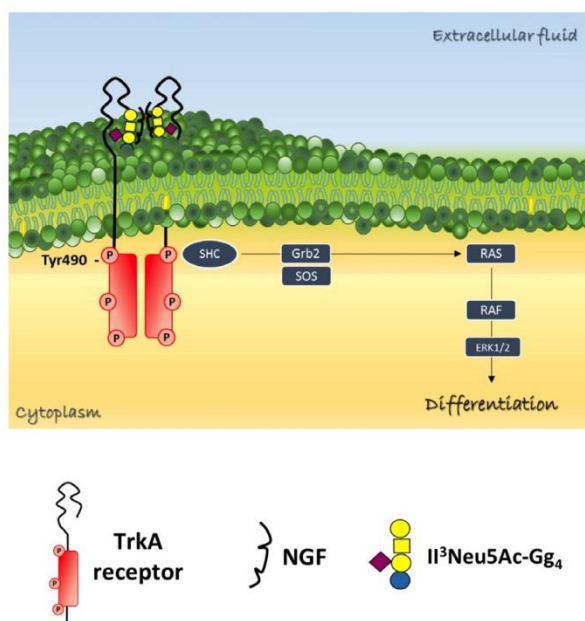
To obtain evidence about the formation of an  $\text{II}^3\text{Neu5Ac-Gg}_4$ –TrkA complex, we prepared a tritium-labeled photoactivable  $\text{II}^3\text{Neu5Ac-Gg}_4$  by chemical techniques (Fig. 1). Photolabeling experiments with photoactivable glycosphingolipids were introduced several years ago (Loberto *et al.* 2003; Mauri *et al.* 2004) and were used to ascertain the interaction of glycosphingolipids with different proteins, such as the insulin receptor (Kabayama *et al.* 2007), the receptor CD9 (Ono *et al.* 2001), the cytoskeleton tubulin (Palestini *et al.* 2000), the membrane protein caveolin 1 (Fra *et al.* 1995), the kinase Lyn (Chiricozzi *et al.* 2015), and the neuronal protein TAG1 (Loberto *et al.* 2003).

After incubation with the tritium-labeled photoactivable  $\text{II}^3\text{Neu5Ac-Gg}_4$ , cells were washed once with PBS to remove the non-cell-associated compound. The subsequent UV-light exposition transforms the photoactivable group into a nitrene, which rapidly covalently links to neighboring compounds (Mauri *et al.* 2004). According to this mechanism, and recalling that the exogenous  $\text{II}^3\text{Neu5Ac-Gg}_4$  does not become component of the cell membranes, any interaction of the tritium-labeled  $\text{II}^3\text{Neu5Ac-Gg}_4$  photoactivable derivative with proteins yields to tritium-labeled  $\text{II}^3\text{Neu5Ac-Gg}_4$ –protein stable complexes that should involve the extracellular domain of transmembrane proteins or of GPI-anchored proteins. By SDS–PAGE separation, followed by radiomaging of the blotted material, we recognized few bands and one of these bands showed a molecular mass of 140 kDa. A specific signal for TrkA was found overlapping the radiolabeled band, suggesting a direct interaction between  $\text{II}^3\text{Neu5Ac-Gg}_4$  and TrkA (Fig. 8).

Over these experimental data, we used molecular modeling tools to predict whether  $\text{II}^3\text{Neu5Ac-Gg}_4$  can increase the TrkA–NGF complex stability, favoring their intermolecular interactions. In fact, even if NGF is not synthesized by N2a cells (Leon *et al.* 1994), it is present in our experimental conditions since the culture medium used contains serum (Figure S3). We started from the crystallized structure of



**Fig. 10** Diagram of the proposed mechanism for GM1-mediated neurodifferentiation in Neuro2a cells. The TrkA activation by autophosphorylation is regulated by GM1-enriched receptor environment. GM1 modulates TrkA activity by stabilizing the TrkA-nerve growth factor (NGF) complex with its oligosaccharide portion. The TrkA-GM1 interaction is represented as a side-by-side interaction. GM1 triggers the phosphorylation of Tyr490 promoting the differentiation signaling. ERK, extracellular signal-regulated protein kinases 1 and 2; Grb2, growth factor receptor-bound protein 2; Gab1, Grb2-associated binder-1; RAS, GTP-binding protein; RAF, serine/threonine kinase; SHC, transforming protein 1; SOS, son of sevenless.



TrkA receptor, which is resolved as a dimer in the presence of NGF. The crystal structure of the TrkA-NGF complex is characterized by a pocket, which can be occupied by water molecules, as showed in another crystallographic structure of the same complex (PDB ID: 1WVW). By *in silico* analysis, we found that the  $\text{II}^3\text{Neu5Ac-Gg}_4$  perfectly fits within this space (Fig. 9). Moreover, the energy associated to the TrkA- $\text{II}^3\text{Neu5Ac-Gg}_4$  complex, approx.  $-6.6$  kcal/mol, becomes approx.  $-11.5$  kcal/mol when NFG belongs to the complex. This suggests that the  $\text{II}^3\text{Neu5Ac-Gg}_4$  stabilizes the TrkA-NGF interaction, and suggests a specific molecular recognition process between the  $\text{II}^3\text{Neu5Ac-Gg}_4$  and a specific extracellular domain of the TrkA receptor.

The information available in literature clearly shows that any experimental model capable to modify the local plasma membrane GM1 content, promotes N2a differentiation. GM1 is a natural amphiphilic compound with a structure that combines the ceramide lipid moiety with the soluble oligosaccharide chain. Altogether, our results point out that the GM1 oligosaccharide is the structure portion responsible for the neurodifferentiative properties exerted by GM1 (Fig. 10). The GM1 oligosaccharide directly interacts with TrkA receptor resulting in TrkA-mediated neuritogenesis.

Neuronal differentiation is characterized by an enhancement of several glycosyltransferases activity leading to an increase

in PM ganglioside content (Aureli *et al.* 2011). Ceramide is the aglycone necessary for glycan protrusion into the extracellular environment and for interaction with functional proteins. GM1 exhibits its oligosaccharide chain to the TrkA receptor. Molecular dynamic calculations confirm that the GM1 oligosaccharide perfectly fits with a TrkA domain stabilizing the TrkA-NGF interaction, allowing a rapid auto phosphorylation of the receptor cytosolic portion.

The still open question is whether the  $\text{II}^3\text{Neu5Ac-Gg}_4$ -TrkA interaction is due to a broad plasma membrane increase of GM1 or to a membrane reorganization, leading to a new TrkA environment enriched of GM1. We reported this latter possibility because silencing plasma membrane sialidase Neu3, with consequent less hydrolysis of polysialylated gangliosides and with reduced production of GM1 at the plasma membrane level, we promoted the neurite elongation (Valperta *et al.* 2007). We discussed this in term of membrane reorganization and local concentration of GM1.

#### Acknowledgments and conflict of interest disclosure

This work was supported by the 2015–2016 contract from FIDIA S.p.a. in favor of S.S. The authors declare that they have no conflict of interest.

## Supporting information

Additional Supporting Information may be found online in the supporting information tab for this article:

**Figure S1.** This figure shows the morphological characterization of N2a cells untreated or treated with GM1,  $\text{II}^3\text{Neu5Ac-Gg}_4$ , and saccharide derivative for 48 h.

**Figure S2.** This figure shows the MS and chromatography analysis of  $\text{II}^3\text{Neu5Ac-Gg}_4$ .

**Figure S3.** This figure shows the evaluation of NGF expression in N2a cells.

**Appendix S1.** Supplementary Materials and methods.

## References

- Acquotti D., Cantu L., Ragg E. and Sonnino S. (1994) Geometrical and conformational properties of ganglioside GalNAc-GD1a,  $\text{IV}^6\text{GalNAcIV}^3\text{Neu5AcII}^3\text{Neu5AcGgOse}_4\text{Cer}$ . *Eur. J. Biochem.* **225**, 271–288.
- Allende M. L. and Panzetta P. (1994) *In vitro* modulation of changes in ganglioside patterns of differentiating neurons in the presence of an anti-GM1 antibody. *J. Neurosci. Res.* **37**, 497–505.
- Aureli M., Loberto N., Lanteri P., Chigorno V., Prinetti A. and Sonnino S. (2011) Cell surface sphingolipid glycohydrolases in neuronal differentiation and aging in culture. *J. Neurochem.* **116**, 891–899.
- Aureli M., Mauri L., Ciampa M. G., Prinetti A., Toffano G., Secchieri C. and Sonnino S. (2016) GM1 ganglioside: past studies and future potential. *Mol. Neurobiol.* **53**, 1824–1842.
- Bachis A., Rabin S. J., Del Fiacco M. and Mocchetti I. (2002) Ganglioside prevent excitotoxicity through activation of TrkB receptor. *Neurotox. Res.* **4**, 225–234.
- Brodeur G. M., Minturn J. E., Ho R., Simpson A. M., Iyer R., Varela C. R., Light J. E., Kolla V. and Evans A. E. (2009) Trk receptor expression and inhibition in neuroblastoma. *Clin. Cancer Res.* **15**, 3244–3250.
- Chigorno V., Pitto M., Cardace G., Acquotti D., Kirschner G., Sonnino S., Ghidoni R. and Tettamanti G. (1985) Association of gangliosides to fibroblasts in culture: a study performed with GM1 [14C]-labelled at the sialic acid acetyl group. *Glycoco. J.* **2**, 279–291.
- Chigorno V., Valsecchi M., Acquotti D., Sonnino S. and Tettamanti G. (1990) Formation of cytosolic ganglioside-protein complex following administration of photoreactive ganglioside GM1 to human fibroblasts in culture. *FEBS Lett.* **263**, 329–331.
- Chiricozzi E., Ciampa M. G., Brasile G., Compostella F., Prinetti A., Nakayama H., Ekyalongo R. C., Iwabuchi K., Sonnino S. and Mauri L. (2015) Direct interaction, instrumental for signaling processes, between LacCer and Lyn in the lipid rafts of neutrophil-like cells. *J. Lip. Res.* **56**, 129–141.
- Coskun U. and Simons K. (2011) Cell membranes: the lipid perspective. *Cell Struct.* **19**, 1543–1548.
- Da Silva J. S., Hasegawa T., Miyagi T., Dotti C. G. and Abab-Rodriguez J. (2005) Asymmetric membrane ganglioside sialidase activity specifies axonal fate. *Nat. Neurosci.* **8**, 606–615.
- Duchemin A. M., Ren Q., Mo L., Neff N. H. and Hadjiconstantinou M. (2002) GM1 ganglioside induces phosphorylation and activation of Trk and Erk in brain. *J. Neurochem.* **81**, 696–707.
- Facci L., Leon A., Toffano G., Sonnino S., Ghidoni R. and Tettamanti G. (1984) Promotion of neurogenesis in mouse neuroblastoma cells by exogenous gangliosides. Relationship between the effect and the cell association of ganglioside GM1. *J. Neurochem.* **42**, 299–305.
- Farooqui T., Franklin T., Pearl D. K. and Yates A. J. (1997) Ganglioside GM1 enhances induction by nerve growth factor of a putative dimer of TrkA. *J. Neurochem.* **68**, 2348–2355.
- Ferrari G., Anderson B. L., Stephens R. M., Kaplan D. R. and Greene L. A. (1995) Prevention of apoptotic neuronal death by GM1 ganglioside. Involvement of Trk neurotrophin receptors. *J. Biol. Chem.* **270**, 3074–3080.
- Fra A. M., Masserini M., Palestini P., Sonnino S. and Simons K. (1995) A photo-reactive derivative of ganglioside GM1 specifically cross-links VIP21-caveolin on the cell surface. *FEBS Lett.* **375**, 11–14.
- Fukuda Y., Fukui T., Hikichi C. et al. (2014) Neurotrophin promotes NGF signaling through interaction of GM1 ganglioside with Trk neurotrophin receptor in PC12 cells. *Brain Res.* **1596**, 13–21.
- Ghidoni R., Sonnino S., Tettamanti G., Wiegandt H. and Zambotti V. (1976) On the structure of two new gangliosides from beef brain. *J. Neurochem.* **27**, 511–515.
- Hakomori S., Handa K., Iwabuchi K., Yamamura S. and Prinetti A. (1998) New insights in glycosphingolipid function: 'glycosignaling domain', a cell surface assembly of glycosphingolipids with signaltransducer molecules, involved in cell adhesion coupled with signaling. *Glycobiology* **8**, xi–xix.
- Huang E. J. and Reichardt L. F. (2003) Trk receptors: roles in neuronal signal transduction. *Ann. Rev. Biochem.* **72**, 609–642.
- IUPAC-IUBMB JCoBN, (1998) Nomenclature of glycolipids. *Carbohydr Res* **312**, 167–175.
- Kabayama K., Sato T., Saito K., Loberto N., Prinetti A., Sonnino S., Kinjo M., Igarashi Y. and Inokuchi J. (2007) Dissociation of the insulin receptor and caveolin-1 complex by ganglioside GM3 in the state of insulin resistance. *Proc. Natl Acad. Sci. USA* **104**, 13678–13683.
- Kuhn R. and Wiegandt H. (1963) Die Konstitution der Ganglio-N-tetraose und des Gangliosids. *Gl Chem. Ber.* **96**, 866–880.
- Kwak D. H., Kim S. M., Lee D. H., Kim J. S., Kim S. M., Lee S. U., Jung K. Y., Seo B. B. and Choo Y. K. (2005) Differential expression patterns of gangliosides in the ischemic cerebral cortex produced by middle cerebral artery occlusion. *Mol. Cell* **20**, 354–360.
- Ledeen R. W. and Wu G. (2015) The multi-tasked life of GM1 ganglioside, a true factotum of nature. *Trends Biochem. Sci.* **40**, 407–418.
- Leon A., Buiuiani A., Dal Toso R., Fabris M., Romanello S., Aloeo L. and Montalcini R. L. (1994) Mast cells synthesize, store, and release nerve growth factor. *Proc. Natl Acad. Sci. USA* **91**, 3739–3743.
- Lipariti M., Lazzaro A., Zanoni R., Mazzari S., Toffano G. and Leon A. (1991) Monosialoganglioside GM1 reduces NMDA neurotoxicity in neonatal rat brain. *Exp. Neurol.* **113**, 301–305.
- Loberto N., Prioni S., Prinetti A., Ottico E., Chigorno V., Karageorgos D. and Sonnino S. (2003) The adhesion protein TAG-1 has a ganglioside environment in the sphingolipid-enriched membrane domains of neuronal cell in culture. *J. Neurochem.* **85**, 224–233.
- Lubineau A., Auge J. and Drouillard B. (1995) Improved synthesis of glycosylamines and a straightforward preparation of N-acetylglycosylamines as carbohydrate-based detergents. *Carbohydr. Res.* **266**, 211–219.
- Masserini M., Freire E., Palestini P., Calappi E. and Tettamanti G. (1992) Fuc-GM1 ganglioside mimics the receptor function of GM1 for cholera toxin. *Biochemistry* **31**, 2422–2426.
- Mauri L., Prioni S., Loberto N., Chigorno V., Prinetti A. and Sonnino S. (2004) Synthesis of radioactive and photoactivable ganglioside derivatives for the study of ganglioside-protein interaction. *Glycoconj. J.* **20**, 11–23.
- Mehlen P., Rabizadeh S., Snipas S. J., Assa-Munt N., Salvesen G. S. and Bredesen D. E. (1988) The DCC gene product induces apoptosis by a mechanism requiring receptor proteolysis. *Nature* **395**, 801–804.

- Miyagi T. and Yamaguchi K. (2012) Mammalian sialidases: physiological and pathological roles in cellular functions. *Glycobiology* **22**, 880–896.
- Mocchetti I. (2005) Exogenous gangliosides, neuronal plasticity and repair and the neurotrophins. *Cell. Mol. Life Sci.* **62**, 2283–2294.
- Mosmann T. (1983) Rapid colorimetric assay for cellular growth and survival: application to proliferation and cytotoxicity assays. *J. Immunol. Methods* **65**, 55–63.
- Mutoh T., Tokuda A., Miyadai T., Hamaguchi M. and Fujiki N. (1995) Ganglioside GM1 binds to the Trk proteins and regulates receptor function. *Proc. Natl Acad. Sci.* **92**, 5087–5091.
- Mutoh T., Tokuda A., Inokuchi J. and Kuriyama M. (1998) Glucosylceramide synthase inhibitor inhibits the action of nerve growth factor in PC12 cells. *J. Biol. Chem.* **273**, 26001–26007.
- Naim M., Bhat S., Rankin K. N. *et al.* (2007) Solvated interaction energy (SIE) for scoring protein-ligand binding affinities. I. Exploring the parameter space. *J. Chem. Inf. Model.* **47**, 122–133.
- Ono M., Handa K., Sonnino S., Withers D. A., Nagai H. and Hakomori S. (2001) GM3 ganglioside inhibits CD9-facilitated haptotactic cell motility: coexpression of GM3 and CD9 is essential in the downregulation of tumor cell motility and malignancy. *Biochemistry* **40**, 6414–6421.
- Palestini P., Pitto M., Tedeschi G., Ferraretto A., Parenti M., Brunner J. and Masserini M. (2000) Tubulin anchoring to glycolipid-enriched, detergent resistant domains of the neuronal plasma membrane. *J. Biol. Chem.* **275**, 9978–9985.
- Rabin S. J., Bachis A. and Mocchetti I. (2002) Gangliosides activate Trk receptors by inducing the release of neurotrophin. *J. Biol. Chem.* **277**, 49466–49472.
- Rodriguez J. A., Piddini E., Hasegawa T., Miyagi T. and Dotti C. G. (2001) Plasma membrane ganglioside sialidase regulates axonal growth and regeneration in hippocampal neurons in culture. *J. Neurosci.* **21**, 8387–8395.
- Roisen F. J., Bartfeld H., Nagele R. and Yorke G. (1981) Ganglioside stimulation of axonal sprouting in vitro. *Science* **214**, 577–578.
- Schengrund C. L. (2015) Gangliosides: glycosphingolipids essential for normal neural development and function. *Trends Biochem. Sci.* **40**, 397–406.
- Schengrund C. L. and Prouty C. (1988) Oligosaccharide portion of GM1 enhances process formation by S20Y neuroblastoma cells. *J. Neurochem.* **51**, 277–282.
- Schneider J. S., Sendek S., Daskalakis C. and Cambi F. (2010) GM1 ganglioside in Parkinson's disease: results of five year open study. *J. Neurol. Sci.* **292**, 45–51.
- Singleton D. W., Lu C. L., Collella R. and Roisen F. J. (2000) Promotion of neurite outgrowth by protein kinase inhibitors and ganglioside GM1 in neuroblastoma cells involved MAP kinase ERK1/2. *Int. J. Dev. Neurosci.* **18**, 797–805.
- Sonnino S., Chigorno V., Acquotti D., Pitto M., Kirschner G. and Tettamanti G. (1989) A photoreactive derivative of radiolabeled GM1 ganglioside: preparation and use to establish the involvement of specific proteins in GM1 uptake by human fibroblasts in culture. *Biochemistry* **28**, 77–84.
- Sonnino S., Chigorno V., Valsecchi M., Pitto M. and Tettamanti G. (1992) Specific ganglioside-cell protein interactions: a study performed with GM1 ganglioside derivative containing photoactivable azide and rat cerebellar granule cells in culture. *Neurochem. Int.* **20**, 315–321.
- Sonnino S., Nicolini M. and Chigorno V. (1996) Preparation of radiolabeled gangliosides. *Glycobiology* **6**, 479–487.
- Sonnino S., Mauri L., Chigorno V. and Prinetti A. (2006) Gangliosides as components of lipid membrane domains. *Glycobiology* **17**, 1R–13R.
- Sonnino S., Chigorno V., Aureli M., Masilamani A. P., Valsecchi M., Roberto N., Prioni S., Mauri L. and Prinetti A. (2011) Role of gangliosides and plasma membrane associated sialidase in the process of cell membrane organization. *Adv. Exp. Med. Biol.* **705**, 297–316.
- Svennerholm L. (1957) Quantitative estimation of sialic acids II A colorimetric resorcinol hydrochloric acid method. *Biochim. Biophys. Acta* **24**, 604–611.
- Takki-Luukkainen I. T. and Miettinen T. (1959) Presence of sialic acid and hexosamine in proteins of the aqueous humour. *Acta Ophthalmol.* **37**, 138–142.
- Tettamanti G. (1986) *Gangliosides and Neuronal Plasticity*. Meeting ISIN. Liviana Press, Springer, Verlag, Paris, France.
- Tettamanti G., Bonali F., Marchesini S. and Zambotti V. (1973) A new procedure for the extraction, purification and fractionation of brain gangliosides. *Biochim. Biophys. Acta* **296**, 160–170.
- Valperta R., Valsecchi M., Rocchetta F., Aureli M., Prioni S., Prinetti A., Chigorno V. and Sonnino S. (2007) Induction of axonal differentiation by silencing plasma membrane-associated sialidase Neu3 in neuroblastoma cells. *J. Neurochem.* **100**, 708–719.
- Wiegand H. and Bucking H. W. (1970) Carbohydrate components of extraneuronal gangliosides from bovine and human spleen, and bovine kidney. *Eur. J. Biochem.* **15**, 287–292.
- Wood E. R., Kuyper L., Petrov K. G., Hunter R. N., Harris P. A. and Lackey K. (2004) Discovery and in vitro evaluation of potent TrkA kinase inhibitors: oxindole and aza-oxindoles. *Bioorg. Med. Chem. Lett.* **14**, 953–957.
- Wu G., Lu Z. H. and Ledeen R. W. (1995) Induced and spontaneous neuritogenesis are associated with enhanced expression of ganglioside GM1 in the nuclear membrane. *J. Neurosci.* **15**, 3739–3746.
- Yu R. K., Nakatani Y. and Yanagisawa M. (2009) The role of glycosphingolipid metabolism in the developing brain. *J. Lipid Res.* **50**, S440–S445.
- Zakharova I. O., Sokolova T. V., Vlasova Y. A., Furaev V. V., Rychkova M. P. and Avrova N. F. (2014) GM1 ganglioside activates ERK1/2 and Akt downstream of Trk tyrosine kinase and protects PC12 cell against hydrogen peroxide toxicity. *Neurochem. Res.* **39**, 2262–2275.
- Zoli M., Benfanti F., Pich E. M., Toffano G., Fuxe K. and Agnati L. F. (1990) Aspects of neuronal plasticity in the central nervous system – IV. Chemical anatomical studies on the aging brain. *Neurochem. Int.* **16**, 437–449.